Spatial and temporal dynamics of the RNA silencing response

Cover Linocut by Marian Groenenboom
A leaf with chlorotic patterns caused by virus infection, and a petunia flower in which the floral colour is suppressed by RNA silencing.
Print PrintPartners Ipskamp
ISBN 978-90-393-4957-1

Spatial and temporal dynamics of the RNA silencing response

Spatiale en temporele dynamica van de RNA silencing reactie
(met een samenvatting in het Nederlands)

Proefschrift

ter verkrijging van de graad van doctor aan de Universiteit Utrecht
op gezag van de rector magnificus, prof. dr. J.C. Stoof,
ingevolge het besluit van het college voor promoties
in het openbaar te verdedigen op
vrijdag 28 november 2008 des middags te 12.45 uur.

door

Maria Anna Cornelia Groenenboom

geboren op 29 juni 1979
te Tilburg

Promotor: Prof. dr. P. Hogeweg

The studies described in this thesis were financially supported by the Netherlands Organisation for Scientific Research (NWO) through grant number 050.50.202 of the BioMolecular Informatics program.

Contents

1 General Introduction **1**
1.1 RNA silencing . . . 2
1.2 Transgene induced silencing . . . 2
1.2.1 Post-transcriptional silencing . . . 3
1.2.2 Transcriptional silencing . . . 5
1.3 Antiviral silencing . . . 6
1.3.1 Virus replication . . . 6
1.3.2 The pathway of antiviral silencing . . . 7
1.3.3 Silencing suppressors . . . 8
1.4 Other silencing phenomena . . . 9
1.4.1 Gene regulation by miRNA . . . 9
1.4.2 piRNAs . . . 10
1.5 Evolutionary conservation . . . 10
1.5.1 Different species . . . 10
1.5.2 The key proteins of RNA silencing . . . 13
1.6 Outline of this thesis . . . 15

2 The RNA Silencing Pathway: the Bits and Pieces That Matter **17**
2.1 Introduction . . . 18
2.2 Results . . . 20
2.2.1 Biological background and description of core model 20
2.2.2 Dynamics of core model . . . 21
2.2.3 Deficiencies of core model . . . 22

2.2.4 Biological background and description of extended models . . . 23
2.2.5 Dynamics of extended models . . . 24
2.2.6 Parameters dependence and predictions . . . 28
2.3 Discussion . . . 33
2.4 Materials and Methods . . . 35

3 The dynamics and efficacy of antiviral RNA silencing: a model study 39
3.1 Introduction . . . 40
3.2 Methods . . . 41
3.2.1 Model description: Viral replication . . . 42
3.2.2 Model description: Antiviral RNA silencing . . . 44
3.2.3 Parameters . . . 46
3.3 Results . . . 47
3.3.1 Viral growth in a silencing defective system . . . 47
3.3.2 Virus induced silencing . . . 48
3.3.3 Observed ratio of siRNAs . . . 54
3.4 Discussion . . . 56
3.5 Appendix . . . 58

4 RNA silencing can explain chlorotic infection patterns on plant leaves 61
4.1 Background . . . 62
4.2 Methods . . . 64
4.2.1 Intracellular model . . . 64
4.2.2 Tissue level model . . . 65
4.3 Results and Discussion . . . 66
4.3.1 Infection patterns without RNA silencing . . . 66
4.3.2 Infection patterns with silencing, without siRNA movement . . . 67
4.3.3 Infection patterns with siRNA movement . . . 68
4.3.4 Alternative equilibria depend on influx of siRNAs . . . 71
4.3.5 Combined single- and double-stranded RNA cleavage by Dicer . . . 73
4.3.6 Effect of amplification . . . 75
4.4 Conclusions . . . 77
4.5 Appendix . . . 79

5 Viral suppression of RNA silencing **83**
5.1 Introduction 84
5.2 Methods 86
5.3 Results and Discussion 89
5.3.1 Suppressors that target siRNA or dsRNA 89
5.3.2 Suppressors that target Argonaute 94
5.4 Conclusion 99
5.5 Appendices 102
5.5.1 Basic model 102
5.5.2 siRNA binding 105
5.5.3 dsRNA binding 105
5.5.4 Targeting Argonaute for degradation 107
5.5.5 Inactivating Argonaute 107
5.5.6 Parameter values 108

6 Summarising Discussion **111**
6.1 Scope 112
6.2 Review and Discussion 112
6.3 Analysing the models 116
6.4 Future directions 116
6.5 Conclusion 118

Bibliography **119**

Nederlandse samenvatting **131**

Curriculum vitae **137**

List of publications **139**

Dankwoord **141**

CHAPTER 1

General Introduction

1.1 RNA silencing

In 2006 Andrew Fire and Craig Mello received the Nobel Price in Physiology or Medicine for their discovery that double-stranded RNA can suppress target gene expression in the worm *Caenorhabditis elegans*. Their discovery was a major step in the understanding of unexplained phenomena in other eukaryotes, for example plants and fungi. These homology-dependent RNA based mechanisms are now collectively called RNA silencing. The term RNA silencing covers various types of RNA-based mechanisms in eukaryotes that use small pieces of RNA to suppress target gene expression. The small pieces of RNA are 20-26 nt long and provide the sequence specificity of RNA silencing by base-pair complementarity. RNA silencing is crucial for defence against viruses, gene regulation, control of transposons and development.

In this thesis we develop mathematical and spatially explicit models to study RNA silencing. We focus on transgene induced silencing and antiviral silencing. In this chapter we will discuss the background and mechanisms of transgene induced silencing and antiviral silencing. Furthermore, we will shortly discuss the various other silencing phenomena; and we conclude with an overview of the work discussed in this thesis.

1.2 Transgene induced silencing

Transgene induced silencing is silencing triggered by a high level of expression of transgenes. This type of RNA silencing is one of the first silencing phenomena studied and also the starting point of the research described in this thesis.

The discovery of transgene induced silencing started with the unexpected results of Napoli et al. [108] and Van der Krol et al. [149] in 1990. In an attempt to create more intensely coloured Petunia flowers, both groups tried to over-express chalcone synthase by the introduction of an extra chalcone synthase gene. Chalcone synthase is a key enzyme in the bio-synthesis of diverse flavonoids, leading to the production of flower pigments. The extra gene, however, did not lead to more heavily pigmented flowers. 20 to 40% of the transgenic plants produced white flowers or flowers with white patches. The chalcone synthase mRNA was reduced 50 fold in the white-flowering plants [108, 149]. The phenomenon was called co-suppression, in which RNAs of a transgene and an homologous endogenous gene are co-ordinately suppressed. van Blokland et al. [148] showed

that the transcription rate of the endogenous chalcone synthase gene and the transgene did not differ between white and purple tissues. These results indicated that the expression of the genes remained unaltered, and that the produced mRNA was degraded by an unknown mechanism. Other experiments showed that antisense RNA, transcribed from a transgene, could also be used to down-regulate the expression of a gene [143].

Co-suppression was used in many experiments. Very interesting was the idea to create transgenic plants that expressed a viral sequence instead of extra copies of an endogenous gene [41, 89]. If the inserted gene co-suppressed the virus, it would be possible to create virus specific resistance. Indeed, most transgenic plants became highly resistant to the virus, some were susceptible but recovered, and some were still fully susceptible.

Co-suppression and RNA mediated virus resistance in plants were collectively called Post-Transcriptional Gene Silencing (PTGS). The mechanism of PTGS remained unknown until Dougherty and Parks [42] linked different experiments to each other in 1995 and proposed that sense and antisense suppression are mediated by the same cellular pathway. The pathway they proposed lacked detail but the general idea turned out to be correct. They suggested that aberrant or over-expressed RNA was recognised by RNA-dependent RNA polymerase (RDR). RDR would then produce small pieces of RNA that could bind to the target mRNA. The small RNA-mRNA complex could be recognised by a second factor that induced cleavage of the mRNA. They suggested that this mechanism was probably not restricted to plants.

Indeed other experiments have shown that transgene induced silencing occurs in flies [111], algae [160] and in fungi under the term quelling [26, 127]. It was also discovered that post-transcriptional silencing of transgenes was not the only mode of silencing. Transgenes could also be silenced transcriptionally. In transcriptional gene silencing the expression of the gene is more permanently altered by chromatin modifications.

1.2.1 Post-transcriptional silencing

How post-transcriptional silencing is triggered by the expression of transgenes is still largely unknown. It has been shown however, that high expression of transgenes induces silencing [33, 72, 82, 111, 113], and that RDR plays an important role [31, 49]. Our modelling will shed light on the initiation of RNA silencing by highly expressed genes.

The generally accepted pathway of post-transcriptional gene silencing is shown in Figure 1.1. The single stranded RNA produced by the trans-

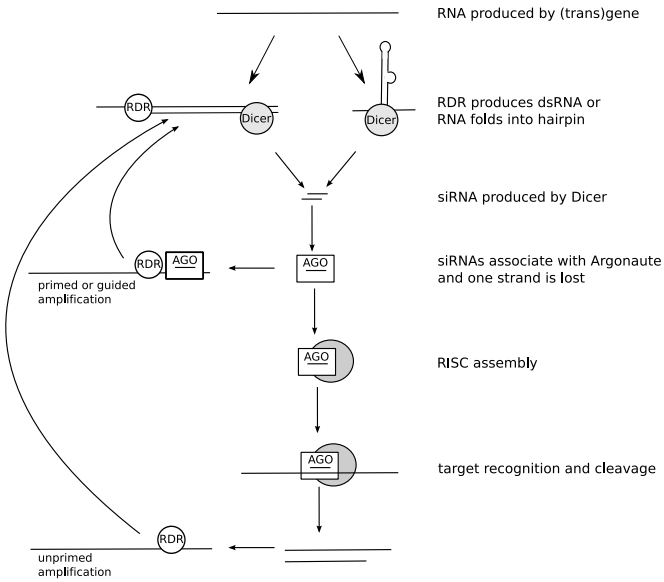

Figure 1.1: A schematic representation of the pathway of transgene induced RNA silencing. RNA produced by the transgenes is either recognised by RDR that synthesises a dsRNA trigger, or the RNA folds in long enough hairpins. The dsRNA structures are cleaved by Dicer into primary siRNAs. siRNA associates with Argonaute (AGO) and the guide strand is kept in the complex. Multiple proteins assemble with the Argonaute-siRNA complex and form RISC. RISC is guided by the siRNA to the target, that is cleaved. Secondary siRNAs can be produced in an amplification pathway in an unprimed, primed or guided manner.

genes triggers RDR to produce a dsRNA trigger [55], or the folded transgene RNA contains hairpins that serve as dsRNA triggers. The latter is for example the case when the transcript contains inverted repeats [24]. The dsRNA is cleaved by an RNase III-like nuclease named Dicer into small interfering RNAs (siRNAs) of 21-25 nucleotides long. siRNAs associate with a protein from the Argonaute family [69]. The Argonautes are essential for all types of RNA silencing. The so called passenger strand of the double stranded siRNA is cleaved and disposed of by the Argonaute protein, the strand that is kept is called the guide strand. Other proteins assemble to the Argonaute-siRNA complex and together they form the RNA Induced Silencing Complex, RISC. RISC is guided to the target RNA by the single-stranded siRNA, and after binding the target RNA is cleaved. The RISC stays intact and can continue with the next target. In this way RNA complementary to the siRNAs will be degraded, and the gene is silenced.

In addition to this primary cleavage pathway there is a secondary amplification pathway. The amplification pathway leads to the production of secondary siRNAs through RDR. There can be three types of amplification: unprimed, primed and guided amplification. Unprimed amplification is the production of dsRNA from a single RNA strand, that can be either a full length RNA or an RNA that is cleaved by RISC. The product dsRNA can be cleaved into siRNA by a Dicer. This process could also be involved in the initiation of transgene induced silencing. In primed and guided amplification the siRNA-Argonaute complex binds to a singe stranded RNA and serves as a primer for RDR. In the case of primed amplification the siRNA-Argonaute complex is lost after binding to a single stranded RNA, whereas with guided amplification the siRNA-Argonaut complex merely serves as guide and stays intact after priming amplification for RDR. Amplification can lead to a phenomenon called transitivity: the production of secondary siRNAs from a region beyond the original region that triggered silencing.

Transgene induced silencing was discovered when researchers artificially increased gene expression. The natural role of this mechanism is most likely the control of transposons. Transposons are selfish nucleic acid elements that can move and copy themselves through genomes. They can change gene coding sequence or alter gene expression. Additionally, they can provide sites for recombination during meiosis and lead to chromosome rearrangements. Transposons could trigger RNA silencing for two reasons: they often have multiple inverted repeats (IRs) that form dsRNA transcripts [139]; and their high copy number could trigger silencing. Transposons are under tight control of RNA silencing, and RNA silencing deficient mutants show enhanced expression of transposons [142, 160]. As is the case with transgenes, transposons can trigger both post-transcriptional and transcriptional silencing (reviewed by Girard and Hannon [56]).

1.2.2 Transcriptional silencing

Although we only consider post-transcriptional silencing in this thesis, we here shortly summarise a recent review on transcriptional silencing by Grewal and Jia [57]. Transcriptional silencing is the formation of condensed, hetero-chromatic regions in DNA that are inaccessible and not easily transcribed. Transgenes and transposons are known to trigger transcriptional silencing. The key elements Dicer, Argonaute and RDR of the post-transcriptional silencing pathway are also active in the transcriptional silencing pathway. Although the exact variant of Dicer, RDR and Argonaute proteins used in transcriptional silencing differ for different species,

the general process is similar in fungi, plants and animals.

As is the case for post-transcriptional gene silencing, the exact mechanism of how transcriptional silencing is initiated is largely unknown. siRNAs that match the genomic region to be silenced are produced, meaning that an initial dsRNA trigger is cleaved into siRNAs by Dicer. siRNAs associate with Argonaute, and this complex can be used for primed or guided amplification to produce more siRNAs. The Argonaute-siRNA complex alone or associated with other proteins is thought to recruit DNA methyltransferase and chromatin remodelling proteins to the right place, after which hetero-chromatin is assembled. Once a hetero-chromatic region is formed it has to be maintained. A specific RNA polymerase is still able to transcribe hetero-chromatic regions and produces RNA. RDR synthesises dsRNA from this RNA and siRNAs are produced by Dicer. These siRNAs again associate with Argonaute and the hetero-chromatic region is maintained. Additionally, it is possible that siRNAs or the siRNA-AGO complex moves into the cytoplasm to eliminate transcripts that escaped from the nucleus.

1.3 Antiviral silencing

In this thesis we study antiviral silencing in Chapter 3-5. RNA silencing has a very important antiviral role in plants and invertebrates [38, 97, 150]. In antiviral silencing siRNAs are produced that lead to sequence specific degradation of the virus. Viruses encode silencing suppressors that counteract the RNA silencing response. Natural antiviral silencing is most extensively studied in plants.

1.3.1 Virus replication

To understand antiviral silencing, we first have to look into virus replication. All viruses can trigger RNA silencing, and in this thesis we focus on the largest group of plant viruses: plus-strand RNA viruses. The virus enters the cell with packaged plus-strand RNA that is translated using host ribosomes. Most plus-strand RNA viruses encode for one big polyprotein that is autocleaved into functional proteins. All plus-strand RNA viruses encode an RNA-directed RNA polymerase (RdRP, RDR is used for cellular RdRP). RdRP associates with plus-strand RNA and synthesises a complementary minus-strand. The plus- and minus-strand can stay shortly attached to each other, forming double-stranded RNA. When the dsRNA

splits, the plus and the minus-strand can associate with RdRP again. Multiple RdRPs can associate to the minus-strand, a process known as semi-conservative replication. Additionally, RdRP may have a preference to associate with the minus-strand. These processes lead to a production of more plus than minus-strands. This is considered useful for the virus, because plus-strand RNA is used for translation, and is packaged in virions that can move from cell to cell.

Other types of viruses are minus-strand RNA viruses, dsRNA viruses and DNA viruses. All RNA viruses trigger RNA silencing with dsRNA or with hairpins in the folded RNA. DNA viruses do not produce dsRNA and they can only trigger silencing through hairpins in their RNA.

1.3.2 The pathway of antiviral silencing

In Figure 1.2 a schematic presentation of antiviral RNA silencing is shown. The pathway of antiviral silencing is very similar to post-transcriptional transgene induced silencing. Double-stranded siRNAs are cleaved from viral RNA by Dicer. Plants have a number of Dicers, each Dicer is involved in the production of small RNAs from a specific length, or they function in different pathways [12]. siRNAs associate with an Argonaute and one strand is selected: the guide strand. When the siRNA duplex is cleaved from dsRNA it is perfectly complementary and there is a 50% chance that either strand is selected as guide strand. Selection of the plus-strand will lead to a complex targeting the minus-strand and vice versa. Cleavage of dsRNA by Dicer therefore leads to equal ratios of siRNAs targeting the plus- or minus-strand. Equal ratios have been found for several plus-strand RNA viruses [66, 165]. However, ratios strongly biased towards plus-stranded RNAs have also been observed. These siRNAs mapped to hairpins in the viral genome [66, 101]. This means that Dicer can also cleave siRNAs from hairpins. When the siRNA is cleaved from an imperfect hairpin from the plus strand, the selected strand will only match the minus strand. These results indicate that plant Dicers have the ability to target both dsRNA and ssRNA.

The Argonaute-siRNA complex associates with the components of RISC and forms the active RISC complex that is guided to the target RNA by the siRNA. A perfect match leads to cleavage of the target. siRNA produced by direct cleavage from the virus are called primary siRNAs. In addition, siRNAs can be produced by a secondary response through RDR. As with transgene induced silencing, there are three possible modes of amplification: unprimed, primed and guided amplification.

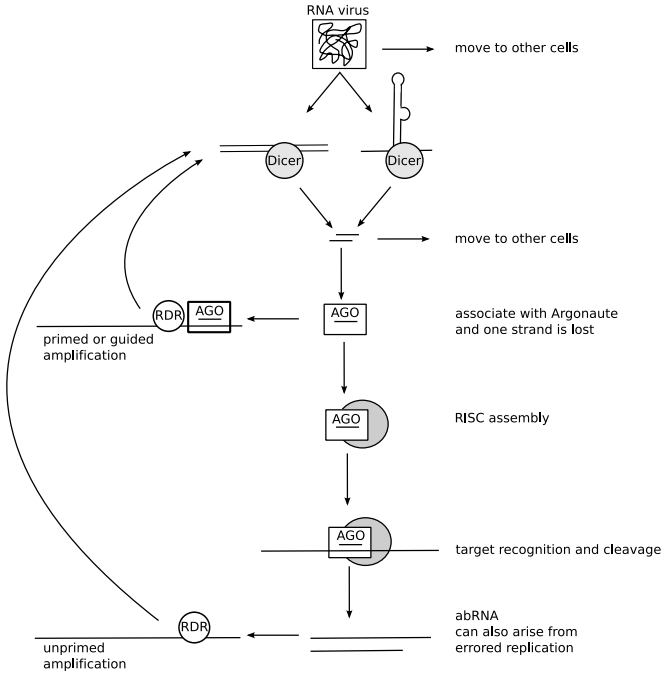

Figure 1.2: A schematic representation of the pathway of antiviral silencing. The virus produces dsRNA during replication, or the viral RNA folds into hairpins. These dsRNA structures are cleaved by Dicer into primary siRNAs. siRNA associates with Argonaute (AGO) and the guide strand is kept in the complex. Multiple proteins assemble with the Argonaute-siRNA complex and form RISC. RISC is guided by the siRNA to the target, that is cleaved. Secondary siRNAs can be produced in an amplification pathway in an unprimed, primed or guided manner.

1.3.3 Silencing suppressors

In Chapter 5 of this thesis we study virus encoded proteins that counter the RNA silencing response. These proteins are called viral suppressors of RNA silencing. Suppressors can target different steps in the silencing pathway.

One widespread strategy is the binding of siRNAs, inhibiting the formation of siRNA-Argonaute complexes and the active RISC. siRNAs can spread from cell-to-cell and siRNA binding can possibly prevent spread of the silencing response. siRNA binding suppressors are present in different virus genera, for example P15 in pecluviruses, γB in hordeiviruses, P21 in closteroviruses, HC-Pro in potyviruses and P19 in tombusviruses [98].

Other virus encoded silencing suppressors can bind all lengths of dsRNA,

and would be able to protect dsRNA from Dicer cleavage in addition to the sequestering of siRNAs [98]. Examples are CP (or P38) of *Turnip crinkle virus* a carmovirus, and P14 of *Pothos latent virus* an Aureusvirus.

The last group of silencing suppressors can interact with Argonaute, namely the 2b suppressor of cucumoviruses and P0 of poleroviruses. P0 has been shown to trigger Argonaute degradation, resulting in a failure in the assembly of active RISC [8, 13]. Additionally, P0 results in a decrease in the number of secondary siRNAs, most likely because an siRNA-AGO complex is needed for primed or guided amplification. Silencing suppressor 2b of cucumoviruses also targets Argonaute. When the suppressor binds to Argonaute it is still able to bind double-stranded siRNAs but is no longer able to 'slice' the passenger strand, making formation of an active RISC complex impossible [169]. Interaction of silencing suppressors with Argonaute also affects host gene regulation by RNA silencing, resulting in severe abnormalities in development [8, 13].

1.4 Other silencing phenomena

1.4.1 Gene regulation by miRNA

Although we do not consider gene regulation by microRNA (miRNA) further in this thesis, here follows a short overview of the discovery of miRNAs and the pathway by which they regulate gene expression. The first evidence of gene regulation by RNA silencing stems from observations in *C. elegans*. The gene *lin-4* was found to encode antisense small RNAs that regulate *lin-14* gene expression [85, 157]. These miRNAs are conserved among eukaryotes and crucial in development [84]. A large difference with the previously discussed RNA silencing mechanisms is that miRNA precursors are encoded in the host genome and transcribed intentionally. The precursors, primary miRNAs, are transcribed in the nucleus and have a specific hairpin-like structure that is recognised by an RNase III (Drosha or Dicer). The RNase produces an double-stranded pre-miRNA of about 70nt long, that is transported into the cytoplasm where it is cleaved by Dicer into the final miRNA. The miRNAs associate with Argonaute and RISC proteins, and guide RISC to the target RNA. In gene regulation the miRNA-RISC complex is also referred to as micro-ribunucleoprotein (miRNP). miRNAs can result in translational repression or degradation of the target [118]. In plants miRNAs are mostly perfectly matched to their target, resulting in degradation, while in animals miRNAs match imperfectly and result in translational repression. In both plants and animals

the number of miRNAs seems to increase for increasing complexity of the organism [83, 159].

miRNAs are expressed in a tissue-specific manner during development, and are crucial for survival, reproduction and brain function in most animals (reviewed in [79]). In plants knockout of Dicer reduces production of miRNAs, and these plants display defects in leaf morphology, flowering time, floral patterning or even die (reviewed in [159]).

1.4.2 piRNAs

siRNA and miRNA are both dependent on Dicer for cleavage to their final size. There are also Dicer-independent small RNAs: piRNAs. piRNAs are cleaved by Piwi proteins, a specific group of Argonaute proteins. piRNAs are somewhat longer than the other small RNAs. piRNAs are, like miRNAs encoded on the genome, and they are involved in silencing of transposons in the germline of animals [78].

1.5 Evolutionary conservation

The RNA silencing pathway has been assembled at the root of the eukaryotic lineage from proteins that stem from different ancestors [135]. The last common ancestor of eukaryotes possessed Argonaute, Dicer and RDR. Although prokaryotes do not posses the RNA silencing pathway, they have an independently evolved homologous mechanism very similar to RNA silencing. It is suggested that RNA silencing was primarily used as a defence mechanism against viruses and transposons, and that the miRNA pathway has evolved later in animals and plants.

1.5.1 Different species

We here discuss the types of RNA silencing observed in different species, because not all eukaryotes are capable of all types of RNA silencing. We split up the eukaryotes in four kingdoms: plants, animals, fungi and protists. The protists are not one monophyletic group, but contain the organisms that do not belong to one of the other groups. We here shortly review silencing phenomena observed in all four kingdoms.

Fungi

The majority of fungi possess the silencing machinery. An early, surprising, observation in this kingdom was that the model organism *Saccharomyces cerevisiae* is incapable of any type of RNA silencing. Pioneering work on RNA silencing in fungi has been done in *Neurospora crassa*. The first type of silencing discovered in *N. crassa* is transgene induced silencing, named quelling. Quelling is dose dependent, only high expression of transgenes triggers silencing [27, 127]. Quelling has been shown to function only post-transcriptionally [26, 50]. Recently it has been shown that RNA silencing also has an antiviral role in fungi [133]. miRNAs have not yet been identified in fungi.

N. crassa possesses two other gene silencing mechanisms that appear to be unrelated to RNA silencing: Repeat Induced Point-mutation (RIP, reviewed in [51]) and Meiotic Silencing of Unpaired DNA (MSUD, reviewed in [136]). RIP detects duplicated sequences in the genome and mutates them. RIP acts only during the sexual cycle and mutated sequences are often targets for DNA methylation. MSUD is a process in which an unpaired gene in meiosis triggers silencing of all homologous sequences.

Fission yeast, *Schizosaccharomyces pombe*, is capable of both transcriptional and post-transcriptional silencing [137], while it has only one copy of Argonaute, RDR and Dicer. Transcriptional silencing of transposons is very well studied in *S. pombe* [171].

Plants

Most work in this thesis will be focused on plant RNA silencing. The main model organisms of this kingdom are the plants *Arabidopsis thaliana* and *Nicotiana benthamiana*, and the green algae *Chlamydomonas reinhardtii*.

Plants are capable of antiviral silencing, transcriptional and post-transcriptional transgene and transposon induced silencing [14]. miRNAs regulate gene expression in plants and both miRNAs and their targets are conserved throughout plant evolution [102, 159]. Interestingly, miRNAs have also been observed in the green alga *C. reinhardtii*, but none of these is present in moss or vascular plants [170]. Green algae are also capable of transcriptional and post-transcriptional transposon induced silencing [18].

RNA silencing in plants has shown to spread over plant tissue, into the phloem and new leaves [153]. This phenomenon, also known as systemic silencing, can prevent spread of viruses into newly developing tissues. Some viruses cannot invade out of the phloem, possibly because RNA silencing

is already active in those tissues [8].

The RNA silencing response in plants is amplified through RDR, this is also known as transitivity. Amplification in plants is bidirectional, meaning that siRNAs are produced both up- and downstream of the initial silencing trigger. Amplification leads to a specific class of siRNAs that seem to play a role in the spread of RNA silencing through the plant [54, 63]. In our models we will simplify by modelling only one type of siRNA that both associates with Argonaute and spread from cell to cell.

Animals

RNA silencing in animals is extensively studied in *C. elegans*, *Drosophila melanogaster* and mouse or human cells. In *C. elegans* and *D. melanogaster* all previously discussed types of RNA silencing are present. Amplification through RDR is not widespread through the animal kingdom and has only been found in *C. elegans* and *Branchiostoma floridae* [155].

Although capable of RNA silencing, the introduction of dsRNA in mammalian cells triggers apoptosis, therefore RNA silencing in mammals cannot be triggered by dsRNA. The introduction of siRNAs does result in RNA silencing [45], and currently many experiments test the ability of siRNA delivery into cells to target viral infection, for example hepatitis B [22]. Additionally, siRNA introduction could be used to treat cancer. However, a number of problems in vivo hinders the development of effective siRNA therapy. Problems are for example efficient targeted delivery, low transfection efficiency, the short half-life of siRNA, and the stimulation of non-specific immune responses [119].

There is, however, increasing evidence that antiviral RNA silencing or miRNAs could be involved in mammalian defence against viruses [34, 80]. For example knockdown of Dicer (both the miRNA producing Drosha and Dicer) increased HIV replication [145].

Protists

In this group RNA silencing has not been so extensively studied as in plants and animals. In the ciliate *Paramecium tetraurelia* dsRNA introduction and high expression of transgenes leads to post-transcriptional silencing [52, 53].
Ciliates have two nuclei: The germ line nucleus is called the micronucleus and is silent during normal cell growth; the macronucleus is transcriptionally active. During sexual reproduction the macronucleus is derived

from the zygotic micronucleus. The ciliate *Tetrahymena thermophila* uses a mechanism very similar to small RNA mediated transcriptional silencing to delete DNA during the transition of micronucleus to macronucleus [164]. Small RNAs are produced that trigger chromatin modifications and finally lead to the deletion of the selected region [91].
The slime mold *Dictyostelium discoidum* also possesses multiple RNA silencing pathways, and is capable of gene regulation through miRNA and transposon silencing [64].

1.5.2 The key proteins of RNA silencing

Although the complete pathway of RNA silencing does not have a prokaryotic ancestor, the key proteins of the RNA silencing pathway have prokaryotic homologs [135]. We here discuss the three key proteins of RNA silencing and their roots.

The Argonautes

One group of essential proteins for RNA silencing is the Argonaute protein family [69]. Argonaute proteins can bind small RNAs and are part of the RNA silencing effector complexes, RISC in post-transcriptional silencing and RITS in transcriptional silencing. Argonautes are also involved in the production of piRNAs. Argonaute proteins can be classified into three groups: Argonaute-like, Piwi-like and the *C. elegans* specific group. Argonaute was first described in *A. thaliana* where leaves from the AGO1 mutant resembled the Argonaute squid (hence the name Argonaute). Piwi was first described in *D. melanogaster*, Piwi mutants developed P-element induced wimpy testis. Argonaute-like and Piwi-like proteins are present in bacteria, archaea and eukaryotes (reviewed in [20]).

Homologs of Argonaute and Piwi have been found both in bacteria and archaea, but the archaeal homologs are more similar to the eukaryotic Argonaute [3]. The original function of Argonaute and Piwi was most likely similar to RNase H endonucleases [93, 167], that degrade RNA in DNA:RNA hybrids (for example to remove RNA primers in DNA replication).

The Argonautes have undergone mechanistic changes from DNA-dependent to RNA-dependent and can now recognise double- or single-stranded RNA and cleave RNA. Within the eukaryotes the number of different Argonaute proteins present varies greatly. Humans have 8 Argonaute proteins, *D. melanogaster* has 5, *A. thaliana* has 10, *S. pombe* has only 1 and *C.*

elegans has 26. *S. cerevisiae* and two parasitic organisms (*Tripanosoma cruzi* and *Leishmania major*) have lost their Argonaute proteins and the other parts of the RNA silencing machinery [147].

Dicer

Dicers are conserved among eukaryotes [107]. They are RNase III large proteins that can have helicase, dsRNA binding, RNase and PAZ (Piwi/Argonaute/Zwille) domains. Interestingly, the RNase III and helicase parts that form Dicer have very different evolutionary backgrounds: RNase III stems from bacterial and the helicase from archaeal roots [135]. The PAZ domain interacts with the 2 nt overhangs of small RNAs.

Protists, fungi, *C. elegans* and vertebrates have only one Dicer, *Drosophila* and mosquito have two, and plants have four Dicer genes. Although plant Dicers are named Dicer-like, plant and animal Dicers appear to be orthologous [20]. In this thesis we will refer to Dicer and Dicer-like as Dicer. Each of the plant Dicers has its own specialised role and handles for example small RNA of a specific length [12]. A recent phylogenetic study suggests that the four plant Dicers are the result of early gene duplication in plants [107]. Although multicellular animals have only one Dicer, they encode another RNase III endonuclease, Drosha, that is used to cleave the primary miRNA encoded in the genome into the pre-miRNA that is transported out of the nucleus. Plants do not encode Drosha and use Dicer-like1 to cleave primary miRNA.

Dicer can interact with Argonaute proteins and recently a conserved binding site in vertebrate Dicers has been identified [129]. The vertebrate binding site binds to all vertebrate Argonautes and the authors suggested that organisms with multiple Dicers will have more specific binding sites to regulate its specific task.

RDR

When RDR was initially detected in plants it was thought that the cellular RDR catalysed viral replication. Now it is known that the opposite is true and that RDR is part of the plant antiviral response. RDRs are used in the secondary RNA silencing response and in synthesis of triggers of RNA silencing. RDRs are not present in *Drosophila* and mammals. However, the widespread occurrence of RDRs in eukaryotes suggests that they were present in the common ancestor of eukaryotes [155], meaning that *Drosophila* and mammals have lost RDR, and therefore the complete secondary

response of RNA silencing. The most likely ancestor of the eukaryotic RDR, are bacteriophage proteins that function as DNA-dependent RNA polymerases [135]. As is the case with the Argonautes, they have evolved in the eukaryotes towards RNA-dependence.

Because no RDR is present in *Drosophila* and mammals, these species are incapable of amplification and transitivity (spreading of silencing beyond the initial trigger).

1.6 Outline of this thesis

In this thesis we use mathematical and computational models to study RNA silencing. We focus on post-transcriptional silencing phenomena induced by highly expressed (trans)genes, the introduction of dsRNA or by virus infection.

The pathways of transgene induced and virus induced silencing are very similar, and make use of the same proteins Dicer, RISC and RDR. To study if this core pathway is able to explain silencing induced by highly expressed transgenes, transposons and dsRNA, we develop a concise mathematical model in **Chapter 2**. We will show that the pathway cannot respond in a dose dependent manner as is necessary for transgene induced silencing. We propose and analyse a few small extensions to the pathway that would allow for a consistent explanation for dsRNA induced silencing, transgene and transposon induced silencing, and avoidance of self-reactivity.

Because natural antiviral silencing is triggered by the presence of a replicating virus, we extend our concise model with viral dynamics in **Chapter 3**. We model a plus-strand RNA virus, because these viruses represent the largest group of plant viruses. The dynamics of antiviral RNA silencing and a virus are complex, because both influence each other. We show that, depending on the strength of the silencing response, different temporal viral growth patterns can occur. Silencing can decrease viral growth, cause oscillations, or clear the virus completely. Our model can explain various observed phenomena, even when they seem contradictory at first: the diverse responses to the removal of RDR; different viral growth curves; and the great diversity in observed siRNA ratios.

Virus infection in plants results in a variety of symptoms. One common symptom is the formation of chlorotic tissue in leaves. Chlorotic and healthy tissue co-occur on a single leaf and form patterns, for example concentric circles or rings, mosaic patterns, vein clearing and spots. It has been suggested that the occurrence of these infection patterns is linked

to the interaction between viruses and RNA silencing. To investigate if RNA silencing can play a role in symptom development we combine our intracellular mathematical model of RNA silencing with a spatial model of plant tissue in **Chapter 4**. We observe that, due to the spread of viruses and the RNA silencing response, different patterns can occur that resemble experimentally observed symptoms on plant leaves.

In **Chapter 5** we complete the circle of RNA silencing and virus growth with the addition of silencing suppressors to the model. We study four types of suppressors and show that some suppressors are more efficient than others. Binding siRNA or dsRNA is always advantageous for intracellular viral growth and viral spread. Targeting Argonaute increases virus levels intracellularly, but can hinder virus spread over the leaf tissue when the binding rate of the suppressor is too low. Although strong binding to Argonaute increases both virus levels and virus spread, siRNA levels are increased, while they are decreased when the suppressor targets siRNA or dsRNA.

CHAPTER 2

The RNA Silencing Pathway: the Bits and Pieces That Matter

Marian Groenenboom, Stan Marée and Paulien Hogeweg
Theoretical Biology/Bioinformatics Group, Utrecht University
Padualaan 8, 3584 CH Utrecht, The Netherlands.

PLoS Comput Biol. 2005, **1(2)**

Abstract

Cellular pathways are generally proposed on the basis of available experimental knowledge. The proposed pathways, however, may be inadequate to describe the phenomena they are supposed to explain. For instance, by means of concise mathematical models we are able to reveal shortcomings in the current description of the pathway of RNA silencing. The silencing pathway operates by cleaving siRNAs from dsRNA. siRNAs can associate with RISC, leading to the degradation of the target mRNA. We propose and analyse a few small extensions to the pathway: a siRNA degrading RNase, primed amplification of aberrant RNA pieces, and cooperation between aberrant RNA to trigger amplification. These extensions allow for a consistent explanation for various types of silencing phenomena, such as virus induced silencing, transgene and transposon induced silencing, and avoidance of self-reactivity, as well as for differences found between species groups.

2.1 Introduction

RNA silencing protects the eukaryotic cell against viruses and transposons. Viruses produce double-stranded RNA (dsRNA) during reproduction, which can trigger the silencing of viral RNA [28, 123]. RNA silencing can also be triggered by a sufficiently high expression of transgenes, a mechanism known as co-suppression or transgene induced silencing [82, 108, 111, 149]. The activation of transgene induced RNA silencing is directly linked to the activity of RNA-dependent RNA polymerase (RDR): overexpression of RDR significantly reduces the number of transgenes needed to induce RNA silencing [49]. RNA silencing deficient mutants show enhanced expression of transposons [142, 160]. Transposons could trigger RNA silencing for two reasons: they often have multiple inverted repeats (IRs) that form dsRNA transcripts [139]; and their high copy number could trigger silencing.

The currently proposed pathway of RNA silencing is shown in Figure 2.1. Generally, the process is initiated by the cleavage of dsRNA by Dicer. Dicer, an RNase III-class enzyme, processes dsRNA into small interfering RNAs (siRNAs) 21-25 nt long. siRNAs can then be incorporated into the RNA induced silencing complex (RISC) and "guide" the complex via antisense base-pairing. This results in cleavage of the target mRNA near the centre of the siRNA. We refer to the aberrant pieces of RNA after cleav-

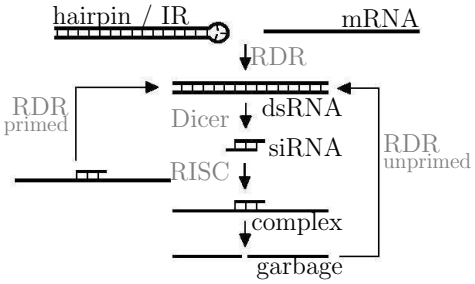

Figure 2.1: The standard pathway of RNA silencing (based on Figure 1 in Hutvágner and Zamore [70]).

age as "garbage RNA". Sijen et al. [138] found that a substantial fraction of the siRNAs in *Caenorhabditis elegans* is not derived directly from the introduced dsRNA. To explain this, two amplification routes have been proposed: primed and unprimed amplification [90, 94, 130]. In both cases RDR synthesises dsRNA: in the case of primed amplification siRNA binds to mRNA to initiate dsRNA synthesis, whereas in the case of unprimed amplification the mere presence of aberrant garbage RNA is sufficient to trigger RDR. In short, the generally accepted pathway of RNA silencing consist of the degradation of mRNA via RISC and an amplification pathway through RDR.

Although it sounds reasonable that such a pathway would suffice to mount responses against both viruses and transposons, we here show that the proposed pathway has severe limitations. We will show that it cannot correctly describe observations on transient and sustained silencing, and dose dependency. Moreover, such a pathway would be extremely vulnerable for mounting responses against self. Finally, we will show that it cannot describe transgene induced silencing at all. We will then propose three different additions to the mechanism: (i) a siRNA degrading RNase; (ii) primed amplification of garbage RNA; and (iii) activation of RDR dependent on the number of garbage RNAs. The proposed models each give a consistent explanation for various types of silencing phenomena, that is, virus induced silencing, transgene and transposon induced silencing, protection against self-reactivity, as well as for differences found between species groups. The extensions, however, do differ in the dynamics they predict, which could be used to experimentally discriminate between them.

2.2 Results

2.2.1 Biological background and description of core model

We study the RNA silencing pathway using concise differential equation models with mass action kinetics. There is strong evidence that there is a common core pathway of RNA silencing present in all organisms capable of RNA silencing. We focus on the experimentally derived common core of RNA silencing (Figure 2.1 and the description in Section 2.1), which is the basis for our model. We directly translate this pathway into a system of four coupled ordinary differential equations,

$$\frac{dM}{dt} = i - d_m M - pM - bSM, \qquad \frac{dD}{dt} = pM - aD,$$
$$\frac{dS}{dt} = anD - d_s S - bSM, \qquad \frac{dG}{dt} = bSM - d_g G,$$

in which M, D, S and G describe the number of mRNA, dsRNA, siRNA and aberrant garbage pieces, respectively. mRNA is transcribed with a rate i and degraded with a rate d_m. dsRNA is synthesised from mRNA by RDR with a small rate p, and is cleaved into n siRNAs with rate a. siRNA can associate with mRNA via RISC with rate b. For simplicity we do not implement the formation of RISC explicitly in our model; instead the siRNA–mRNA complex is directly degraded into aberrant garbage RNA. d_s and d_g describe the degradation of siRNAs and aberrant garbage pieces, respectively.

dsRNA can also enter the pathway in other ways than through RDR: a virus can produce dsRNA; dsRNA can be introduced or injected; or a transcript with IRs can form dsRNA. We simulate the introduction of dsRNA by a stepwise intracellular increase of the amount of dsRNA.

To allow for the formation of secondary siRNAs we extend the model with the two amplification pathways:

$$\frac{dM}{dt} = i - d_m M - pM - bSM - \mathbf{g_2 SM}, \qquad \frac{dD}{dt} = pM - aD + \underline{g_1 G} + \mathbf{g_2 SM},$$
$$\frac{dS}{dt} = anD - d_s S - bSM - \mathbf{g_2 SM}, \qquad \frac{dG}{dt} = bSM - d_g G - \underline{g_1 G},$$

The underlined term $g_1 G$ describes the unprimed amplification: the synthesis of dsRNA from aberrant garbage RNA by RDR; and the bold term $g_2 SM$ describes primed amplification: the synthesis of dsRNA primed by the presence of a siRNA on mRNA. We consider the pathway with and without the amplification terms.

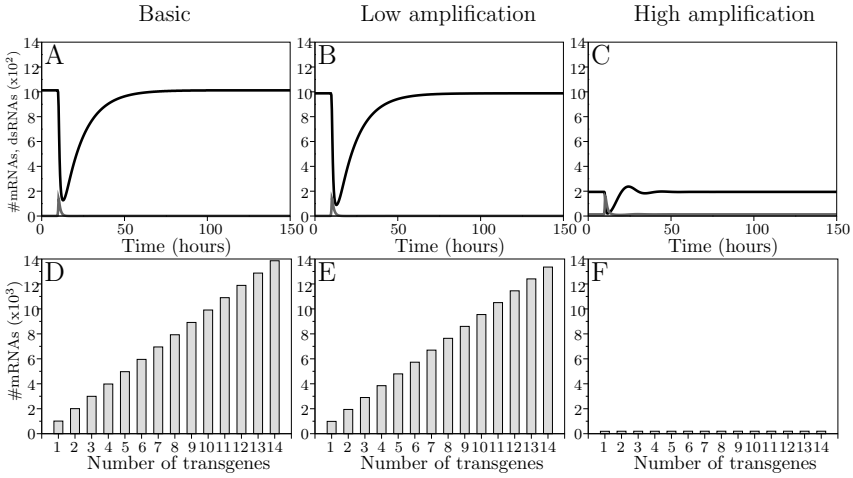

Figure 2.2: Dynamics of the standard models: (A) and (B) show that after dsRNA introduction, only transient responses are possible for the standard model without or with low amplification, whereas (C) shows that with high amplification an arbitrary amount of dsRNA causes sustained silencing. Grey lines indicate dsRNA levels, black lines mRNA levels. (D) and (E) show that an increase in copy number leads to a proportional increase in mRNA levels for the model without or with low amplification, whereas (F) shows that mRNA levels have become independent of copy number in the model with high amplification. RNA levels are expressed in number of molecules per cell. Parameter values can be found in Table 2.1.

2.2.2 Dynamics of core model

The behaviour of the pathway as modelled above is shown in Figure 2.2. The upper panels show the effect of introducing dsRNA, homologous to an endogenous gene. We first study the model without amplification, which should be representative for mammals, in which RDR has not been found [141]. In mammals, dsRNA or siRNAs have to be continuously supplied to keep a gene silenced. In accordance, the model without amplification allows only for transient responses: siRNAs derived from the dsRNA cause a strong decrease in the amount of mRNA, after which the default equilibrium is re-established (Figure 2.2A). Since the system has only one attractor, the cell will always return to this attractor, which is the state with normal levels of mRNA. Only when dsRNA is continuously supplied, the gene stays silenced. Amplification of the response via RDR is observed in nematodes, plants, slime molds and fungi. The dynamics of the core model with primed or unprimed amplification are very similar; we therefore only

show the results obtained for primed amplification. At a low amplification rate the dynamics do not differ from the model without amplification (Figure 2.2B), but at a high amplification rate the default equilibrium becomes unstable, resulting in perpetual silencing (Figure 2.2C). Although the cell will remain in the default state as long as siRNAs and dsRNA are completely absent, a single dsRNA strand or siRNA suffices to trigger silencing.

A model of RNA silencing should also be able to explain transgene induced silencing. We therefore analysed the effect of increasing the number of gene copies. We here assume that each gene copy has the same transcription rate, given by parameter i. In the model without or with a low rate of amplification, an increasing copy number leads to a proportional increase in mRNA levels (Figure 2.2D and E). In contrast, when the amplification rate is high, the amount of mRNA does not depend on the number of gene copies (Figure 2.2F). In this regime, the cell is always in the silenced state, and therefore the amount of mRNA per cell cannot increase. Thus, transgene induced silencing is not possible in the core model, whether or not amplification is taken into account.

2.2.3 Deficiencies of core model

The core model without amplification is capable of explaining only transient responses. In contrast, in plants RNA silencing can be sustained even after removal of the trigger [112, 128], and in *C. elegans* silencing can persist for even more than one generation [48]. Intuitively it seemed plausible that amplification of the response could solve this problem. The core pathway with amplification, however, results in all-or-none type of behaviour: either sustained silencing is impossible, or a single dsRNA strand or siRNA is sufficient to trigger perpetual silencing. This actually means that the dynamics of the core pathway with amplification imply inevitable destruction of self.

This problem of self-destruction has also been observed by Bergstrom et al. [10]. In their model study, they added unidirectional amplification, to obtain a transient silencing response. Amplification in plants, however, can be bidirectional [77], so unidirectionality cannot be the sole mechanism that prevents responses to self. Moreover, although unidirectional amplification can prevent sustained responses, it will not prevent transient responses directed against self, implying the unrealistic scenario of an infinite series of auto-destructive responses.

Another major deficiency of the core pathway is that it cannot describe

or explain transgene induced silencing. Mathematical analysis of the equations shows that the incapability of transgene induced silencing and the all-or-none type of behaviour are inherent properties of the core pathway: the qualitative dynamics do not change when some or all of the mass action terms in the models are replaced by Michaelis-Menten kinetics (see Section 2.4).

We conclude, that to alleviate the limitations discussed above, the core model should be qualitatively altered. A qualitative difference could be either a missing step in the pathway, or some cooperative effect between RNAs. On the other hand, taking, for example, more details of the RISC complex formation into account, would not make the model qualitatively different, and, therefore, the model would still suffer from the same limitations. That is, this model study shows that the core pathway, which is generally presented as being the basic mechanism, with extensions of the pathway simply being (subtle) modifications of it, is essentially incomplete, and can therefore not be considered to be the core of the pathway.

2.2.4 Biological background and description of extended models

We aim to find extensions to the core pathway that are able to provide insight in the type of interactions needed to explain the complexity of RNA silencing. These extended pathways should be able to describe dose dependent responses; the possibility of both transient and sustained responses; transgene or transposon induced silencing; and avoidance of self-reactivity. All extended models need to include at least one of the amplification pathways in order to account for secondary siRNAs and to allow for sustained silencing.

In the first extension we propose that in addition to the non-specific siRNA degradation a specific siRNA degrading RNase with saturating kinetics is involved ("RNase model"). Such a protein has recently been found in *C. elegans* [75]. We assume that the RNase has Michaelis Menten kinetics:

$$\frac{dM}{dt} = i - d_m M - pM - bSM - g2SM, \qquad \frac{dD}{dt} = pM - aD + g2SM,$$
$$\frac{dS}{dt} = anD - \frac{\mathbf{d_r S}}{\mathbf{1} + \mathbf{kS}} - d_s S - bSM - g2SM, \qquad \frac{dG}{dt} = bSM - d_g G.$$

The maximum rate of siRNA degradation by the RNase is given by $\frac{d_r}{k}$. The nonspecific degradation of siRNAs has to be included in the RNase model: since the RNase has a saturated response, the siRNA levels would

go to infinity without this nonspecific degradation.

In our second extension, we generalise the primed amplification process. Whereas in the standard model the process was limited to the amplification of mRNA, we assume here that siRNAs can also bind to garbage mRNA to trigger dsRNA synthesis ("garbage model"):

$$\frac{dM}{dt} = i - d_m M - pM - bSM - g_2 SM, \qquad \frac{dD}{dt} = pM - aD + g_2 SM + \mathbf{g_3 SG},$$
$$\frac{dS}{dt} = anD - d_s S - bSM - g_2 SM - \mathbf{g_3 SG}, \qquad \frac{dG}{dt} = bSM - d_g G - \mathbf{g_3 SG}.$$

The rate of dsRNA synthesis by primed amplification of garbage RNA is given by g_3.

As a third extension we consider a revised unprimed amplification. We explore the possibility that either RDR is activated by the presence of garbage RNA, or that there is another form of cooperation between garbage RNA pieces and RDR. This has been implemented by replacing the mass action unprimed amplification by a sigmoid (unprimed) amplification ("sigmoid model"):

$$\frac{dM}{dt} = i - d_m M - pM - bSM, \qquad \frac{dD}{dt} = pM - aD + \frac{\mathbf{g_1 G^2}}{\mathbf{1 + kG^2}},$$
$$\frac{dS}{dt} = anD - bSM - g2SM, \qquad \frac{dG}{dt} = bSM - d_g G - \frac{\mathbf{g_1 G^2}}{\mathbf{1 + kG^2}}.$$

The maximum rate of unprimed dsRNA synthesis by RDR is given by $\frac{g_1}{k}$.

2.2.5 Dynamics of extended models

The problem with the primed and unprimed amplification in the core pathway is that the number of secondary siRNAs per primary siRNA is basically independent of the initial dose. Consequently, amplification either results in explosion of the reaction, in the case that the number of secondary siRNAs per primary siRNA is larger then one, or the reaction will die out, in the case that the number of secondary siRNAs per primary siRNA is smaller than one. In contrast, in the extended pathways the number of secondary siRNAs becomes dose dependent by introducing a positive feedback into the system. In the RNase model, dose dependency is caused by the saturation of the siRNA degrading RNase: small numbers of siRNAs are rapidly degraded by the enzyme, while at larger numbers the enzyme becomes saturated, which leads to larger amounts of siRNAs. In the garbage and sigmoid model, the cooperation between garbage and siRNAs, and between garbage pieces themselves, respectively,

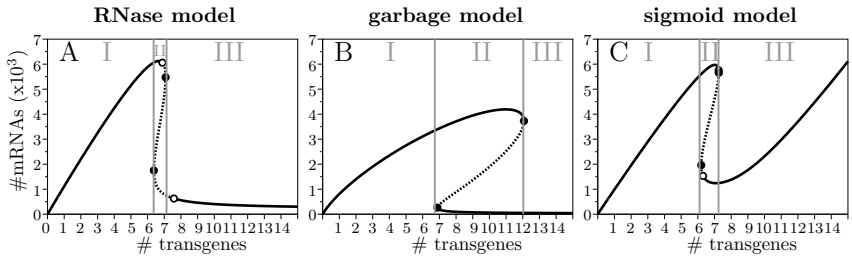

Figure 2.3: Bifurcation diagrams of the extended models showing transgene induced silencing: solid lines indicate stable equilibria; dashed lines unstable equilibria; open circles Hopf bifurcations; and closed circles fold bifurcations. The dynamic behaviours in region I, II and III are shown in Figure 2.4.

lead to dose dependency.

The behaviour of the extended models is more complex than the core model. We can distinguish three main regions of qualitatively different behaviour. One way to switch the system to another qualitatively different behaviour is by changing the number of gene copies present in the cell. The bifurcation diagrams with the three regions for all three extended models are shown in Figure 2.3A, B, and C. Plotted is the equilibrium amount of mRNA against the number of copies of a gene; a stable equilibrium is indicated with a solid line, an unstable with a dashed line. In region I, there is only one attractor: after a perturbation, the system will always return to this attractor. In region II, there are two attractors, and the system can end up in either one of them. In region III, there is again only one attractor. We will first discuss each region separately, with the corresponding types of dsRNA induced silencing, and then we will continue discussing the bifurcation diagram as a whole, to understand the process of transgene induced silencing. In the first region, when there are few copies present, there is only one stable equilibrium. In this default equilibrium, there are low numbers of siRNAs and dsRNA. In this region, mRNA can be silenced transiently by the introduction of homologous dsRNA (Figure 2.4A, B, and C): when dsRNA is introduced, siRNAs derived from dsRNA cause a strong, rapid decrease of the amount of mRNA, after which the default equilibrium is slowly re-established. Transient silencing after dsRNA injection has been observed in nematodes, flies, and zebrafish [76, 88, 103]. Unlike the core pathway, the extended pathways are stable in face of responses against self: a low dose of dsRNA will cause a smaller response than a high dose, and a single dsRNA strand has a negligible effect. This

is due to the fact that the amplification in all extended pathways is flux dependent. It means that as long as the copy number is not too high, a low dose of dsRNA will always result in only a small response, and sustained silencing cannot be triggered.

The second region, with an intermediate copy number, is bistable; that is, there are two attractors: the default state and the silenced state. (There is a third equilibrium, which is of the saddle type. The stable manifold of the saddle separates the basins of attraction of the two stable equilibria.) When starting in the default state (dsRNA and siRNAs are almost completely absent), the introduction of a small dose of dsRNA will cause a transient silencing response, after which the default equilibrium is re-established (see Figure 2.4D, E, and F, dashed lines). A high dose of dsRNA, however, can bring the system from the default equilibrium into the basin of attraction of the silenced equilibrium, which means that sustained silencing is triggered (Figure 2.4D, E, and F, solid lines). Sustained silencing has been demonstrated in *C. elegans*, where silencing can persist and even be transmitted to the next generation [48]. Also in plants infected with a virus carrying a gene homologous to a plant gene, silencing of the endogenous gene persists even after removal of the virus [128]. The silencing response in plants can also be transmitted via grafting with very high efficiency from silenced stocks to non-silenced stocks [112].

The existence of two attractors prevents undesired sustained responses: only when the amount of dsRNA exceeds a threshold value is the sustained response mounted. Unfortunately, until now few experiments have focused on the correlation between the dsRNA dose and the duration of the silencing response. Lipardi et al. [90] showed that in *Drosophila* embryo extract, doses below a threshold concentration failed to induce RNA silencing, while ten times higher doses were able to trigger silencing. This study indicates the existence of a threshold; the duration of the response, however, has not been investigated. The results of Li et al. [88] also indicate the existence of a threshold: they showed that in zebrafish (*Danio rerio*) embryos small doses of dsRNA lead to partial phenotypic changes only, while high doses of dsRNA lead to more than 50% partial and 35% full phenotypic changes. The partial phenotypic effects could indicate that there was only a transient response in the embryos, while the full phenotypic changes triggered by a high dose of dsRNA could indicate a sustained response.

In the garbage model, the amounts of mRNA, dsRNA, and siRNAs are stable in both attractors, but in the RNase and the sigmoid model,

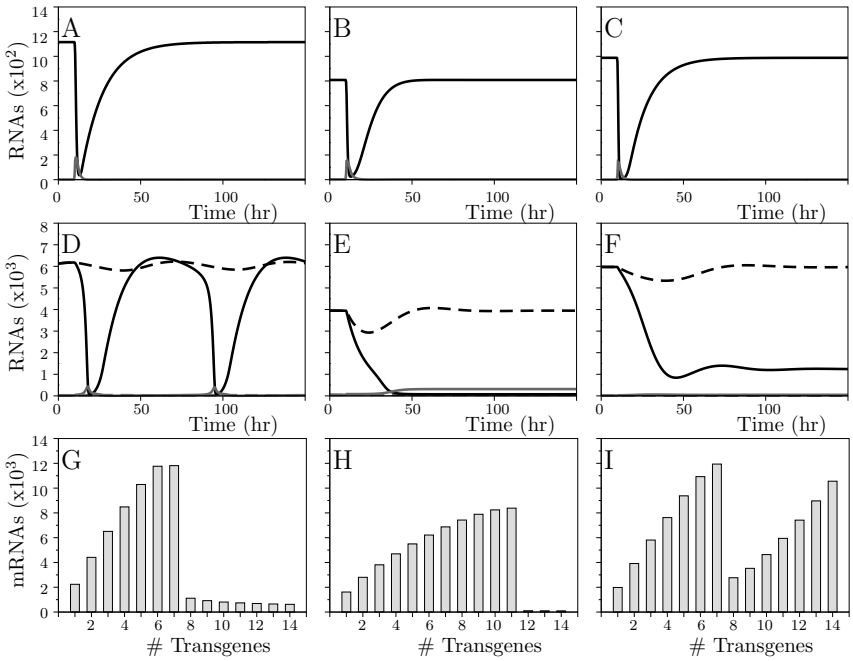

Figure 2.4: Dynamics of the proposed models. Grey lines indicate dsRNA levels, black lines mRNA levels. A, B and C show transient silencing after dsRNA introduction in the RNase, garbage and sigmoid model, respectively. D, E and F show timeplots of the behaviour in the bistable region after introduction dsRNA: a low dose has only a small effect (dashed lines), but a high dose of dsRNA causes sustained silencing, or, in the RNase model, large oscillations (solid lines). G, H and I show bar graphs of transgene induced silencing, in the RNase, garbage and sigmoid model, respectively. Parameter values can be found in Table 2.1.

oscillations can occur in this region. The oscillations around the default equilibrium are always of small amplitude, but around the silenced equilibrium they can become large. The region with oscillations is much smaller in the sigmoid model than in the RNase model. We therefore show dynamics with oscillations for the RNase model and without oscillations for the sigmoid model (Figure 2.4D and F, respectively).

Finally, in the third region, with a high copy number, only the silenced state, with low levels of mRNA and high levels of siRNAs, is stable. The introduction of additional dsRNA will have only a small effect on the already largely reduced amount of mRNA. When a gene is present at very high copy numbers, its mRNA will be silenced continuously.

Technically, the transitions between the regions can be characterised

by different bifurcations. In the garbage model, the default state and the silenced state disappear due to fold bifurcations (Figure 2.3, closed circles) when the number of transgenes is respectively increased or decreased. In the other two models, shortly before the fold bifurcations the equilibria become unstable due to Hopf bifurcations (Figure 2.3, open circles), which leads to oscillatory behaviour around the equilibria. These oscillations then disappear due to homoclinic connection bifurcations. When, by changing the number of transgenes, a fold or homoclinic connection bifurcation is passed, the dynamics immediately jump to the other equilibrium (or around it, in the case that there are oscillations).

The bifurcation diagram depicts the process of transgene induced silencing. In Figure 2.4G, H, and I we plot bar graphs, where each bar indicates the equilibrium amount of mRNA for a certain number of gene copies, to compare our results to the graphs obtained experimentally in *Drosophila* by Pal-Bhadra et al. [111]. They inserted one to ten copies of a full *Adh* transgene using different insertion sites. Stocks with the same copy number showed similar mRNA levels, independent of where the genes were inserted into the genome. One copy resulted in a normal amount of mRNA, while up to five copies, an extra copy resulted in a proportional increase in mRNA levels. However, when a sixth copy was inserted, RNA silencing was triggered, indicated by the presence of siRNAs, and dramatically decreased mRNA levels. At even higher copy numbers, the amount of mRNA was lying around the amount expected for one or two copies only. The bar graphs we obtained with our models are in close correspondence: the amount of mRNA in the cell initially increases with increasing numbers of transgenes; however, when the number of transgenes is increased beyond a threshold level, RNA silencing is triggered.

2.2.6 Parameters dependence and predictions

There is only a limited amount of experimentally measured parameters available, which are generally obtained for different model organisms. Moreover, the range of measured values can often be very large. We, therefore, do not focus on specific parameter values, but instead use mean values to show the qualitative dynamics. We then vary the parameter values and infer what kind of qualitative and quantitative changes are to be expected to accompany such parameter changes. When data are available, we compare these model predictions with experiments in which specific parameters have been varied.

Table 2.1: Parameter values used in the models (mol^{-1} means per molecule). The default values used for the basic model are also used for the extensions, except when indicated otherwise.

Model	Par.	Meaning	Value	Units
Core	d_m	decay rate mRNA	0.14	hr^{-1} (half-life 5 hr) [1]
	d_s	decay rate siRNA	2	hr^{-1} (half-life 21 min)[2]
	d_g	decay rate garbage RNA	2.8	hr^{-1} (half-life 15 min)
	i	transcription rate mRNA	160	hr^{-1} $cell^{-1}$
	p	rate of dsRNA synthesis from mRNA	0.002	hr^{-1}
	a	rate of dsRNA cleavage by Dicer	2	hr^{-1}
	n	number of siRNAs cleaved from one dsRNA	10	
	b	rate of siRNA–mRNA complex formation	0.008	cell $mol^{-1}hr^{-1}$
Unprimed	g_1	unprimed ampl. rate	0.02	hr^{-1} (low)
			0.4	hr^{-1} (high)
Primed	g_2	primed amplification rate	0.0002	cell mol^{-1} hr^{-1} (low)
			0.002	cell mol^{-1} hr^{-1} (high)
RNase	d_r	degradation rate	160	hr^{-1}
	k	saturation constant	0.2	cell mol^{-1}
Garbage	g_2	primed amplification rate	0.0008	cell mol^{-1} hr^{-1}
	g_3	primed amplification rate of garbage	0.0008	cell mol^{-1} hr^{-1}
Sigmoid	g_1	unprimed amplification rate	0.002	cell $mol^{-1}hr^{-1}$
	k	saturation constant	0.00001	$cell^2$ mol^{-2}
	b	rate of siRNA–mRNA complex formation	0.04	cell mol^{-1} hr^{-1}

[1] mRNA half-lives vary greatly between different species. Yeast mRNA half-lives vary from minutes to 1.5 hours [154]. In humans the median half-life is 10 hours [162], and there are mRNAs which are stable for more than 24 hours. Plant mRNA half-lives vary from less than one hour to several days, with an average of several hours [144].

[2] We here take siRNA half-life to be 21 minutes, as is measured in human cells [23].

The default parameters are given in Table 2.1. We assumed stable mRNA (half-life 5 h), a 20x faster decay of garbage pieces (half-life 15 min), and slightly more stable siRNAs (half-life 21 min, as measured in human cells [23])). The other parameters are chosen such as to depict the full capabilities of the models.

We distinguish five types of qualitatively different effects that can be caused by changing parameter values (Figure 2.5). The changes in behaviour can be described in terms of the threshold, which is the number of

transgenes needed to trigger silencing; and in terms of the bistable point, which is the lower bound of the bistable region. Note that in the sigmoid model, the amount of mRNA in the cell always increases again at high copy numbers.

Type I behaviour occurs in the garbage model when changing parameters n, b and g, and in all three models when changing p. Changing these parameters does not influence the bistable point (that is, the value above which sustained silencing can be triggered), but moves the threshold to different copy number and mRNA levels. This means that the size of the bistable region changes: when the threshold is lower than the bistable point there is no bistable region, and transgene silencing is triggered at low copy numbers. When the threshold becomes very high the bistable region is very large: only a very high copy number triggers silencing, while sustained silencing triggered by the introduction of dsRNA becomes possible in a large region.

Type II behaviour is typical for the RNase and sigmoid model. In both models changes in the parameters n, b, $g_{1,2}$ and k result in type II behaviour; as well as d_r in the RNase model; and d_g in the sigmoid model. Parameter changes move the bistable point and the threshold in the following manner: a low threshold coincides with an even lower bistable point; a high threshold with an even higher bistable point. This means that, in contrast to type I behaviour, the bistable region disappears when the threshold is high, and sustained silencing becomes impossible. In the sigmoid model also the possibility of transgene induced silencing disappears, since there is no noticeable decrease in mRNA levels beyond the threshold. In the RNase model this is not the case: mRNA levels will always decrease with sufficiently high copy number, although this point sometimes lies outside of the graphs in Figure 2.5.

Type III behaviour occurs for changes in d_m in all three models. In this case the threshold moves to different copy numbers, but the amount of mRNA at the threshold remains the same. Instead the initial slope of the mRNA level changes. The bistable point is not affected, and since the threshold moves, the bistable region can increase or decrease in size (and even disappear).

Type IV behaviour is typical for changes in d_s and d_g in the garbage model. These parameters scale the complete bifurcation diagram.

Type V behaviour occurs in the RNase and the sigmoid model for changes in d_s. In this case, the only thing that changes, is the amount of mRNA just after transgene silencing is triggered.

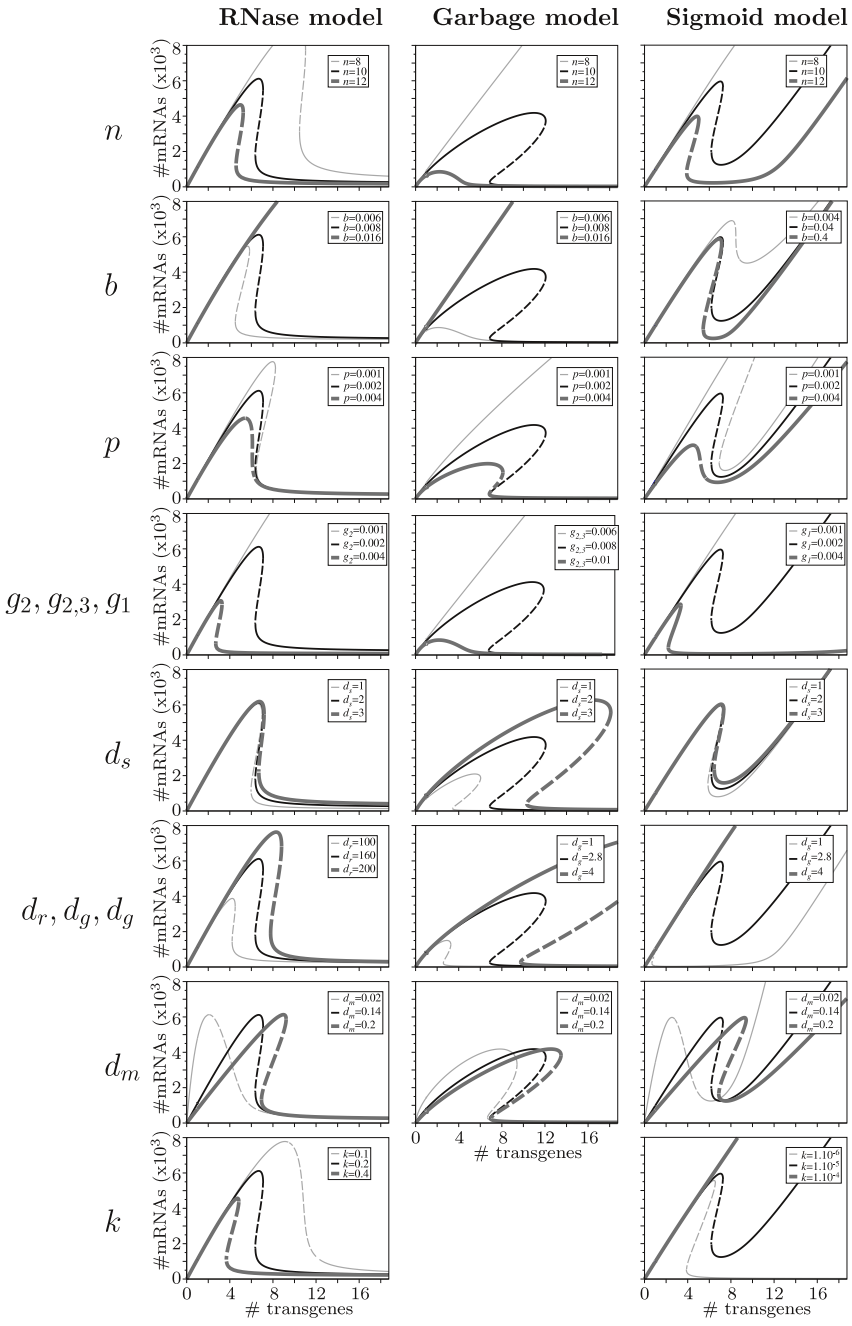

Figure 2.5: Changes in the Bifurcation Diagrams of Figure 2.3 due to changing parameter values. The black lines indicate the standard parameter values, the thin light grey lines a lower value, and the bold dark grey lines a higher value for the corresponding parameter.

Changes in the threshold value of gene copies have been experimentally observed. Several studies suggest that the amount of transcribed mRNA plays an important role in the ability of transcripts to trigger transgene induced silencing. When a transgene is under control of a 35S promoter with a double enhancer, the gene is transcribed at such a high rate that a single transgene can be sufficient to trigger silencing [47]. Also in petunia the strength of the promoter correlated with the frequency and degree of silencing [122], and plants homozygous for a transgene are much more often silenced than hemizygous plants [33, 36, 40, 72, 113, 122]

These observations are consistent with our models: when a gene is more highly expressed (in our models described by a higher value of i, the transcription rate), less copies are needed to trigger silencing. This is because changing i effectively rescales the x-axis of the bifurcation diagrams.

Our models suggest that the amount of dsRNA per mRNA is a major factor determining the threshold. When more dsRNA per mRNA is produced, the threshold to trigger transgene silencing will be lower. For example, an increase in the parameter p, the rate of dsRNA synthesis by RDR, results in all models in a decrease of the threshold. An increase in amplification (g) will have a similar effect. Our results are in line with experimental observations: Forrest et al. [49] showed that in strains which overexpressed RDR, the number of transgenes required to induce silencing is decreased. Likewise, transcripts with tandem IRs, which produce much more dsRNA per mRNA, have shown to be very efficient inducers of RNA silencing [125, 139]. Finally, transposons often contain long IRs and are present in high copy numbers, both of which we have shown to induce silencing.

These experimental results are consistent with our models, but they do not make it possible to distinguish between them. Instead, we need experiments in which certain specific parameters are varied. For example, the models predict a completely different effect of the overexpression of RISC (all its components have to be overexpressed). In the garbage and RNase model, RISC overexpression leads to an increase and ultimately disappearance of the threshold. In the sigmoid model, we find the complete opposite: the disappearance of the threshold is not caused by RISC overexpression, but by RISC underexpression (Figure 2.5).

2.3 Discussion

The extended models each provide a unified framework for different RNA silencing phenomena. They provide consistent explanations for (i) dose dependent dsRNA induced silencing; (ii) stability against self-directed responses; (iii) the dependence of transgene induced silencing on RDR; (iv) the effect of IRs; (v) multiple copies; (vi) efficient promoters; and (vii) the ability of transposons to trigger silencing.

Previously it has been proposed that transgene induced silencing is triggered only if the number of transgenes exceeds a threshold level [33, 72, 82, 111, 113]. It has also been observed that the overexpression of RDR reduces the threshold [49]. Our models support the threshold hypothesis and give a mechanistic explanation for it: we propose that the amount of dsRNA per transcript matters.

The extensions also explain differences in RNA silencing phenomena in different species groups. According to our extended models, in organisms that have RDR homolog(s), like plants, fungi, nematodes and cellular slime molds, silencing can be induced by transgenes, inverted repeats, transposons and dsRNA. In contrast, we have shown here that organisms without RDR are unable to trigger transgene induced silencing. Accordingly, experiments have shown that plants with a mutation in RDR are no longer able to bring about transgene induced silencing, while virus (dsRNA) induced silencing is still possible in these strains [31]. The presence of an RDR in *Drosophila* is currently disputed. Some experiments strongly suggest the presence in *Drosophila* of an RDR or a protein that functions as an RDR [90, 111, 156]. Other experiments, however, argue against the presence of such an enzyme (a BLAST search, for example, does not yield an RDR homolog) [19, 126, 168]. Since high transgene numbers (without IRs) are capable of inducing RNA silencing in *Drosophila*, our model suggests that a protein with the same function as RDR must be present. Mammals lack RDR, and in agreement with our models, they are capable of only transient silencing induced by siRNAs [17] (in mammals dsRNA triggers several non-specific responses [25, 120]; sustained silencing in mammals can only be accomplished by continuous expression of siRNAs).

We did not include the effect of siRNAs on DNA chromatin, which is referred to as transcriptional silencing or heterochromatinisation. Transcriptional silencing plays a role in transposon silencing [61, 74, 100, 105]. Nolan et al. [109], however, recently showed that in the fungus *Neurospora crassa* the LINE1-like transposon, *Tad*, is post-transcriptionally silenced and not significantly methylated, indicating that transposon induced si-

lencing in *N. crassa* can be independent of DNA methylation. Also in *Drosophila* transgene induced silencing has been shown to be solely post-transcriptional [111]. Although heterochromatinization can play an important role in transposon silencing, our model study indicates that the addition of heterochromatinization alone, i.e. the stop in transcription, to the core pathway will not make transgene silencing possible. Heterochromatinisation will only decrease mRNA transcription, and does not provide the necessary positive feedback.

Although it has been shown recently that RISC can perform multiple rounds of cleavage [60], we assume only one cleavage per RISC complex. Adding multiple turnover of RISC, however, does not affect the qualitative behaviour of the model (unpublished data).

We proposed three different additions to the pathway. We here suggest some ways of testing or rejecting experimentally the predictions made by the different extensions. In the parameter section, we have already discussed the different behaviour of the sigmoid model when RISC is overexpressed. Another difference is that only in the sigmoid model, after silencing is triggered, even higher copy numbers will cause an increase in mRNA levels again. Such an increase, however, can also indicate other sigmoid responses in the pathway, for example in Dicer or RISC. Sigmoid kinetics alone are not able to allow for low mRNA levels when copy numbers become very large. It can be argued, however, that a combination of heterochromatinization with a sigmoid response will be able to keep mRNA levels silenced.

Recently, a siRNA degrading RNase has been found in *C. elegans* [75]. The pathway with the siRNA degrading RNase, however, is able to cause transgene silencing only when it degrades siRNAs very rapidly and when it saturates quickly. In fact, even when this is the case, this pathway only limitedly allows for sustained RNA silencing, because the parameter range for sustained silencing is very small. We would like to see experiments that focus on the correlation between the dose of dsRNA and the duration of the silencing response. Such experiments will give insights into the existence of a positive feedback and will show if there is a bistable region. The next step would be to investigate the dependence of both the threshold and the size of the bistable region on gene copy numbers, and how this depends on changes in parameters. These observations can then be compared with the dependencies predicted in the parameter section.

The garbage model could be tested by investigating the possibility of siRNAs to serve as primers for RDR on aberrant garbage pieces. When

that is possible, we expect that this primed amplification of garbage is a missing step in the RNA silencing pathway. It represents only a small addition to the currently known pathway, but it has a large impact on the dynamics, making transgene and transposon silencing, as well as dose dependent sustained silencing, possible for a wide range of parameters. Therefore, we conclude that in RNA silencing it is "the bits and pieces" that matter.

2.4 Materials and Methods

Mathematical proof of limitations of core pathway

In this section we prove that the core pathway, with or without amplification, is incapable of transgene induced silencing and sustained silencing.

In transgene induced silencing the amount of mRNA in the cell initially increases when the number of transgenes is increased, but a further increase in the number of transgenes leads to a sudden drop in the equilibrium amount of mRNA, due to RNA silencing [111]. This implies that two different copy numbers can lead to exactly the same equilibrium amount of mRNA (see Figure 3 or Figure 1 in Pal-Bhadra et al. [111]). We refer to the equilibrium for a low copy number as the default state, and to the equilibrium for a high copy number as the silenced state. Despite the high transcription of mRNA, in the silenced state the amount of mRNA remains low, due to the high levels of dsRNA and siRNAs which are present. Consequently, when it would be possible to keep the amount of mRNA in the cell constant (cf. patch clamp techniques in neuroscience), there should exist mRNA levels for which there are at least two stable equilibria in the system, each with a different amount of dsRNA. Mathematically, this requirement can be studied by considering the variable M as a fixed parameter m. Then for a certain interval of values of m there should exist at least two stable equilibria, which implies the existence of at least three equilibria, since one equilibrium will be unstable. We here will show that the previously proposed pathway cannot fulfil this requirement, and consequently is not able to describe and explain transgene induced silencing.

The requirement is analysed by studying the equilibrium dsRNA (D) level. Without amplification the dsRNA dynamics consist of two parts only: a positive influx (pm) and a decay by Dicer (aD). In Figure 2.6 we depict the influx and breakdown of D as a function of D. To obtain an equilibrium the influx should balance the breakdown, that is, the depicted lines should cross. Hence, without amplification there will be one equilib-

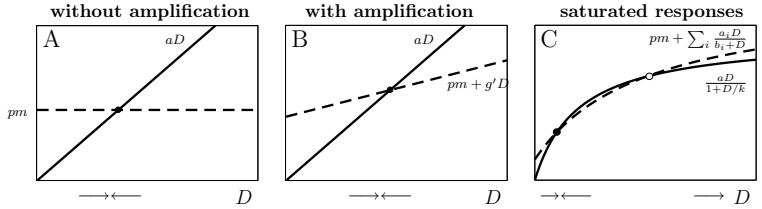

Figure 2.6: Equilibrium analysis of the models based on the previously proposed pathway. Transgene induced silencing requires the existence of two stable equilibria with different dsRNA (D) levels for one fixed value of mRNA (m). Shown here are the influx (dashed line) and breakdown (solid line) of D as a function of D. Equilibria are found when influx balances breakdown, i.e. where these lines cross. Both without and with amplification there exists only one stable equilibrium; when mass action terms are replaced by saturated responses, there can be zero, one or two equilibria, of which at most one is stable. The pathway is therefore unable to describe transgene induced silencing.

rium only (Figure 2.6). Thus, each gene copy number leads to a unique mRNA level, it can therefore only be the case that the equilibrium mRNA level monotonically rises with increasing transgene copy number (Figure 2.2D). The addition of either primed or unprimed amplification does not allow for an increase in the number of stable equilibria. This can be derived by solving for equilibria by means of putting both dS/dt and dG/dt to zero:

$$\frac{dS}{dt} = 0 \quad \Rightarrow \quad S = \frac{anD}{d_s + bm + g_2 m} = qD \qquad (\text{where } q = \frac{an}{d_s + bm + g_2 m})$$

$$\frac{dG}{dt} = 0 \quad \Rightarrow \quad G = \frac{bmS}{d_g + g_1} = \frac{bmqD}{d_g + g_1} = q'D \quad (\text{where } q' = \frac{bmq}{d_g + g_1})$$

This means that the amplification terms can be written as a linear function of D, which can never result in more than one stable equilibrium (see Figure 2.6B):

$$g_1 G + g_2 mS = g_1 q'D + g_2 mqD = g'D \qquad (\text{where } g' = g_1 q' + g_2 mq)$$

When mass-action terms are replaced by Michaelis Menten kinetics, the amplification can be rewritten as a sum of saturated responses as well: $\sum_i \frac{a_i D}{b_i + D}$. When the breakdown is not saturated, this still trivially leads to one equilibrium only. However, when breakdown by Dicer shows a saturated response, more than one equilibrium can be found (but also no equilibria, in the case that the saturation is very rapid). To allow for at least two stable equilibria, the line $g(D) = pm + \sum_i \frac{a_i D}{b_i + D}$ should cross the line $f(D) = \frac{aD}{1 + D/k}$ at least three times, because a second equilibrium will

always be unstable. (Note that since in this analysis m can be treated as a constant, the term pm could as well have a more complicated -for example, saturated- dependency on m.) This, however, is never possible. The model can be rescaled to $f(D) = \frac{D}{1+D}$. Consider the ratio of both functions:

$$R(D) = \frac{g(D)}{f(D)} = \frac{pm}{D} + pm + \sum_i \frac{a_i(1+D)}{b_i+D}$$

Equilibria are found when $R(D) = 1$; to obtain three equilibria the derivative of $R(D)$ should have at least two roots:

$$\frac{dR}{dD} = -\frac{pm}{D^2} + \sum_i \frac{a_i(b_i-1)}{(b_i+D)^2} = 0$$

$$\sum_i \frac{a_i(b_i-1)}{(b_i+D)^2} = \frac{pm}{D^2}$$

However, by multiplying both sides with the monotonically increasing function $(1+D)^2$, it can be shown that there is at most one root, since the left hand side is a monotonically increasing function of D:

$$\frac{d(\sum_i \frac{a_i(b_i-1)(1+D)^2}{(b_i+D)^2})}{dD} = \sum_i \frac{2a_i(b_i-1)^2(1+D)}{(b_i+D)^3} \geq 0 \qquad \text{(for all } D \geq 0)$$

while the right hand side is a monotonically decreasing function:

$$\frac{d(\frac{pm(1+D)^2}{D^2})}{dD} = -\frac{2(1+D)}{D^3} < 0 \qquad \text{(for all } D \geq 0)$$

Consequently, dR/dD has only one root, and there will be at most two equilibria, from which at most one is stable (Figure 2.6C). Thus, in the previously proposed pathway transgene induced silencing is impossible.

Likewise, model dynamics describing sustained responses require multiple steady states for a unique set of parameters. This requirement is implicitly equivalent to the previous one, since the existence of a second stable equilibrium (with a lower mRNA level) automatically implies that the same equilibrium mRNA level can be found for a lower transgene copy number. That is, the previously proposed pathway can neither describe or explain transgene induced silencing, nor sustained silencing triggered by injecting dsRNA.

Programs used

The timeplots in Figure 2.2 and 2.3 are produced with GRIND, a computer program for the study of differential equation models by means of numerical integration, steady state analysis, and phase space analysis (*http://theory.bio.uu.nl/rdb/software.htm*). The bifurcation diagrams are produced with CONTENT, an integrated environment for bifurcation analysis of dynamical systems (*http://www.math.uu.nl/people/kuznet/CONTENT/*).

Acknowledgements

We thank M. van Hoek and T. Sijen for helpful comments on the manuscript. This research was funded by the Netherlands Organisation for Scientific Research (NWO) through grant number 050.50.202 of the Bio-Molecular Informatics program.

CHAPTER 3

The dynamics and efficacy of antiviral RNA silencing: a model study

Marian Groenenboom and Paulien Hogeweg
Theoretical Biology/Bioinformatics Group, Utrecht University
Padualaan 8, 3584 CH Utrecht, The Netherlands.

BMC Systems Biology 2008, **2**:28

Abstract

Mathematical modelling is important to provide insight in the complicated pathway of RNA silencing. RNA silencing is an RNA based mechanism that is widely used by eukaryotes to fight viruses, and to control gene expression. We here present the first mathematical model that combines viral growth with RNA silencing. The model involves a plus-strand RNA virus that replicates through a double-strand RNA intermediate. The model of the RNA silencing pathway consists of cleavage of viral RNA into siRNA by Dicer, target cleavage of viral RNA via the RISC complex, and a secondary response. We found that, depending on the strength of the silencing response, different viral growth patterns can occur. Silencing can decrease viral growth, cause oscillations, or clear the virus completely. Our model can explain various observed phenomena, even when they seem contradictory at first: the diverse responses to the removal of RNA-dependent RNA polymerase; different viral growth curves; and the great diversity in observed siRNA ratios. The model presented here is an important step in the understanding of the natural functioning of RNA silencing in viral infections.

3.1 Introduction

RNA silencing is an evolutionary conserved regulation system and has an antiviral role in plants and some animals [38, 97, 150]. The key mediators of RNA silencing are small RNAs [61, 62], that are cleaved from stem loop RNA or long stretches of double-strand RNA (dsRNA) by the enzyme Dicer [11, 48]. The general view is that in antiviral silencing small interfering RNAs (siRNAs) are cleaved from long stretches of dsRNA, that are produced by the virus as intermediates in replication. The double-stranded siRNA associates with the protein complex RISC. The siRNA strand with the 5' lowest stability is selected to guide the RISC complex to the target. The siRNA-RISC complex cleaves the target and will stay intact to continue to the next target [60, 115]. However, the long stretches of dsRNA that are formed during replication may not be accessible for Dicer [1], and recently it has been suggested that viral single-strand RNA (ssRNA) is cleaved into siRNAs [101].

In the primary silencing response siRNA is cleaved directly from viral RNA. In addition, in plants there can be a secondary response in which host encoded RNA-dependent RNA polymerase (RDR) creates dsRNA

that can be cleaved into one or more siRNAs.

We here present the first model study that combines viral growth with RNA silencing. Previous models focused either on virus dynamics or on RNA silencing separately, or on direct siRNA delivery for clinical applications of RNA silencing [5, 10, 30, 59, 124].

Previously we modelled the RNA silencing pathway and investigated the ability of RNA silencing to silence endogenous genes, transposons and dsRNA, and the role of the primary and secondary response in these cases [59]. Antiviral silencing differs from these processes, because the virus itself is replicating. We here model a replicating plus-strand RNA virus, and we extend our model of the silencing pathway with the kinetics of RISC, siRNA loaded RISC, Dicer and RDR, since we expect that the ability of the pathway to silence viruses will strongly depend on these proteins.

We study virus induced RNA silencing and its efficacy to reduce viral infections in a single compartment system. We find that RNA silencing can alter viral growth in five qualitatively different ways, and we compare the behaviour in these regions to experimentally observed growth curves. We investigate the effect of different Dicer cleavage modes, and the impact of the secondary response. Lastly, we vary Dicer single- and double-strand cleavage rates and find that our model provides an explanation for the wide range of observed siRNA ratios.

3.2 Methods

In short, the model consists of the following processes: The virus replicates itself through dsRNA, that is produced via virus encoded RNA-dependent RNA polymerase (RdRP). Viral double- or single-strand RNA is degraded by host encoded Dicer into siRNAs, that have a plus- or minus-strand polarity. Via RISC the siRNAs cause degradation of either viral plus- or minus-strand RNA. In addition, siRNAs can be synthesised through the secondary pathway that involves synthesis of dsRNA by host encoded RDR. The model of the primary pathway can apply to both plants and animals, the model with secondary pathways applies to plants only [132]. We build up the mathematical model in a stepwise manner, starting with a model of viral replication. We then expand the model with the primary and finally the secondary silencing pathway. Each equation of the full model will consist of viral replication ($\mathcal{V}$), the primary ($\mathcal{P}$) and the secondary pathway. At the end of each equation we define $\mathcal{V}$ and $\mathcal{P}$.

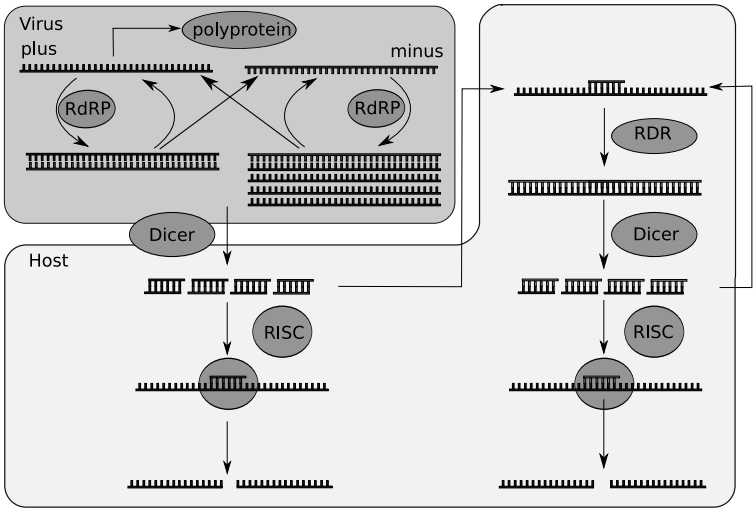

Figure 3.1: Schematic representation of plus-strand RNA virus replication (dark box) and the RNA silencing pathway (light box). Viral plus- and minus-strand RNA is replicated by RdRP, including semi conservative synthesis of multiple plus strands from a single minus-strand template. The formed dsRNA dissociates into single-strand RNA. Viral single- and double-stranded RNA can be cleaved by Dicer into siRNA. siRNA associates with RISC and cleaves the target RNA. siRNAs can guide or prime amplification of the response through host encoded RDR, or viral ssRNA is amplified in an unprimed manner. The primary pathway is shown on the left, the secondary on the right.

3.2.1 Model description: Viral replication

In plants the majority of viruses are plus-strand RNA viruses, that replicate via viral encoded RdRP. Our model of viral replication is based on the replication cycle shown in the box "Virus" in Figure 3.1.

$$\text{RdRP} \quad \frac{dR}{dt} = \frac{rP}{(P+k_t)} - d_r R + h(D_p + R_a) - \{o(1-f)P + ofM + o_d D_m\}\mathcal{F} \equiv \mathcal{V}_r \tag{3.1}$$

$$\text{+RNA} \quad \frac{dP}{dt} = -o(1-f)P\mathcal{F} + hD_p + hR_a - dP - \frac{vP^5}{k_v^5 + P^5} \equiv \mathcal{V}_p \tag{3.2}$$

$$\text{−RNA} \quad \frac{dM}{dt} = -ofM\mathcal{F} + hD_p - dM + hD_m(1 - \frac{1}{D_m})^{(R_a - D_m)} \equiv \mathcal{V}_m \tag{3.3}$$

$$\text{Virions} \quad \frac{dV}{dt} = \frac{vP^5}{k_v^5 + P^5} \equiv \mathcal{V}_v \tag{3.4}$$

$$\text{dsRNA} \qquad \frac{dD_p}{dt} = o(1-f)P\mathcal{F} - hD_p \equiv \mathcal{V}_{dp} \tag{3.5}$$

$$\text{dsRNA} \qquad \frac{dD_m}{dt} = ofM\mathcal{F} - hD_m(1-\frac{1}{D_m})^{(R_a-D_m)} \equiv \mathcal{V}_{dm} \tag{3.6}$$

$$\text{act.RdRP} \qquad \frac{dR_a}{dt} = ofM\mathcal{F} + o_dD_m\mathcal{F} - hR_a \equiv \mathcal{V}_{ra} \tag{3.7}$$

As indicated R, P, M and V represent the number of viral RdRP molecules, plus-strand RNAs, minus-strand RNAs and virions, respectively. D_p, D_m and R_a represent the number of dsRNA complexes produced from the plus-strand, dsRNA complexes from the minus-strand and the total number of RdRPs producing plus-strand RNA from a minus-strand template, respectively.

RdRP is not packaged in the virions, therefore the first step in replication is the translation of RdRP from the viral plus strand with maximum rate r and saturation constant k_t. RdRP associates with plus- or minus-stranded RNA with maximum rate o to synthesise a complementary strand. f sets the preference of RdRP for the minus strand. We assume that the minus-strand is the preferred template for dsRNA synthesis. The complex formation ($\mathcal{F}$) between RdRP and RNA strands is saturated for both viral RNA and RdRP (the Beddington-DeAngelis functional response [9, 35]):

$$\mathcal{F} = \frac{R}{R+P+M+D_m+k_r} \tag{3.8}$$

with saturation constant k_r. Semi-conservative synthesis of multiple plus-strands from a single minus-strand template is incorporated in the model. RdRP can associate with D_m (dsRNA complexes formed from the minus strand) with maximum rate o_d. In the case of D_p a single RdRP is present on the complex, and the entire complex dissociates with rate h into RdRP and a plus- and minus-strand. Multiple RdRPs are present on D_m, and each RdRP produces one product strand and then dissociates with rate h. However, the complex still exists after dissociation of one RdRP. The D_m complex disappears when the last RdRP dissociates. The chance that only one RdRP is present is $(1-\frac{1}{D_m})^{(R_a-D_m)}$ and therefore the dissociation rate of D_m is $hD_m(1-\frac{1}{D_m})^{(R_a-D_m)}$.

The virus produces virions that consist of plus-strand RNA and coat proteins. We simplify here by using the number of plus-stranded RNA instead of modelling a separate coat protein. The virion production has a maximum rate of virion production v and a Michaelis Menten constant k_v. d and d_r are the decay rates of viral ssRNA and RdRP respectively.

3.2.2 Model description: Antiviral RNA silencing

Primary response

The viral replication model is extended to include viral induction of the RNA silencing pathway. The scheme is shown in Figure 3.1. The $\mathcal{V}$ terms represent the parts of the equations modelling viral replication, and are defined in Equation 3.1-3.7.

RdRP
$$\frac{dR}{dt} = \mathcal{V}_r + \mathcal{G}_d(D_p + R_a) \equiv \mathcal{V}_r + \mathcal{P}_r \tag{3.9}$$

+RNA
$$\frac{dP}{dt} = \mathcal{V}_p - \frac{b_2 R_m P}{P + k_{ri}} - \mathcal{G}_s P \equiv \mathcal{V}_p - \mathcal{P}_p \tag{3.10}$$

−RNA
$$\frac{dM}{dt} = \mathcal{V}_m - \frac{b_2 R_p M}{M + k_{ri}} - \mathcal{G}_s M \equiv \mathcal{V}_m - \mathcal{P}_m \tag{3.11}$$

dsRNA
$$\frac{dD_p}{dt} = \mathcal{V}_{dp} - \mathcal{G}_d D_p \equiv \mathcal{V}_{dp} - \mathcal{P}_{dp} \tag{3.12}$$

dsRNA
$$\frac{dD_m}{dt} = \mathcal{V}_{dm} - \mathcal{G}_d D_m \equiv \mathcal{V}_{dm} - \mathcal{P}_{dm} \tag{3.13}$$

act.RdRP
$$\frac{dR_a}{dt} = \mathcal{V}_{ra} - \mathcal{G}_d R_a \equiv \mathcal{V}_{ra} - \mathcal{P}_{ra} \tag{3.14}$$

+siRNA
$$\frac{dSi_p}{dt} = \left(\mathcal{G}_s P + 0.5\mathcal{G}_d(D_p + D_m) - d_{si} Si_p - b_1 Si_p R_f\right) \equiv \mathcal{P}_{sip} \tag{3.15}$$

free RISC
$$\frac{dR_f}{dt} = i - d_r R_f - b_1 R_f (Si_p + Si_m) \equiv \mathcal{P}_{rf} \tag{3.16}$$

+RISC
$$\frac{dR_p}{dt} = b_1 R_f Si_p - d_r R_p \equiv \mathcal{P}_{rp} \tag{3.17}$$

Variables Si_p, Si_m, R_f, R_p and R_m represent siRNA cleaved from plus-strands, siRNA from minus-strands, free RISC, RISC loaded with Si_p, and RISC loaded with Si_m, respectively. We do not show the equations for Si_m and R_m since they have the same form as the equations for Si_p and R_p. The equation for the virions is unaltered (Equation 3.4).

Viral RNA is cleaved into siRNAs by Dicer. We simplify here by using only a single type of Dicer. $\mathcal{G}_d$ And $\mathcal{G}_s$ are the Dicer cleavage functions for dsRNA and ssRNA respectively.

$$\mathcal{G}_d = \frac{c_d D_i}{D_p + D_m + k_d} \qquad \mathcal{G}_s = \frac{c_s D_i}{P + M + k_d} \tag{3.18}$$

D_i is the number of Dicer molecules present in the host. Dicer can cleave siRNAs from dsRNA with maximum rate c_d, and from ssRNA with rate c_s. When Dicer cleaves both single- and double-strand RNA, we use the following function:

$$\mathcal{G}_{d,s} = \frac{c_{d,s} D_i}{D_p + D_m + P + M + k_d} \tag{3.19}$$

that is saturated for all possible Dicer targets. When Dicer cleaves dsRNA a 1-1 ratio of siRNAs targeting the plus- and minus-strand is produced. When studying the effects of Dicer cleavage rate, we always use the total rate, that is, $c_d + 2c_s$.

siRNAs associate with rate b_1 with RISC to form siRISC: the active RISC complex that will cause the breakdown of viral RNA. One strand of the siRNA is kept in siRISC, and since that strand consists of a short stretch of either plus- or minus-strand viral RNA, it will match to the complementary strand. The target of the active RISC is the RNA strand that matches the incorporated siRNA. siRISC cleaves the target RNA with maximum rate b_2. k_{ri} is the saturation constant of the siRISC cleavage function. d_{si} and d_r are the siRNA and RISC decay rates.

Secondary response

In addition to the primary response, the silencing pathway can include a secondary response. Host-encoded RDR synthesises dsRNA from single-strand substrates, that are cleaved into secondary siRNAs. In vitro RDR has two modes of action: primed and unprimed amplification [94, 130]. In the case of primed amplification siRNA binds to ssRNA and serves as a primer for RDR. In the case of unprimed amplification, RDR synthesises dsRNA from ssRNA without a primer. Recently, a third possibility has been proposed: RDR is guided by a siRNA to the ssRNA after which unprimed amplification takes place [110, 140]. The model is expanded with the three amplification terms:

$$\mathcal{A}_u = \frac{a_u}{(P + M + k_a)} \tag{3.20}$$

$$\mathcal{A}_g = \mathcal{A}_p = \frac{a_{p,g}}{((Si_p + Sis_p)M + (Si_m + Sis_m)P + k_a)} \tag{3.21}$$

Where $\mathcal{A}_u$ is unprimed amplification, $\mathcal{A}_p$ is primed amplification and $\mathcal{A}_g$ is guided amplification. We study the amplification pathways separately. In the case of guided amplification, the siRNAs are not removed when they guide amplification, in contrast to primed amplification. Amplification produces dsRNA that is not used for virus replication (D_e). This dsRNA is degraded into secondary siRNAs with a plus- or minus-strand polarity; Sis_p and Sis_m respectively. Since Dicer now cleaves D_e in addition to D_p

and D_m, the Dicer cleavage functions $\mathcal{G}_d$ and $\mathcal{G}_{d,s}$ are saturated for D_e:

$$\mathcal{G}_d = \frac{c_d D_i}{D_p + D_m + D_e + k_d} \qquad \mathcal{G}_{d,s} \quad = \frac{c_{d,s} D_i}{D_p + D_m + D_e + P + M + k_d} \tag{3.22}$$

$\mathcal{V}$ and $\mathcal{P}$ represent the parts of the equations that describe virus replication and the primary silencing pathway, and are defined in Equation 3.1-3.7 and Equation 3.9-3.17. The equations altered by the secondary response are:

$$\text{+RNA} \qquad \frac{dP}{dt} = \mathcal{V}_p - \mathcal{P}_p - \frac{b_2 R_{sm} P}{P + k_{ri}} - \mathcal{A}_u P - \mathcal{A}_p(Si_m + Sis_m)P - \mathcal{A}_g(Si_m + Sis_m)P \tag{3.23}$$

$$\text{−RNA} \qquad \frac{dM}{dt} = \mathcal{V}_m - \mathcal{P}_m - \frac{b_2 R_{sp} M}{P + k_{ri}} - \mathcal{A}_u M - \mathcal{A}_p(Si_p + Sis_p)M - \mathcal{A}_g(Si_p + Sis_p)M \tag{3.24}$$

$$\text{+siRNA} \qquad \frac{dSi_p}{dt} = \mathcal{P}_{sip} - \mathcal{A}_p Si_p M \tag{3.25}$$

$$\text{sec.}D \qquad \frac{dD_e}{dt} = \mathcal{A}_p((Si_m + Sis_m)P + (Si_p + Sis_p)M) + \mathcal{A}_g((Si_m + Sis_m)P + (Si_p + Sis_p)M) + \mathcal{A}_u(P + M) - \mathcal{G}_d D_e \tag{3.26}$$

$$\text{sec.}Si_p \qquad \frac{dSis_p}{dt} = 0.5\,\mathcal{G}_d D_e - d_{si} Sis_p - b_1 Sis_p R_f - \mathcal{A}_p Sis_p M \tag{3.27}$$

$$\text{sec.RISC} \qquad \frac{dR_{sp}}{dt} = b_1 Sis_p R_f - d_r R_{sp} \tag{3.28}$$

With D_e, Sis_p, Sis_m, R_{sp} and R_{sm} representing dsRNA produced via amplification, secondary siRNA with plus strand polarity, secondary siRNA with minus strand polarity, RISC loaded with Sis_p and RISC loaded with Sis_m, respectively. Again we do not show Si_m, Sis_m and R_m since they have the same form as Si_p, Sis_p and R_p respectively.

The full model can be found in the Section 3.5.

3.2.3 Parameters

Where possible, parameters were taken from literature (Table 3.1). We have estimated the remaining parameters within reasonable ranges as indicated in Table 3.1. When choosing parameters we aimed to show all qualitative outcomes of the model. When more parameters of a specific case are known, we can fit the model to that case, and investigate what behaviour is expected.

Table 3.1: Parameters used in the model with their default value and the studied range. #mol is number of molecules.

par.	meaning	value	units	studied range
r	maximum translation rate x #ribosomes	75000	#mol hr^{-1}	30,000 - 750,000 [1]
o	max rate of complex formation ssRNA	1	hr^{-1}	0.1 - 5
o_d	max rate of complex formation dsRNA	100	hr^{-1}	0 -1000
f	ratio of binding plus or minus RNA	0.9	-	0 - 1
h	dsRNA-RDR splitting rate	10	hr^{-1}	1 - 1,000
v	max virion production rate	500	#mol hr^{-1}	0 - 50,000
D_i	number of Dicer molecules	500	#mol	0 - 5,000
c_d	max Dicer cleavage rate for dsRNA	3	#mol hr^{-1}	0 - 20
c_s	max Dicer cleavage rate for ssRNA	3	#mol hr^{-1}	0 - 20
b_1	rate of RISC activation	0.005	#mol $^{-1}$ hr^{-1}	0 - 1
b_2	RISC target cleavage rate	20	#mol $^{-1}$ hr^{-1}	0 - 1,000 [2]
i	translation of RISC	100	#mol hr^{-1}	0 - 1,000
a	amplification (a_u, a_p and a_g)	100	#mol hr^{-1}	0 - 400
d_r	decay RDR and RISC	0.1	hr^{-1}	0 - 0.5
d	decay viral ssRNA	0.5	hr^{-1}	0 - 2
d_{si}	decay siRNA	2	hr^{-1}	0 - 5 [3]
k_v	saturation of virion production	10,000	#mol	1 - 100,000
k_d	saturation of Dicer cleavage	10,000	#mol	1 - 100,000
k_t	saturation constant for translation	1,000	#mol	1 - 10,000
k_{ri}	saturation of RISC cleavage	1,000	#mol	1 - 10,000
k_r	saturation of complex formation	1,000	#mol	1 - 10,000
k_a	saturation amplification	1000	#mol	1 - 10,000

[1] [92, 114], [2] [60], [3] [23]

3.3 Results

3.3.1 Viral growth in a silencing defective system

We first study the growth of a plus-strand RNA virus in a silencing defective system. The viral replication cycle is shown in Figure 3.1, and the model description can be found in Section 3.2.1.

In the default setting our model results in a sigmoid growth of viral plus-strands (Figure 3.2A). Sigmoid growth curves for plus-strand RNA

viruses in silencing defective systems have been observed for example for West Nile virus [46], Japanese encephalitis virus [146] and vesicular stomatitis virus in *C. elegans* [158]. In our model, after initialisation with 10 viral plus-strands, the number of free plus-strands initially decreases, because they become part of the RdRP-RNA complex. After this decrease, the virus grows exponentially and then growth saturates due to the saturation in the production of RDR and in the dsRNA complex formation. In the equilibrium the number of plus-strand RNA is an order of magnitude higher than the number of minus strands.

Depending on the initial dose and growth parameters, the virus can expand to the equilibrium as shown in Figure 3.2A, or it dies out immediately. An increase in o, o_d, h and r causes faster initial growth of the virus. A decrease in k_r and k_t has the same effect. A sigmoid curve with a higher equilibrium can be obtained by increasing o, o_d and r, and by decreasing h. Changing v does not have a large effect on viral growth, except when the timing of virion production is too early (when k_v is low).

The plus-to-minus ratio is controlled by f, the preference that RDR has for minus-strands. When increasing f the plus-to-minus ratio becomes increasingly biased towards the plus strand (Figure 3.2B). The virus is only capable of expanding when f lies between 0.009 and 0.988, and the ratio of plus-to-minus strands can vary from less then 1 up to 100. Parameter o_d can also increase the plus-to-minus ratio: when more RdRPs are able to bind to minus RNA, the ratio can become more skewed. However, the dsRNA complex has to stay intact long enough to observe this effect.

By varying the above parameters we can adjust the viral growth curve to fit different viruses.

3.3.2 Virus induced silencing

Primary response

We add the host primary RNA silencing defence to the viral growth model. Dicer cleaves dsRNA or ssRNA into siRNAs, that associate with free RISC and will target either the plus- or minus-strand. The primary RNA silencing pathway can alter the viral growth pattern substantially: it can slow down and decrease viral growth, cause oscillations, or can result in complete virus clearance.

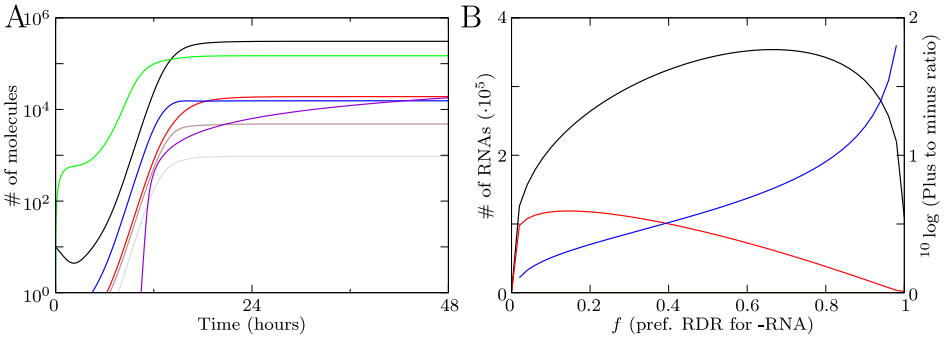

Figure 3.2: Viral growth in a silencing deficient system.(A) Timeseries of virus growth showing the number plus-strand RNA (black); minus-strand RNA (red); free RDR (green); dsRNA complex from plus strand (grey), dsRNA complex from minus strand (brown); RDRs active on minus strands (blue); and the number of virions (violet). (B) The effect of f on the number of plus and minus strands, with plus-strand RNA (black) and minus-strand RNA (red). The blue line shows the effect on the plus-to-minus strand ratio.

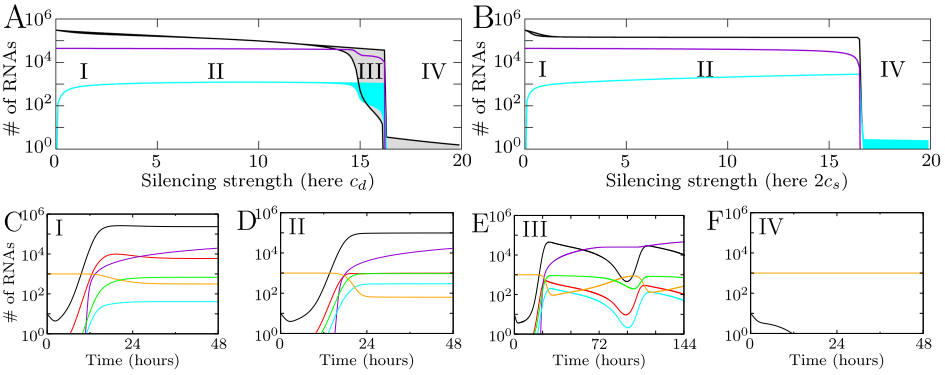

Figure 3.3: Four qualitative different outcomes of viral growth and silencing. (A) and (B) Bifurcation diagrams for increasing silencing strength. For varying silencing strength the number of plus-strand RNAs 100 hours post infection is shown. Black lines indicate plus-strand RNA, violet lines the number of virions produced, and cyan lines the total number of siRNAs. In the filled area a single peak or multiple oscillations of the number of plus-strand RNAs or the number of siRNAs occur. (A) Dicer cleaves dsRNA and (B) Dicer cleaves ssRNA. (C)-(F) show typical timeseries of behaviour in the four regions for $c_d = 2$, $c_d = 6$, $c_d = 8$ and $c_d = 10$. Timeplots show plus-strand RNA (black); minus-strand RNA (red); total number of virions (violet); free siRNA (cyan); free RISC (orange); active RISC (green). Virions can only be formed when virus levels are sufficiently high.

The important silencing parameters are the RISC activation rate (b_1), the RISC cleavage rate (b_2), the number of Dicers (D_i), the influx of free RISC (i), and the siRNA production rate (c_d and c_s). All these parameters determine the rate at which RNA silencing degrades viral RNA. We refer to this effect as the silencing strength. We will use one parameter as an example to study the effect of silencing strength.

As the functioning of Dicer in virus derived siRNAs is not resolved yet, we investigate three different Dicer activity modes: Dicer can cleave either only dsRNA, only ssRNA or both.

Dicer on dsRNA
In this setting Dicer cleaves only dsRNA and therefore siRNAs targeting the plus- and minus-strand are always present in equal amounts.

To investigate the effect that RNA silencing has on viral growth we vary the silencing strength. We do this by varying any of the silencing parameters according to the ranges in Table 3.1. As an example we here use the siRNA production rate c_d by Dicer. For each value of c_d we plot the number of viral plus-strand RNA, siRNA and virions present 100 hours (4.2 days) post infection. Maximum and minimum values are monitored from 10 hours onwards.

When silencing strength increases, we observe four possible effects of silencing. The four regions of different behaviour are shown in the bifurcation diagram in Figure 3.3A. In Figures 3.3C-F timeseries of the behaviour in the different regions are shown.

For a low silencing strength, in region I, virus levels are slightly decreased. A timeseries of this behaviour is shown in Figure 3.3C. A small peak in virus levels occurs, after which a decreased equilibrium amount of RNA is reached.

When silencing strength increases, viral growth is delayed and the equilibrium is decreased (Region II). The delayed virus growth results in a later timing and thereby decrease of virion production.

A further increase in silencing strength leads to the behaviour in region III, where oscillations in viral RNA levels occur (grey area in Figure 3.3A, and timeplot in Figure 3.3E). The oscillations are caused by the feedback of the system: the silencing response needs the virus to be sustained, but at the same time eliminates it. When silencing decreases viral RNA substantially, less siRNAs can be produced and the weakening silencing response creates the opportunity for the virus to expand again. Each time when the number of plus strands increases, more virions are produced, resulting in a stepwise virion production.

For even higher silencing strength the virus is not able to expand and decreases directly after initiation (Region IV, Figure 3.3F). In this case the virus is not able to produce virions.

The silencing parameters are determined by the host, but the silencing strength is also determined by properties of the virus. Folding and accessibility of viral RNA can limit the amount of RNA accessible for Dicer. Additionally, the RISC cleavage rate depends on target accessibility [16]. Therefore, the virus itself affects silencing strength and the bifurcation diagram can be interpreted in terms of viral properties. In Figure 3.3A a low silencing strength corresponds with a very resistant virus and a high silencing strength with a weaker virus. Therefore, it is possible that a single host type -with fixed silencing parameters- is able to silence one virus, but not the other.

Dicer on ssRNA, and on both ds and ssRNA
Next we assume that Dicer cleaves only ssRNA and has equal affinity for plus- and minus-strands (Figure 3.3B). There are some striking differences between the case where Dicer cleaves long dsRNA and this case. A major difference is that oscillations do not occur, instead region IV follows directly after region II. Additionally, in region II an increase in silencing strength does not affect the amount of virus present, while for dsRNA cleavage by Dicer the amount of virus slopes downward due to increasing silencing strength.

When single and double-stranded RNA cleavage by Dicer are combined, the Dicer cleavage function is saturated for both single- and double-strand RNA. Interestingly, a combined single- and double-strand cleavage by Dicer makes the response more efficient than each case separately (Figure 3.4B).

Secondary response

An important component of the silencing pathway is amplification via RDR. Detailed information on RDRs can be found in Wassenegger and Krczal [155]. RDR -and therefore amplification- has been shown to play an antiviral role in plants, and in RDR knockouts virus accumulated to higher levels and lead to increased symptom severity [106, 121, 131, 161, 163, 166]. Yu et al. [166] have shown that in an RDR defective mutant viral RNA turnover is substantially decreased compared to the wild-type. Several experiments have shown that RDR plays a role in the systemic spread of the virus to the plant meristem and newly emerging leaves [106, 121, 131].

We studied the effect that the secondary response can have. We im-

plement all three types of amplification: primed, unprimed and guided amplification. For each type of amplification we investigate two different Dicer activity modes. Either Dicer can cleave siRNAs from dsRNA only, or Dicer can cleave both dsRNA and ssRNA. The case where Dicer cleaves only ssRNA is not relevant here because the amplification functions through dsRNA.

Again we vary the silencing strength by varying c_d and c_s. As previously we can interpret the results also in terms of viral properties. The addition of the secondary response can have a number of effects. The virus can be cleared for lower silencing strength, and oscillations can be enlarged (Figure 3.4). The most striking is the occurrence of a new region of behaviour, where the virus is able to expand initially but is cleared later. The different types of amplification have different effects.

Unprimed amplification
The solid lines in Figure 3.4C and D show the bifurcation diagram when the gain of unprimed amplification is one siRNA per synthesised RDR transcript. Silencing becomes effective for lower silencing strength when unprimed amplification is added. This means that viruses that could not be silenced with the primary response can be silenced after the addition of the secondary response. When the gain is increased to four siRNAs, there is hardly an effect (dashed lines Figure 3.4C), indicating that maximum efficiency is already reached when the gain is only one siRNA. Interestingly, the oscillations that occurred without amplification have disappeared. When the amplification rate is lower, oscillations occur in the same region as without amplification. With increasing amplification rate the transition to region IV moves to lower silencing strength, cutting off the bifurcation diagram and losing the oscillatory regime.

Primed amplification
At first primed amplification seems to have little effect on silencing (solid lines, Figure 3.4E and F). This is caused by the lack of gain by this amplification route. Primed amplification uses one siRNA to produce a siRNA, resulting in a gain of zero. When four siRNAs are cleaved from an amplified transcript (D_e), there is a clear effect (dashed lines, Figure 3.4E). The oscillations in region III are enlarged to such extent that the virus is cleared after an initial growth peak. This is a new region of behaviour, region IIIa (Figure 3.5). In this region the virus can only produce virions during the initial growth peak, resulting in a strongly decreased virion production. Region IIIa can also occur without amplification for a faster growing virus.

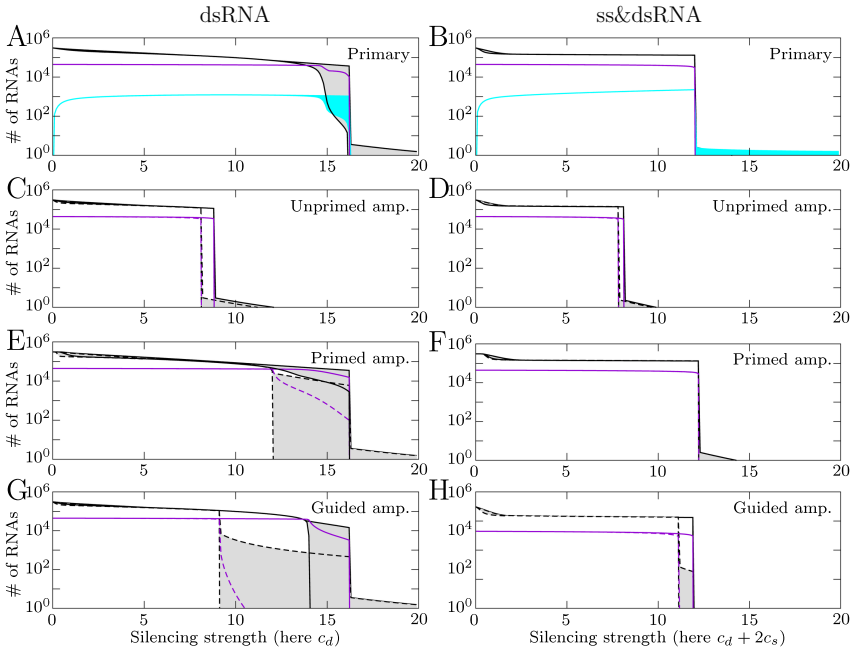

Figure 3.4: Effect of amplification. Bifurcation diagrams for increasing silencing strength. In this case we varied Dicer cleavage rates. On the left, Dicer cleaves dsRNA; on the right Dicer cleaves dsRNA and plus- and minus-strand ssRNA. In the case of Dicer cleaving plus- and minus-strand RNA $c_d = c_s$. Solid black lines show the number of plus-strand RNA 300 hours post infection, violet lines show the number of virions, and cyan lines the total number of siRNAs. Dashed lines show the behaviour when amplification yields four siRNAs per amplified transcript. For clarity the lines representing siRNAs have been omitted in C-H.

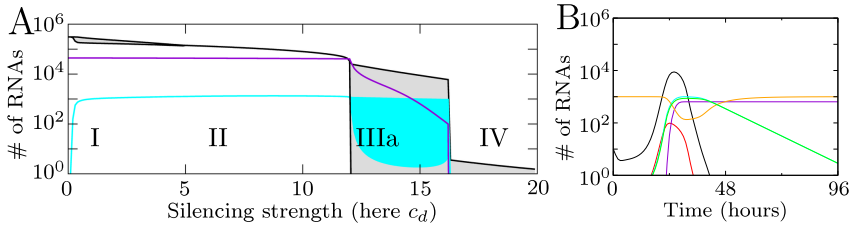

Figure 3.5: Behaviour in region IIIa.(A) Region IIIa shown in a bifurcation diagram for increasing Dicer cleavage rate ($a_p = 100$, 4 siRNAs per amplified transcript). Black lines indicate plus-strand RNA, violet lines the number of virions produced, and cyan lines the total number of siRNAs. (B) A timeplot showing the behaviour in region IIIa ($c_d = 15$) with plus-strand RNA (black); minus-strand RNA (red); total number of virions (violet); total siRNA (cyan); free RISC (orange); active RISC (green).

When the initial growth peak is sufficiently high and silencing is strong, the virus can be cleared after a single peak.

When Dicer cleaves both single- and double-strand RNA, primed amplification has virtually no effect, indicating that sufficient dsRNA cleavage is necessary to benefit from primed amplification.

Guided amplification
Guided amplification does not deplete the siRNAs as primed amplification does. In the oscillatory regime, the oscillations are enlarged and, as with primed amplification, region IIIa behaviour is observed (Figure 3.4G). When Dicer cleaves single- and double-strand RNA this region occurs only when the gain of amplification is higher (Figure 3.4H).

The role of the secondary response
We conclude that enough dsRNA cleavage is necessary to observe an effect of the secondary pathway. Not all virus infections seem to be affected by the secondary response. RDR defective Tobacco (*N. bentamiana*) plants, that are not capable of a secondary response, were only hypersusceptible to some of the tested viruses, while the response to other viruses was not affected [131]. Although these observations seem contradictory, our model suggests that it is an inherent property of the system that, depending on the virus, RDR can or cannot influence the amount of virus accumulation. The initial position of the system in the bifurcation diagram influences the effect of RDR. Depending on the initial position of the system, the removal of RDR can bring the system from region I to II, IIIa to II or III, IV to II or III, or it remains in the same region of behaviour. This means that viral properties such as accessibility of viral single and double-strand RNA to Dicer, availability of ssRNA to RISC, and viral growth rate define the effect that RDR can have.

3.3.3 Observed ratio of siRNAs

Several studies have focused on determining the ratio between plus- and minus-strand derived siRNAs during viral infection. Molnar et al. [101] studied the siRNA origin of *Cymbidium ringspot tombusvirus* in detail. They found that 80% of the siRNAs were derived from the plus-strand. Additionally, they studied *Tobacco mosaic virus* and *Potato virus X*, and found that these siRNA ratios were also biased towards the plus-strand. They suggested that the presence of more plus-strand derived siRNAs increases silencing efficiency, and that Dicer may have a preference for plus-strand RNA. It may be more efficient to mainly target the minus-strand,

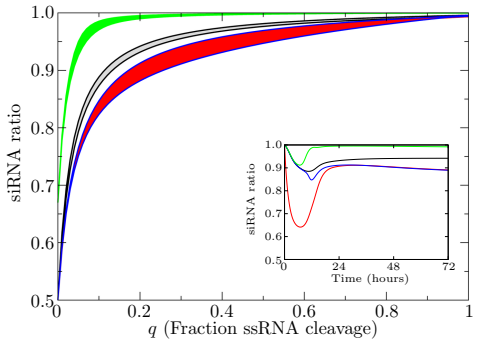

Figure 3.6: siRNA ratios observed for varying Dicer cleavage modes: on the left Dicer cleaves exclusively dsRNA; on the right exclusively ssRNA. Shown are siRNA ratios for the primary pathway (black); primed amplification (green), unprimed amplification (red) and guided amplification (blue). Unprimed and guided amplification result in the same siRNA ratios, the lines lie on top of each other. The inset shows the change in siRNA ratio in time for all studied pathways (fraction of ssRNA cleavage q is 0.2).

because it is present in lower amounts. Pantaleo et al. [115] confirmed the skewed siRNA ratio found by Molnar et al. [101], but reported that the asymmetry was not as pronounced. Ho et al. [66] explored two other viruses and found that for *Turnip crinkle carmovirus* 97.6% of the siRNAs was derived from the plus strand, while for *Turnip mosaic potyvirus* only 58.1% was produced from the plus-strand. The question rises if these different ratios can arise without implementing Dicer preferences for the plus strand.

To investigate whether a preference of Dicer is needed to explain the observed ratios we vary the ratio between single- and double-stranded RNA cleavage by Dicer (q). This ratio may be affected by viral properties as RNA folding and accessibility of single- and double-strand RNA. We keep total Dicer cleavage rate constant and plot the minimum and maximum siRNA ratio observed between 24 and 100 hours post infection (Figure 3.6). The cleavage function is saturated according to the ratio between single- and double-stranded RNA cleavage by Dicer:

$$\mathcal{G}_d = \frac{(1-q)c_d D_i}{(1-q)(D_p+D_m+D_e)+q(P+M)+k_d} \tag{3.29}$$

$$\mathcal{G}_s = \frac{qc_s D_i}{(1-q)(D_p+D_m+D_e)+q(P+M)+k_d} \tag{3.30}$$

We set total Dicer cleavage rate to region I or II (total Dicer cleavage rate is 3) to avoid non-existent siRNA ratio's in region III, IIIa or IV.

When only dsRNA is cleaved, the siRNA ratio will be 0.5, due to the fact that there is always an 0.5 chance that either siRNA strand is selected. The addition of primed amplification can raise this ratio: more minus-strand siRNAs are used for amplification because the plus strand is present in higher amounts. When only ssRNA is cleaved, the ratio follows from the plus-to-minus ratio produced by the virus. We find that when Dicer cleavage rates are intermediate between these two extreme cases, different siRNA ratios can occur for different viruses. In fact, the whole range between 0.5 and 1 is possible, and the experimentally observed ratios can be reached without implementing an extra mechanism or Dicer preference for the plus-strand. When the virus ssRNA has many hairpins and mainly ssRNA is cleaved, we predict a high siRNA ratio. When mainly dsRNA is cleaved we expect a low ratio (Figure 3.6).

The siRNA ratios are shown in ranges between the maximum and minimum because the siRNA ratio changes over time. The trend is that initial siRNA ratio's are close to 1 (almost only plus-strand derived), followed by a decline in siRNA ratio, after which a stable ratio is reached (inset Figure 3.6).

Concluding, when Dicer is capable of both single- and double-strand RNA cleavage, the experimentally observed ratios can be reached without implementing a Dicer preference for the plus-strand.

3.4 Discussion

The RNA silencing pathway functions as an immune system in plants and several animals. We here presented the first model study that combines viral growth and RNA silencing.

In contrast to the previously reported necessity of a nonlinear feedback in amplification to silencing transgenes [59], we showed that antiviral silencing can function without any amplification. In agreement with our results, experiments have shown that plants with a defective RDR are still capable of antiviral silencing [31].

RNA silencing can alter the sigmoid growth pattern of the virus substantially. Wilkins et al. [158] studied viral growth in *C. elegans* with silencing able and silencing deficient hosts. They show that without silencing the virus grows according to a sigmoid curve to $1 \cdot 10^6$, with silencing this curve is flattened and the virus accumulates to $5 \cdot 10^4$. This behaviour is in accordance with our results: in region I and II the virus equilibrium is decreased to similar extent. Dzianott and Bujarski [44] obtained a *Brome*

mosaic virus growth curve in *A. thaliana*. They observed an initial decline in RNA, then a peak of viral growth, after which the concentrations decline toward zero again. We can assume the curve found by Dzianott and Bujarski [44] represents viral growth limited by RNA silencing, because siRNA was found, and virus accumulated to higher levels in a host expressing a silencing suppression protein. This 'peak' behaviour corresponds with the behaviour of our model in region IIIa. Region IIIa occurs only when the virus and the silencing response are fast, with amplification these conditions are more likely to occur.

We studied three cases of Dicer activity modes: Dicer can cleave dsRNA, ssRNA or both. We show that a combined degradation of single- and double-strand RNA by Dicer is more efficient than each case separately.

Sufficient dsRNA cleavage is necessary to observe an effect of the secondary silencing response. Unprimed amplification is able to strongly increase the efficacy of RNA silencing, clearing the virus for much lower silencing strength. Virion production is then not possible, because virus growth is completely silenced. Primed and guided amplification can cause major oscillations that also lead to clearance of the virus, however, the virus is still able to produce virions during the initial growth peak. Moreover, primed amplification can only be beneficial when the siRNA gain through amplification is sufficiently high.

Experiments have shown that viruses accumulate to higher levels in hosts defective in the secondary response [106, 121, 131, 161, 163, 166]. However, some viruses are and some viruses are not limited by RDR (secondary response) [131]. Our model study has shown that such seemingly contradictory results can be explained by a slight change in viral properties that bring the system to a different region of behaviour.

In antiviral silencing a wide range of siRNA ratios has been observed [66, 101, 115]. Our model provides a possible explanation for these observations. Each virus has unique folding properties and accessibility of its RNA, thereby affecting the Dicer cleavage rate on single- and double-strand RNA. Variation in these Dicer cleavage rates can account for the full range of observed siRNA ratios and a preference of Dicer for either the plus- or minus-strand is not needed.

The model presented here studies antiviral silencing on the cellular level, and is a first step in understanding the interactions between viruses and RNA silencing. An interesting extension of the model is the addition of virus encoded silencing suppressors. Although we expect that silencing suppression partly overlaps with decreasing silencing strength, the specific

types of silencing suppressors could affect the RNA silencing response in unexpected ways. Additionally, we plan to extend our model with the spread of virus particles and siRNAs from cell to cell.

We hope that further experimental research will be done to provide more data to test our model. We would be specifically interested in timeseries of viral growth with and without RNA silencing, and in particular in the role of RDR and Dicers on the dynamics of RNA silencing within the cell.

Our work provides an important framework to study natural antiviral silencing. We have shown that various experimentally observed behaviours can be explained, even when they seem contradictory at first.

3.5 Appendix

The full model:

$$\frac{dR}{dt} = \frac{rP}{(P+k_t)} - d_r R - \{o(1-f)P + ofM + o_d D_m\}\mathcal{F} + hD_p + hR_a + \mathcal{G}_d(D_p + R_a)$$

$$\frac{dP}{dt} = -o(1-f)P\mathcal{F} + hD_p + hR_a - dP - \frac{vP^5}{k_v^5 + P^5} - \frac{b_2 R_m P}{P+k_{ri}} - \mathcal{G}_{p,m}P$$
$$- \frac{b_2 R_{sm} P}{P+k_{ri}} - \mathcal{A}_u P - \mathcal{A}_p(Si_m + Sis_m)P - \mathcal{A}_g(Si_m + Sis_m)P$$

$$\frac{dM}{dt} = -ofM\mathcal{F} + hD_p + hD_m(1 - \frac{1}{D_m})^{(R_a - D_m)} - dM - \frac{b_2 R_p M}{M+k_{ri}} - \mathcal{G}_{p,m}M$$
$$- \frac{b_2 R_{sp} M}{P+k_{ri}} - \mathcal{A}_u M - \mathcal{A}_p(Si_p + Sis_p)M - \mathcal{A}_g(Si_p + Sis_p)M$$

$$\frac{dV}{dt} = \frac{vP^5}{k_v^5 + P^5}$$

$$\frac{dD_p}{dt} = o(1-f)P\mathcal{F} - hD_p - \mathcal{G}_d D_p$$

$$\frac{dD_m}{dt} = ofM\mathcal{F} - hD_m(1 - \frac{1}{D_m})^{(R_a - D_m)} - \mathcal{G}_d D_m$$

$$\frac{dR_a}{dt} = ofM\mathcal{F} + o_d D_m \mathcal{F} - hR_a - \mathcal{G}_d R_a$$

$$\frac{dSi_p}{dt} = \mathcal{G}_{p,m}P + 0.5\mathcal{G}_d(D_p + D_m) - d_{si}Si_p - b_1 Si_p R_f - \mathcal{A}_p Si_p M$$

$$\frac{dSi_m}{dt} = \mathcal{G}_{p,m}M + 0.5\mathcal{G}_d(D_p + D_m) - d_{si}Si_m - b_1 Si_m R_f - \mathcal{A}_p Si_m P$$

$$\frac{dR_f}{dt} = i - d_r R_f - b_1 R_f (Si_p + Si_m)$$
$$\frac{dR_p}{dt} = b_1 R_f Si_p - d_r R_p$$
$$\frac{dR_m}{dt} = b_1 R_f Si_m - d_r R_m$$
$$\frac{dD_e}{dt} = \mathcal{A}_u(P+M) + \mathcal{A}_p((Si_m + Sis_m)P + (Si_p + Sis_p)M) - \mathcal{G}_d D_e + \mathcal{A}_g((Si_m + Sis_m)P + (Si_p + Sis_p)M)$$
$$\frac{dSis_p}{dt} = 0.5\mathcal{G}_d D_e - d_{si} Sis_p - b_1 Sis_p R_f - \mathcal{A}_p Sis_p M$$
$$\frac{dSis_m}{dt} = 0.5\mathcal{G}_d D_e - d_{si} Sis_m - b_1 Sis_m R_f - \mathcal{A}_p Sis_m P$$
$$\frac{dR_{sp}}{dt} = b_1 Sis_p R_f - d_r R_{sp}$$
$$\frac{dR_{sm}}{dt} = b_1 Sis_m R_f - d_r R_{sm}$$

Acknowledgements

This work was supported by the Netherlands Organisation for Scientific Research (NWO) through Grant 050.50.202 of the BioMolecular Informatics program.

CHAPTER 4

RNA silencing can explain chlorotic infection patterns on plant leaves

Marian Groenenboom and Paulien Hogeweg
Theoretical Biology/Bioinformatics Group, Utrecht University
Padualaan 8, 3584 CH Utrecht, The Netherlands.

BMC Systems Biology, in press

Abstract

RNA silencing has been implicated in virus symptom development in plants. One common infection symptom in plants is the formation of chlorotic tissue in leaves. Chlorotic and healthy tissue co-occur on a single leaf and form patterns. It has been shown that virus levels in chlorotic tissue are high, while they are low in healthy tissue. Additionally, the presence of siRNAs is confined to the chlorotic spots and the boundaries between healthy and infected tissue. These results strongly indicate that the interaction between virus growth and RNA silencing plays a role in the formation of infection patterns on leaves. However, how RNA silencing leads to the intricate patterns is not known. Here we elucidate the mechanisms leading to infection patterns and the conditions which lead to the various patterns observed. We present a modelling approach in which we combine intra- and inter-cellular dynamics of RNA silencing and viral growth. We observe that, due to the spread of viruses and the RNA silencing response, parts of the tissue become infected while other parts remain healthy. As is observed in experiments high virus levels coincide with high levels of siRNAs, and siRNAs are also present in the boundaries between infected and healthy tissue. We study how single- and double-stranded cleavage by Dicer and amplification by RNA-dependent RNA polymerase can affect the patterns formed. This work shows that RNA silencing and virus growth within a cell, and the local spread of virions and siRNAs between cells can explain the heterogeneous spread of virus in leaf tissue, and therewith the observed infection patterns in plants.

4.1 Background

RNA silencing is an evolutionary conserved mechanism in eukaryotes that has a major role in gene regulation, development, transposon control and defence against viruses.

Antiviral RNA silencing is induced by virus double-stranded RNA (dsRNA) or by specific single-stranded RNA (ssRNA) structures. Double- or single-stranded RNA is cleaved into small interfering RNA (siRNA) by RNase III-like enzymes such as Dicer and Dicer-like [101, 150]. siRNAs associate with the RNA-induced silencing complex (RISC) and guide the complex to complementary sequences that are then destroyed. In addition to the primary response, siRNAs can be produced through a secondary pathway that involves synthesis of dsRNA or siRNA by host encoded

RNA-dependent RNA polymerase (RDR) [7, 94, 155].

The antiviral role of RNA silencing is extensively studied in plants [38, 97, 150]. Virus spread through the plant results in diverse symptoms, for example leaf curling, abnormal leaf or flower development, and patterns on infected leaves. These patterns consist of both chlorotic or necrotic tissue in combination with healthy looking tissue. Different types of patterns that occur are concentric circles or rings, mosaic patterns, vein clearing and spots. Interestingly, virus levels are high in yellow, chlorotic tissue and low in the green, healthy tissue [4]. This means that virus accumulation varies from cell to cell. It has been hypothesised that RNA silencing may play a role in the development of leaf patterns resulting from virus infections [2, 6, 71, 104]. Recent observations by Hirai et al. [65] on mosaic patterns support this hypothesis. They have shown that RNA silencing activity is confined to the yellow spots and the marginal regions of the green spots. Reduced expression of RDR, which is part of the secondary pathway of the silencing response, resulted in smaller or no green tissue. These results strongly suggest that RNA silencing plays a major role in the development of plant symptoms.

Previously we developed a mathematical model of RNA silencing and its interaction with viral growth within a cell [58]. We found that depending on the strength of the silencing response the virus equilibrium can be almost unaffected, oscillations can occur, or the virus can be cleared. Additionally, we found that a change in Dicer cleavage rate is representative for a general change in silencing strength. For a low Dicer cleavage rate the equilibrium amount of virus is slightly decreased and the virus grows slower than without silencing. For high Dicer cleavage rate the virus is not able to grow and is cleared directly after introduction. For intermediate Dicer cleavage rates oscillations in virus levels can occur. When a secondary response is added these oscillations can be enlarged to such extend that the virus is cleared after a single growth peak.

We here study how RNA silencing can explain the development of leaf patterns resulting from viral infection. To this end we use a detailed modelling approach in which we combine an intra-cellular model of viral growth and the RNA silencing pathway with inter-cellular tissue dynamics.

We observe that RNA silencing and virus growth on a tissue can result in a discontinuous spread of the virus: the virus reaches high levels in some cells, while it is suppressed in other cells. We study the conditions for different type of patterns. These patterns could be the basis of plant symptom development. We elucidate the mechanisms leading to these

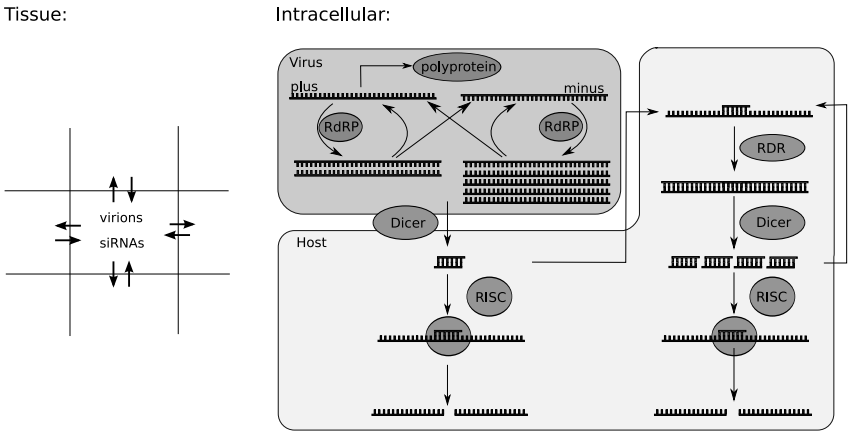

Figure 4.1: Schematic representation of the model. In each grid point the dynamics of a replicating plus-strand RNA virus and antiviral silencing are calculated. Viral plus- and minus-strand RNA is replicated by RdRP. The formed complex dissociates into ssRNA. Virus single-strand and part of the double-stranded RNA can be cleaved into siRNA by Dicer. siRNA associates with RISC and cleaves the target RNA. siRNAs can guide or prime amplification of the response through host encoded RDR, or viral ssRNA is amplified by RDR in an unprimed manner. The full intracellular model can be found in Section 4.5. siRNAs and virions produced in each cell can move from cell to cell on the grid.

patterns and how increased silencing efficiency, siRNA movement and the occurrence of a secondary response relate to the pattern formation.

4.2 Methods

To investigate the formation of infection patterns in plants we model an area of plant tissue on a grid. Each grid point represents a plant cell. Within each cell we calculate virus levels and levels of RNA silencing proteins with a detailed model. Virions and siRNAs can move from cell-to-cell. A schematic representation of the model is shown in Figure 4.1.

4.2.1 Intracellular model

The number of molecules in each cell is calculated with our previously described model of the antiviral RNA silencing pathway and a replicating plus-strand RNA virus [58].

The intracellular model consists of coupled differential equations, rep-

resenting viral plus- and minus-strand RNA, dsRNA, virions, RdRP, siRNA targeting plus or minus-stranded RNA, and free and active RISC. The virus replication cycle starts with the translation of plus-stranded RNA into a poly-protein. After auto-cleavage one of the products is RNA-dependent RNA polymerase (RdRP) that associates with plus-strand RNA to synthesise a complementary strand. The formed dsRNA separates into a plus- and minus-strand that can both associate with RdRP again. We assume that the minus-strand is the preferred template for dsRNA synthesis. Semi-conservative synthesis of multiple plus-strands from a single minus-strand template is incorporated in the model, resulting in a biased plus-to-minus ratio. The virus produces virions that consist of plus-stranded RNA and coat proteins. We simplify here by using the number of plus-stranded RNA instead of modelling a separate coat protein.

Viral double- or single-stranded RNA is degraded by host encoded Dicer into siRNAs, that have a plus- or minus-strand polarity. siRNAs cleaved from dsRNA have a 50% chance of targeting either the plus or the minus strand. siRNAs cleaved from a ssRNA hairpin automatically target strands with the opposite polarity. Via RISC the siRNAs cause degradation of either plus- or minus-stranded viral RNA.

Secondary siRNAs can be synthesised through the amplification pathway that involves synthesis of dsRNA by host encoded RDR. We implement unprimed, primed and guided amplification. Each type of amplification can be studied separately.

All equations are integrated using a timestep of 3.6 seconds. Simulations run for 300 hours, unless indicated otherwise. The equations can be found in Section 4.5.

4.2.2 Tissue level model

To study RNA silencing and viral infection in a tissue we use a spatial model. Each grid point represents a cell for which the intracellular dynamics are calculated with the model described above.

Viruses encode movement proteins that enable the movement of virions from cell-to-cell through plasmodesmata. We implement the movement of virions to the four neighbouring cells in our model. Virions can be unpacked in each cell into naked plus-strand RNA. We chose a 4 neighbourhood because cells share almost no surface area with the diagonal neighbours.

For movement we shift to a particle based system, because we do not want incomplete particles to trigger a reaction in a neighbouring cell.

Movement of particles occurs every timestep (3.6 seconds). A fraction of the total number of virions in the cell is evenly distributed among the four neighbours, and excess virions are distributed randomly among the neighbours. When the number of moving virions is smaller than one, we draw a random number to decide if one virion moves to a random neighbour. With this method we underestimate the heterogeneity of viral spread as compared to Brownian motion. This method is therefore a good worst-case scenario for the study of heterogeneous spread of virus particles.

The silencing response is able to spread from cell-to-cell with a short range silencing signal, most likely siRNAs [63]. We implement the spread of siRNAs in the same way virions move. There is also a long-range silencing signal [15, 43]. Because of the elusive nature of the long range silencing signal, and because we here take only a tissue or leaf area into account we do not include a long range silencing signal.

4.3 Results and Discussion

We vary Dicer cleavage rates as representative for silencing strength to study the effect of RNA silencing on the spread of virus particles over the tissue.

Within the cell three different behaviours can be observed [58]. High Dicer cleavage rate results in fast clearance of the virus. Low Dicer cleavage rate delays viral growth but hardly decreases the virus levels in equilibrium. Intermediate cleavage rate results in oscillating virus levels.

4.3.1 Infection patterns without RNA silencing

We first study virus spread without silencing present. We initialise the tissue with healthy cells and infect one cell in the centre with 10 viral plus strands. After initiation the virus starts to produce virions that spread from cell-to-cell. We fix the fraction of virions leaving a cell to 1% per hour.

The virus spreads rapidly over the entire area and 75 hours post infection (hpi) a circular area of the grid has become infected with the virus. In Figure 4.2A we show the number of virions, the number of siRNAs and the number of plus strands in separate screen-shots. When virions, virus plus-stranded RNA or siRNAs are absent from the cell, it is shown in green. Cells that have virions, plus-stranded RNA or siRNAs are shown in a colour ranging from black to yellow (via red): the colour ramps are shown in Figure 4.2. Also shown is a space-time plot, that is, horizontal

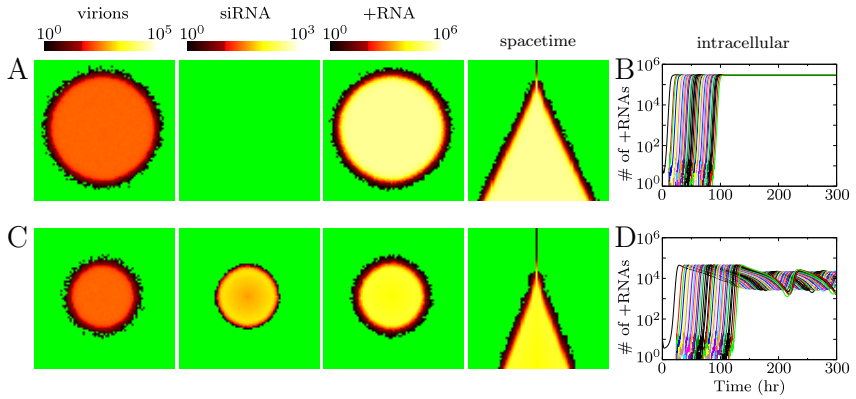

Figure 4.2: Virus spread over plant tissue. (A) and (C) are screen-shots 75 hpi showing the number of virions, siRNAs and +RNA in the cells. (B) and (D) show the intracellular +RNA levels for a row of cells through time. (A) and (B) show results without silencing and (C) and (D) with silencing. Virions move from cell-to-cell, but siRNAs cannot spread.

cross-sections of the grid every hour post infection (1 hpi top row, 75 hpi bottom row). In Figure 4.2B we show time-series of plus-strand accumulation in adjacent cells. The curve starting at 0 hpi is an initially infected cell. The other cells in turn each become infected by the neighbouring cell(s) and in each cell the virus expands to the equilibrium.

4.3.2 Infection patterns with silencing, without siRNA movement

When RNA silencing is active, we initialise the cells with RISC and Dicer. We first assume that Dicer is only capable of cleaving siRNA from viral dsRNA, and that siRNAs cannot move from cell to cell. Even without siRNA movement RNA silencing slows down virus spread over the area (Figure 4.2C). In the space-timeplot can be seen that the infection advances much slower than without the presence of the silencing response. A stronger silencing response slows down the spread of the virus more than a weaker response. We here show results for an intermediate Dicer cleavage rate, that results in oscillatory behaviour within the cells (Figure 4.2D). For high Dicer cleavage rate the virus is cleared immediately after introduction, and is not able to spread from cell to cell, because it is eliminated before virions could be produced.

4.3.3 Infection patterns with siRNA movement

As shown above, without siRNA movement the infection spreads homogeneously over the area. When siRNAs do move from cell to cell, they can limit virus growth in neighbouring cells, resulting in viral growth in some cells and suppression in others. This results in patterns that can spread over the entire area or stay localised to the area around the inoculated site. We observe somewhat different patterns for low and intermediate Dicer cleavage rates and we will discuss results from both possibilities.

Low dsRNA cleavage rate by Dicer

We first study the effects of a low Dicer cleavage rate for all possible siRNA movement rates. Varying the rate of siRNA movement we observe that the virus does not spread uniformly over the area and that patterns are formed.

Low siRNA movement results in a circular pattern that is shown in Figure 4.3A. The virus reaches a high equilibrium in the cells close to the initiation site. The siRNAs produced by these cells inhibit viral growth in a ring of cells around the centre. Virions are unpacked in these cells, but the viral RNA is silenced with the siRNAs from the neighbours. At sufficient distance from the siRNA producing cells, the virus will be able to grow, and these cells will in their turn inhibit viral growth in the next ring. Once a ring is formed it remains stable.

In the time-series (Figure 4.3A) it can be seen that the virus can expand to an equilibrium with high RNA levels in some cells, while in other cells the virus decreases to low RNA levels. We will refer to these cells as "silenced cells". The silenced equilibrium is maintained by siRNA movement: the virus grows to the high equilibrium when siRNA movement is stopped. In silenced cells the siRNA influx suppresses virus replication completely: no dsRNA is formed, and the observed plus-strand RNA levels result from the virion influx from neighbouring cells.

For a higher siRNA movement rate a different pattern occurs (Figure 4.3B). The circular pattern breaks and protrusive waves occur that resemble mosaic-like symptoms. We can distinguish three cell types in this pattern: cells with high virus levels, silenced cells and healthy cells. The healthy spots between the infected patches are surrounded by the silenced cells. Apart from low virus levels in the silenced cells at the edge of the spots there are no virions or other virus particles present in the healthy spots. The siRNAs present in the edge cells seem to "guard" the edges of the healthy spots as described by Hirai et al. [65]. These siRNAs, however,

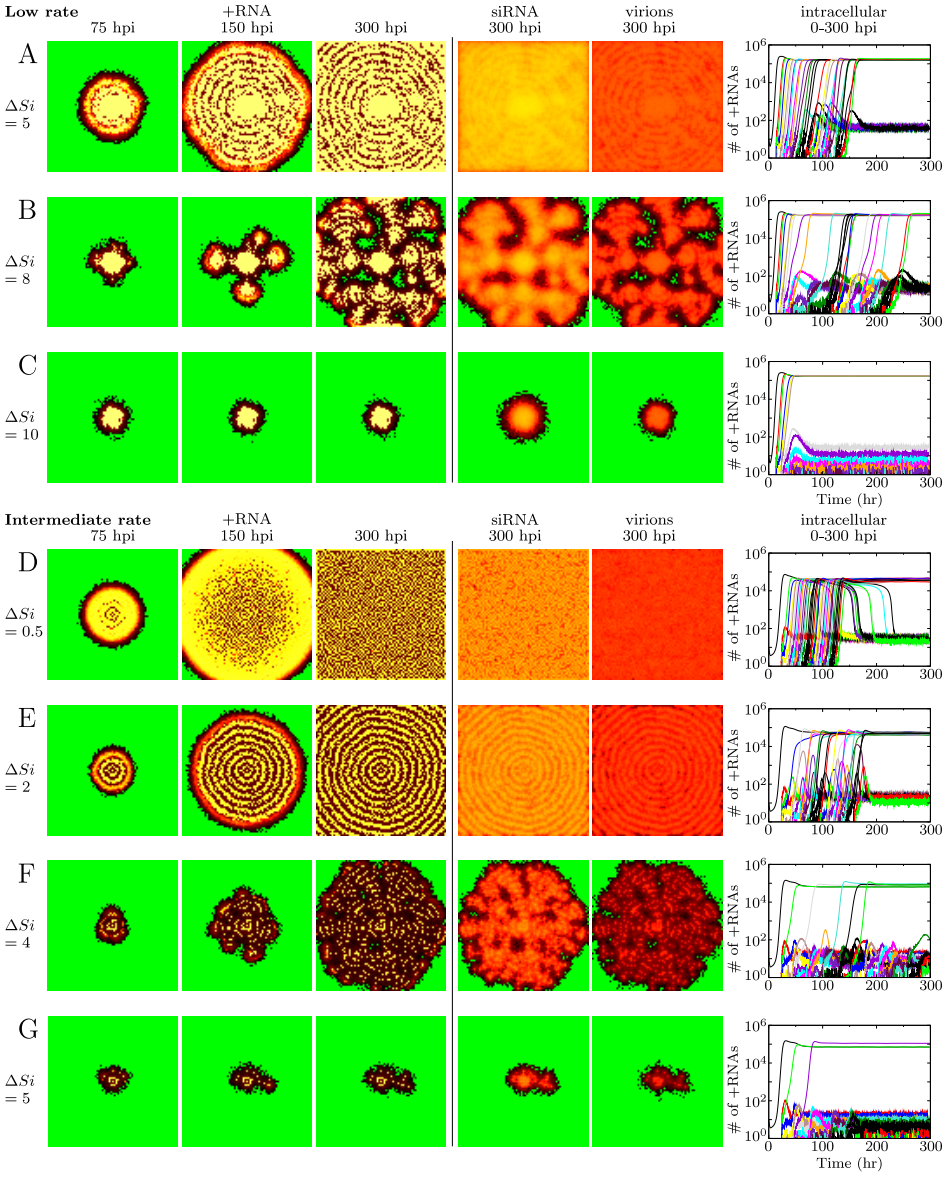

Figure 4.3: Infection patterns caused by RNA silencing. (A-C): low silencing strength (Dicer cleavage rate is 5 cleavages per Dicer per hour). (A) concentric circles, (B) mosaic and (C) local spot. (D-G): intermediate silencing strength (Dicer cleavage rate is 15 cleavages per Dicer per hour). (D) speckle-pattern; (E) concentric circles; (F) mosaic; and (G) local spot. The patterns spread over the entire tissue, except the patterns shown in C and G. In the first three columns the number of +RNAs is shown, column 4 and 5 show siRNA and virions respectively. Also shown is the intracellular amount of +RNA through time for a row of cells. ΔSi gives the percentage of siRNAs that move to neighbouring cells per hour. Colours according to the colour-ramps shown in Figure 4.2.

are not produced by the silenced cells in the edges, but move there from the infected neighbouring cells.

For the maximum siRNA movement rate (10% of the available siRNAs in a cell) the infection is confined to the area around the inoculated site (Figure 4.3C).

Concluding, siRNA movement creates silenced cells in which the virus is suppressed, and cells in which the virus grows to high values. Increasing siRNA movement increases the number of silenced cells, rather than decreasing virus load in all cells.

Intermediate dsRNA cleavage rate by Dicer

When Dicer cleavage rate is intermediate, similar patterns can be observed (Figure 4.3D-G). However, a lower siRNA movement rate is sufficient to generate them. For low siRNA movement rate a speckle pattern occurs. Initially the virus is able to expand considerably in all cells (Figure 4.3D). However, some time after infection virus levels drop in some cells and reach the silenced equilibrium. After 300 hours the pattern is almost completely stable, either cells are at the high or at the low equilibrium. This speckle pattern distinguishes itself from the others by the high initial growth of the virus in all cells: in other patterns virus levels never reach this high levels before declining to the silenced state.

When siRNA movement increases concentric circles are formed as is the case for the lower silencing efficiency (Figure 4.3E). The number of silenced cells increases compared to the speckle pattern. A relatively low siRNA movement rate results in broad bands of virus infection, a higher rate results in very thin bands.

With still higher siRNA movement the thin bands in which the virus reaches high levels break, and a growing ice crystal-like pattern is observed (Figure 4.3F). The pattern consists of protrusive waves, and in only a small number of cells the virus reaches the high equilibrium. Because the infected spots are much smaller compared to the similar mosaic pattern for low silencing strength there are not enough siRNAs to create truly healthy spots.

With even higher siRNA movement rate the protrusive waves are reduced to a local spot, with the possibility of one or two small outbreaks (Figure 4.3G). For low silencing efficiency we also observed a spot pattern (Figure 4.3C). Low silencing efficiency results in a completely infected spot, while higher silencing efficiency results in a small ring-like pattern.

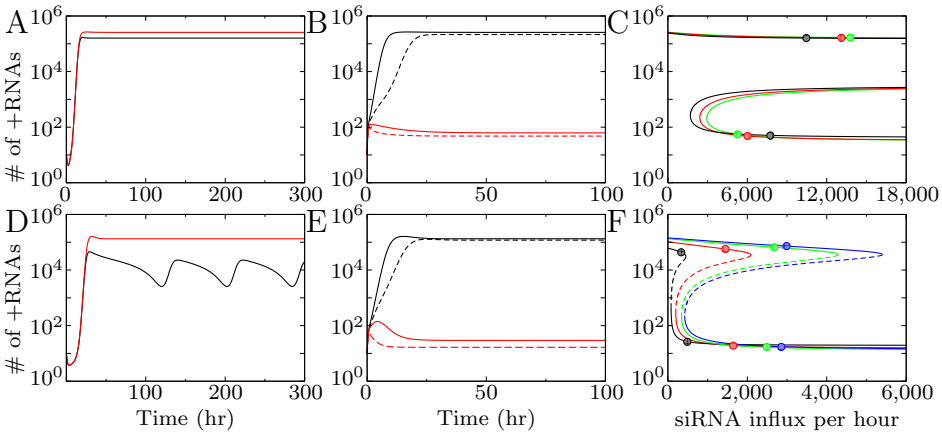

Figure 4.4: The intracellular model with in- and efflux of siRNA and virions. (A-C) low Dicer cleavage rate (5 cleavages per Dicer per hour); (D-F) intermediate Dicer cleavage rate (15 cleavages per Dicer per hour). (A) and (D) time-series for the intracellular model without in and efflux (black) and with efflux (red). (B) and (D) Time-series with in- and efflux showing bistability: low siRNA influx (black lines) results in a high equilibrium, high siRNA influx (red lines) in a low equilibrium. (C) and (F) Bifurcation diagram showing equilibrium values of viral plus-strand RNA for increasing siRNA influx. The different lines are calculated with a fixed virion influx measured for the different patterns in Figure 4.3. ΔSi in (C) from left to right lines: 5% (black), 8% (red), 10% (green); and in (F) from left to right: 0.5% (black), 2% (red), 4% (green), 5% (blue). Circles indicate the position of cells that reached the high and the low equilibrium in the tissue model.

4.3.4 Alternative equilibria depend on influx of siRNAs

As shown in the previous section, virus levels in the spatial model can reach two different equilibria, a high and a low one, while in the intracellular ODE model only a single equilibrium exists. The patterns disappear when siRNA movement is stopped, therefore siRNA movement maintains the silenced equilibrium. To analyse the influence of the tissue dynamics on the cellular dynamics mathematically we add in- and efflux of siRNAs and virions to the intracellular model. Efflux is fixed to the movement parameters used in the tissue model. We measure average virion and siRNA influx in the equilibrium for 4 cells from the centre of the tissue and use these as influx values in the intracellular model.

As an example case we take the parameters and measurements for the mosaic-like pattern for low and intermediate silencing strength shown in Figure 4.3B and F. Without in- and efflux virus levels reach a high equilibrium for low silencing strength, and for intermediate silencing strength

intracellular oscillations occur (black lines Figure 4.4A and D). Efflux of siRNAs and virions results in an increase in virus levels and the oscillations disappear (red lines in Figure 4.4A and D). When virion influx is fixed to the average virion influx measured and siRNA influx is added we observe a bifurcation: Depending on siRNA influx two equilibria occur, a high and a low one, corresponding to the equilibria in the spatial model (Figure 4.4B and E). A low siRNA influx results in virus growth to the high equilibrium, high siRNA influx results in growth to the silenced equilibrium.

We calculate bifurcation diagrams as a function of the siRNA influx. In Figure 4.4C we show the bifurcation diagram for low silencing strength. Each line in the bifurcation diagram is calculated with measurements from different patterns. For all measurements only the high equilibrium exists for low siRNA influx, while for higher siRNA influx there are three equilibria: two stable states separated by an unstable state (Figure 4.4C). Depending on the initial conditions and the siRNA influx the virus can either grow to the high or the low equilibrium. The number of virus RNAs in the high and low equilibrium are similar for the bifurcation lines calculated for different siRNA movement rates. However, the siRNA influx needed to reach the low equilibrium (that is, the bifurcation point) shifts to lower siRNA influx values for lower siRNA movement rate. Low siRNA movement rate increases the effect of silencing within the cell, because less siRNAs leave it and a lower siRNA influx is sufficient to reach the silenced state.

In the spatial model both virion and siRNA influx change over time. Therefore not the final siRNA influx but the combined virion and siRNA influx during the growth phase of the virus determine which equilibrium is reached. Once a stable state is reached a change in siRNA influx has no effect on equilibrium values. Only when siRNA influx is dramatically lowered or when a very large amount of virions would be introduced it would be possible to pass the bifurcation point and move from the silenced to the high state.

For intermediate silencing strength the bifurcation diagram is similar, however due to the lower siRNA efflux and the stronger silencing response within the cell, it is shifted toward lower siRNA influx. The high and the low equilibrium are connected, meaning that an increase in siRNA influx results in a shift from the high equilibrium to the low one. This is the case in the speckle pattern: all cells initially expand to the high equilibrium, but some cells decline to the silenced state later in infection.

To indicate the measured siRNA influx from the patterns shown in

Figure 4.3, we placed circles in the bifurcation diagrams for two high and two low cells (Figure 4.4C and F). For most patterns the equilibrium values are far from the bifurcation points, resulting in a stable pattern unaffected by noise. For the speckle pattern the values are close to the bifurcation point. A slight increase in siRNA influx can push a cell with high virus levels to the silenced state. On the other hand a slight decrease in siRNA influx can result in growth from the silenced state to the high equilibrium. The resulting pattern is at a delicate balance: cells that reach the high equilibrium suppress virus growth in neighbouring cells, and the silenced cells cause a low enough siRNA influx into the cell to stay at the high state.

Concluding, the effect of siRNA influx from neighbouring cells is two-fold. Firstly, siRNA influx creates two coexisting equilibria; secondly, siRNA influx during the initial growth phase of the virus largely determines which equilibrium is reached.

4.3.5 Combined single- and double-stranded RNA cleavage by Dicer

It has been proposed that Dicer can cleave ssRNA in addition to dsRNA [101]. On the cellular level combined single- and double-stranded cleavage by Dicer results in the diverse skewed siRNA ratios that have been observed [58, 66, 101, 115]. Although combined Dicer cleavage of single- and double-stranded RNA can clear the virus for lower Dicer cleavage rates, it can also be less efficient. For the same total Dicer cleavage rate dsRNA cleavage results in somewhat lower plus-strand RNA levels then combined single- and double-strand cleavage [58]. This is due to the skewed siRNA ratio: many siRNAs are produced that target the minus-strand, but few siRNAs are produced that target the plus-strand. This bias results in slightly less efficient silencing, however when the minus strand is completely degraded, the virus is cleared despite the less efficient response.

The complex feedbacks between the intracellular and the spatial model result in an unexpected effect of ssRNA cleavage in the spatial model. While keeping total Dicer cleavage rate constant, increasing ssRNA cleavage by Dicer shifts the silenced equilibrium to higher RNA levels. An increase of virus levels in the silenced equilibrium results in less pronounced patterns and it can even result in disappearance of the silenced state. In Figure 4.5D-F we show patterns for increasing rates of ssRNA cleavage by Dicer 300 hpi. The patterns change from circles to mosaic-like, and the silenced cells change from a dark to a red colour, indicating higher virus

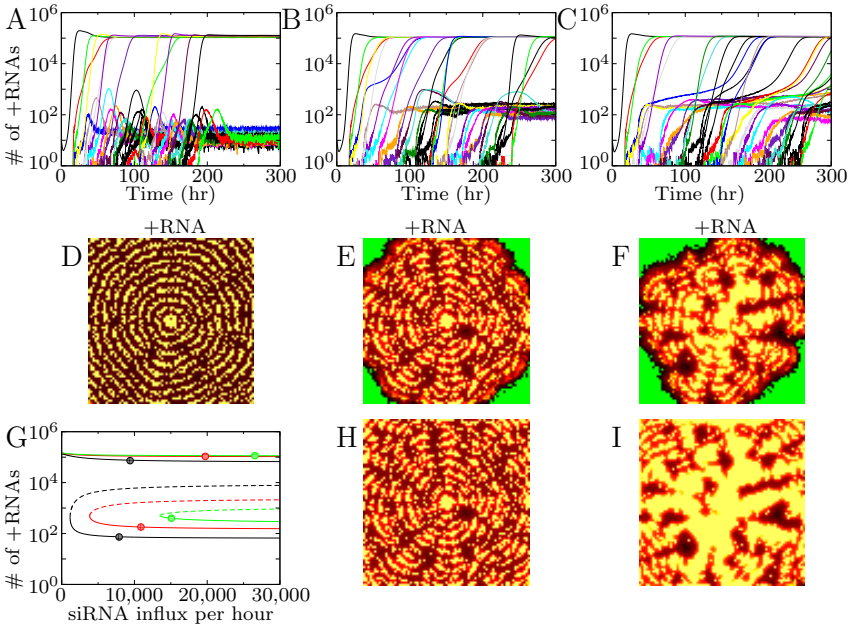

Figure 4.5: Effect of ssRNA cleavage by Dicer on intracellular dynamics and infection patterns. Total Dicer cleavage rate is 10 cleavages per Dicer per hour and ΔSi =4%. (A-C) measured intracellular +RNA levels from spatial model with Dicer cleavage rates: (A) 10 on dsRNA, 0 on ssRNA; (B) 8.5 on dsRNA, 1.5 on ssRNA; (C) 8.05 on dsRNA, 1.95 on ssRNA. (D-E) The infection patterns corresponding to (A-C). Shown are +RNA levels 300 hpi. (G) Bifurcation diagram of intracellular +RNA levels for increasing siRNA influx. The different lines are calculated with parameters from (A) black; (B) red; and (C) green. Circles indicate the position of 2 cells from the spatial model that reached the high or low equilibrium. (H and I) infection patterns showing +RNA levels corresponding to (B) and (C) 450 hpi. Colours according to the colour-ramps in Figure 4.2.

levels in silenced cells. This effect becomes more clear later in infection (Figure 4.5H). Moreover, the infection pattern shown in Figure 4.5F fades out (at 450 hpi, shown in Figure 4.5I), and eventually the entire tissue becomes fully infected.

In Figure 4.5A-C we show how the equilibria change when changing ratio's of double- to single-stranded RNA cleavage by Dicer. We keep total Dicer cleavage rate constant at 10 cleavages per Dicer per hour. To explain the observed siRNA ratios approximately 0-20% of Dicer cleavages should take place on ssRNA [58]. In Figure 4.5A 5% of Dicer cleavages is on ssRNA and in Figure 4.5B 15%. The silenced state clearly shifts to

higher virus levels when ssRNA is cleaved. When more ssRNA is cleaved the equilibrium shifts further upwards until it disappears. In Figure 4.5C we show the behaviour for 19.5% ssRNA cleavage by Dicer, at 20% ssRNA cleavage the silenced state has completely disappeared. The upwards shift of viral RNA levels implies that virus replication is not completely silenced. Indeed dsRNA is produced in the silenced cells.

These results are explained further in the bifurcation diagram in Figure 4.5G. Shown are the equilibrium values of plus-strand RNA as a function of siRNA influx. The different lines represent a varying fraction of ssRNA cleavage by Dicer. The virion influx increases for increasing ssRNA cleavage by Dicer and the silenced state shifts upwards. Additionally, an increasingly higher siRNA influx is needed to reach this equilibrium. The dots indicate the location of cells from the spatial model that reach the high and the low equilibrium. Due to increased siRNA levels the siRNA influx is increased when ssRNA is cleaved by Dicer. However, due to the less efficient silencing within cells, an increasingly higher siRNA influx is needed to reach the silenced state.

This means that, although combined single- and double-stranded RNA cleavage by Dicer can clear the virus at lower Dicer cleavage rate [58], the slight increase in virus equilibrium is disadvantageous at the tissue level as RNA silencing can no longer fully suppress virus replication in silenced cells. However, an advantage of single strand cleavage by Dicer is the slower rate of spread over the tissue.

4.3.6 Effect of amplification

Amplification of silencing through RDR can decrease viral levels in plants [106, 121, 166]. It also affects symptoms observed: plants without a functional RDR become fully infected or die, while plants with RDR show mild chlorosis or mosaic [161, 163].

To study the effect of the secondary response on pattern formation and virus levels we add amplification to the model. At the cellular level RNA silencing with unprimed amplification can clear the virus for much lower silencing strength. Primed and guided amplification can increase oscillations and create a new region of behaviour, in which the virus is degraded after an initial growth peak. It has to be noted that primed amplification can only be beneficial when there is a net siRNA gain [58]. At low Dicer cleavage rate the virus equilibrium is slightly decreased on the cellular level. In the spatial model the addition of amplification can result in a change of patterns (Figure 4.6A). Without amplification almost the

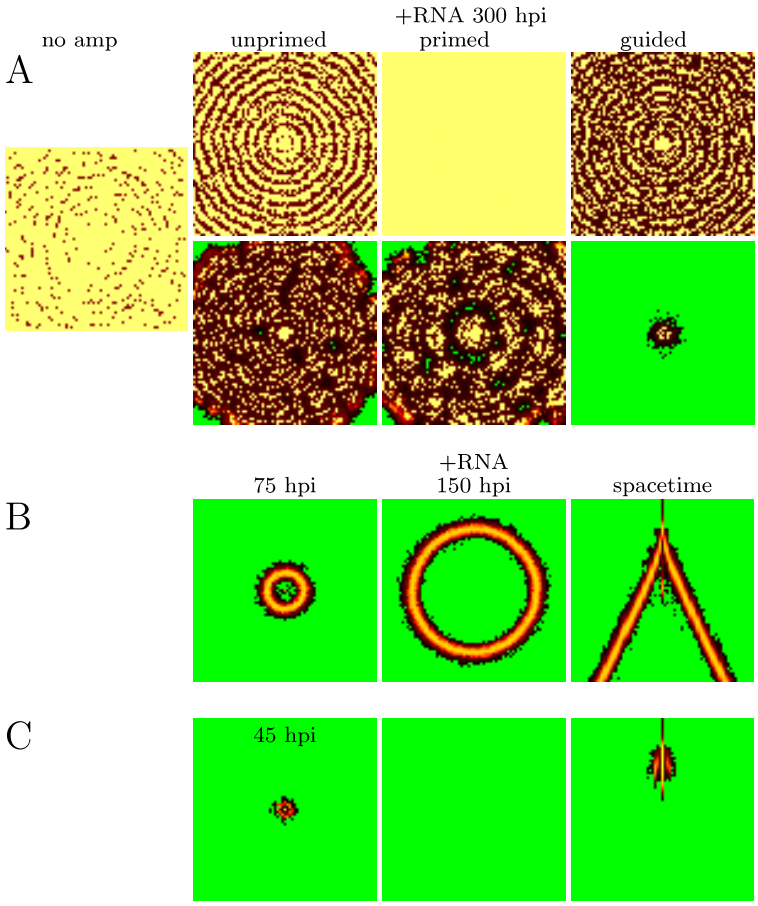

Figure 4.6: Infection patterns with different types of amplification. (A) low double-strand Dicer cleavage rate (5 cleavages per Dicer per hour). Top row shows screen-shots for 1 siRNA per amplified transcript, bottom row 4 siRNAs per amplified transcript. siRNA movement is 4%. Amplification can reduce virus infection to mosaic or circle patterns, while it infected almost the entire tissue without amplification. (B-C) New patterns for intermediate double-strand Dicer cleavage rate (15 cleavages per Dicer per hour) and amplification. (B) zero siRNA movement results in a growing circle that leaves uninfected tissue behind; (C) 5% siRNA movement results in the appearance and disappearance of a spot. Parameters used: (B) primed amplification with 4 siRNAs per amplified transcript; (C) guided amplification with 4 siRNAs per amplified transcript. Colours according to the colour-ramps shown in Figure 4.2.

complete area becomes infected with the virus, with amplification circles or mosaic-like patterns can occur.

Concluding, for low silencing strength amplification has a similar effect to increasing silencing strength or siRNA movement.

New patterns can be observed when the virus is cleared after an initial growth peak at the cellular level. Because the virus can expand and produce virions initially, it is able to spread over the tissue. However, in each cell the virus will be completely degraded by the RNA silencing response. We therefore observe transient patterns that leave healthy tissue behind. These patterns are shown in Figure 4.6B and C. Without siRNA movement a single growing ring occurs, low siRNA movement can lead to a disappearing spot near the infected site. These results indicate that a strong feedback can result in transient infection patterns. When siRNA movement is higher, the feedback becomes smaller due to the efflux of siRNAs, and infection patterns as shown in Figure 4.3 and 4.6A occur.

4.4 Conclusions

We have shown that RNA silencing causes local differences in virus accumulation that can be the basis of different virus symptoms developed in plants. We have studied all qualitatively different patterns that can occur for different parameter values.

When siRNAs spread from cell to cell, we observe patterns that can spread over the entire tissue and consist of alternating healthy and infected tissue. When siRNAs are able to spread quickly we observe localised spots around the infection site. The presence of a secondary response can result in transient patterns that leave healthy tissue behind. In accordance with our results, it has been shown that in absence of a secondary response tissue can get fully infected, while with secondary response patterns develop [161, 163]. The initial appearance of patterns that slowly fade until the entire tissue is infected occurs only when ssRNA is cleaved by Dicer.

In plants a variety of chlorotic patterns caused by viral infection have been observed. Chlorotic tissue contains high virus levels [32]. Some of the patterns of our model resemble infection patterns in plants. When silencing is weak the entire leaf area becomes infected, corresponding to chlorosis of the entire leaf.

When silencing is stronger we observe a mosaic-like pattern that resembles symptoms observed for many mosaic viruses. A difference with the experimentally observed patterns and our simulated patterns is the

scale. We only observe larger scale mosaic when silencing strength is low. When silencing strength is high or when the secondary response is active we observe a small scale mosaic pattern. Our model, however, does not include growth of the tissue, and it has been shown that the healthy spots in mosaic-like patterns come about from cell division of single cells or a cluster of a few cells (reviewed in [32]). Development and growth of our small scale mosaic-like pattern could result in the experimentally observed large scale patterns.

In our model local spots occur when siRNA movement and silencing strength are sufficiently high. The virus infection stays localised to the area around the initially infected cell. We observe two types of spots: spots that are completely infected and ring spots that have a circle of low virus levels in between high levels. Lesions and ring spots are very common local symptoms after inoculation.

Ring patterns similar to our concentric rings have been observed for Tomato ringspot virus [73]. In contrast to our rings, this pattern does not spread over the entire tissue. This could be due to a long range silencing signal that we have not included in our model. Ringspot viruses can also give rise to a large single ring-like spot that resembles the single growing ring that we observed. Tissue at the leading edge of virus infection is infected, tissue in the centre of the ring is healthy. We observe this pattern only when there is a very strong feedback, as for example a secondary response.

We have used a detailed model of both intra- and inter-cellular dynamics of virus replication and RNA silencing. Nevertheless we were able to analyse mathematically (by bifurcation diagram) the intracellular dynamics that lead to alternative equilibria underlying the formation of infection patterns in plants. We have shown that siRNA movement is the driving force behind the pattern formation observed. Additional experiments and parameter validation is necessary to study specific cases and to investigate if siRNA movement in plants is responsible for the formation of infection patterns on leafs.

In conclusion, we have shown that the interplay of RNA silencing and virus growth within a cell, and the spread of virions and siRNAs between cells can explain the variety of viral infection patterns observed in plants.

Acknowledgements

The authors thank Milan van Hoek and Stan Marée for valuable discussions. This work was supported by the Netherlands Organisation for Sci-

entific Research (NWO) through Grant 050.50.202 of the BioMolecular Informatics program.

4.5 Appendix

Intracellular dynamics

The entire intracellular model:

RdRP
$$\frac{dR}{dt} = \frac{rP}{(P+k_t)} - d_r R - \{o(1-f)P + ofM + o_d D_m\}\mathcal{F} + hD_p + hR_a + \mathcal{G}_d(D_p + R_a) \tag{4.1}$$

+RNA
$$\frac{dP}{dt} = -o(1-f)P\mathcal{F} + hD_p + hR_a - dP - \frac{vP^5}{k_v^5 + P^5} - \frac{b_2 R_m P}{P+k_{ri}} - \mathcal{G}_{p,m}P - \frac{b_2 R_{sm} P}{P+k_{ri}} - \mathcal{A}_u P - \mathcal{A}_p(Si_m + Sis_m)P - \mathcal{A}_g(Si_m + Sis_m)P \tag{4.2}$$

−RNA
$$\frac{dM}{dt} = -ofM\mathcal{F} + hD_p + hD_m(1 - \frac{1}{D_m})^{(R_a - D_m)} - dM - \frac{b_2 R_p M}{M+k_{ri}} - \mathcal{G}_{p,m}M - \frac{b_2 R_{sp} M}{P+k_{ri}} - \mathcal{A}_u M - \mathcal{A}_p(Si_p + Sis_p)M - \mathcal{A}_g(Si_p + Sis_p)M \tag{4.3}$$

Virions
$$\frac{dV}{dt} = \frac{vP^5}{k_v^5 + P^5} - d_v V \tag{4.4}$$

dsRNA
$$\frac{dD_p}{dt} = o(1-f)P\mathcal{F} - hD_p - \mathcal{G}_d D_p \tag{4.5}$$

dsRNA
$$\frac{dD_m}{dt} = ofM\mathcal{F} - hD_m(1 - \frac{1}{D_m})^{(R_a - D_m)} - \mathcal{G}_d D_m \tag{4.6}$$

act.RdRP
$$\frac{dR_a}{dt} = ofM\mathcal{F} + o_d D_m \mathcal{F} - hR_a - \mathcal{G}_d R_a \tag{4.7}$$

+siRNA
$$\frac{dSi_p}{dt} = \mathcal{G}_{p,m}P + 0.5\mathcal{G}_d(D_p + D_m) - d_{si}Si_p - b_1 Si_p R_f - \mathcal{A}_p Si_p M \tag{4.8}$$

−siRNA
$$\frac{dSi_m}{dt} = \mathcal{G}_{p,m}M + 0.5\mathcal{G}_d(D_p + D_m) - d_{si}Si_m - b_1 Si_m R_f - \mathcal{A}_p Si_m P \tag{4.9}$$

free RISC
$$\frac{dR_f}{dt} = i - d_r R_f - b_1 R_f(Si_p + Si_m) \tag{4.10}$$

+RISC
$$\frac{dR_p}{dt} = b_1 R_f Si_p - d_r R_p \tag{4.11}$$

−RISC
$$\frac{dR_m}{dt} = b_1 R_f Si_m - d_r R_m \tag{4.12}$$

$$\text{dsRNA amp} \quad \frac{dD_e}{dt} = \mathcal{A}_u(P+M) + \mathcal{A}_p((Si_m + Sis_m)P + (Si_p + Sis_p)M) + \mathcal{A}_g((Si_m + Sis_m)P + (Si_p + Sis_p)M) - \mathcal{G}_d D_e \tag{4.13}$$

$$\text{sec. } +\text{siRNA} \quad \frac{dSis_p}{dt} = 0.5\mathcal{G}_d D_e - d_{si} Sis_p - b_1 Sis_p R_f - \mathcal{A}_p Sis_p M \tag{4.14}$$

$$\text{sec. } -\text{siRNA} \quad \frac{dSis_m}{dt} = 0.5\mathcal{G}_d D_e - d_{si} Sis_m - b_1 Sis_m R_f - \mathcal{A}_p Sis_m P \tag{4.15}$$

$$\text{sec.} + \text{Risc} \quad \frac{dR_{sp}}{dt} = b_1 Sis_p R_f - d_r R_{sp} \tag{4.16}$$

$$\text{sec.} - \text{Risc} \quad \frac{dR_{sm}}{dt} = b_1 Sis_m R_f - d_r R_{sm} \tag{4.17}$$

The biological meaning of the variables is mentioned to the left of the equations. Multiple RdRPs can bind to minus-strand RNA, we refer to these as 'active RdRPs'. +RISC and -RISC are RISC loaded with siRNA with a plus- or minus-strand polarity. The abbreviation 'sec.' stands for secondary and is used to indicate siRNA that is produced through a secondary amplification pathway. Secondary RISC is loaded with secondary siRNA.

All parameter values can be found in Table 4.1, as well as a short description of each parameter. The other terms $\mathcal{F}$, $\mathcal{G}$ and $\mathcal{A}$ are functions for the complex formation between RdRP and RNA strands, Dicer cleavage and amplification, respectively.

The complex formation ($\mathcal{F}$) between RdRP and RNA strands is saturated for both viral RNA and RdRP (the Beddington-DeAngelis functional response [9, 35]):

$$\mathcal{F} = \frac{oR}{R + P + M + D_m + k_r} \tag{4.18}$$

Dicer can cleave double-stranded and single stranded RNA and is saturated for D_e, D_p, D_m, P and M. The Dicer cleavage functions, one for cleaving dsRNA and one for ssRNA, are saturated according to the ratio between single- and double-stranded RNA cleavage (q) by Dicer:

$$\mathcal{G}_d = \frac{(1-q)c_d D_i}{(1-q)(D_p + D_m + D_e) + q(P+M) + k_d} \tag{4.19}$$

$$\mathcal{G}_s = \frac{qc_s D_i}{(1-q)(D_p + D_m + D_e) + q(P+M) + k_d} \tag{4.20}$$

The amplification terms are:

$$\mathcal{A}_u = \frac{a_u}{(P+M+k_a)} \tag{4.21}$$

$$\mathcal{A}_g = \mathcal{A}_p = \frac{a_{p,g}}{((Si_p+Sis_p)M+(Si_m+Sis_m)P+k_a)} \tag{4.22}$$

Where $\mathcal{A}_u$ is unprimed amplification, $\mathcal{A}_p$ is primed amplification and $\mathcal{A}_g$ is guided amplification. We study the amplification pathways separately. In the case of guided amplification, the siRNAs are not removed when they guide amplification, in contrast to primed amplification. Amplification produces dsRNA that is not used for virus replication (D_e). This dsRNA is degraded into secondary siRNAs with a plus- or minus-strand polarity; Sis_p and Sis_m respectively.

Parameters

For the intracellular dynamics we use the parameters previously described [58]. Parameter values can be found in table 4.1. The only intracellular parameter that we vary in this study is the cleavage rate by Dicer (0 to 15 cleavages per Dicer per hour), because it is representative for a general increase in strength of the silencing response [58].

The extra parameters of the spatial model are the percentages of siRNAs and virions that move out of a cell (0 to 10% per hour), and virion unpacking rate.

Table 4.1: Parameter values used. #mol is number of molecules.

Model	Par.	Meaning	Value	units
Intracellular	r	maximum translation rate x #ribosomes	15*5000	#mol hr^{-1}
	o	max rate of complex formation ssRNA	1	hr^{-1}
	o_d	max rate of complex formation dsRNA	100	hr^{-1}
	f	ratio of binding plus or minus RNA	0.9	-
	h	dsRNA-RDR splitting rate	10	hr^{-1}
	v	max virion production rate	500	#mol hr^{-1}
	D_i	number of Dicer molecules	500	#mol
	c_d	max Dicer cleavage rate for dsRNA	0-15	#mol hr^{-1}
	c_s	max Dicer cleavage rate for ssRNA	0-10	#mol hr^{-1}
	b_1	rate of RISC activation	0.005	#mol $^{-1}$ hr^{-1}
	b_2	RISC target cleavage rate	20	#mol $^{-1}$ hr^{-1}
	i	translation of RISC	100	#mol hr^{-1}
	a	amplification (a_u, a_p and a_g)	100	#mol hr^{-1}
	d_r	decay RdRP and RISC	0.1	hr^{-1}
	d	decay viral ssRNA	0.5	hr^{-1}
	d_{si}	decay siRNA	2	hr^{-1}
	d_v	decay virions	0.1	hr^{-1}
	k_v	saturation of virion production	10,000	#mol
	k_d	saturation of Dicer cleavage	10,000	#mol
	k_t	saturation constant for translation	1,000	#mol
	k_{ri}	saturation of RISC cleavage	1,000	#mol
	k_r	saturation of complex formation	1,000	#mol
	k_a	saturation amplification	1000	#mol
Spatial	ΔSi	percentage of siRNAs exiting the cell	0-10	hr^{-1}
	ΔV	percentage of virions exiting the cell	1	hr^{-1}
	u	unpacking rate of virions	2	#mol hr^{-1}

CHAPTER 5

Viral suppression of RNA silencing

Marian Groenenboom and Paulien Hogeweg
Theoretical Biology/Bioinformatics Group, Utrecht University
Padualaan 8, 3584 CH Utrecht, The Netherlands.

In preparation

Abstract

Virus infection in plants is limited by RNA silencing. In turn, viruses can counter RNA silencing with virus encoded silencing suppressors. Silencing suppressors have shown to play a role in symptom devellopment in plants. We here study four different strategies employed by silencing suppressors: siRNA binding, dsRNA binding, degrading Argonaute and inactivating Argonaute. To study the effect of the suppressors on viral accumulation and spread we use a combination of an intracellular and spatially explicit model that couples the cells. We show that the effectiveness of a suppressor within the cell cannot predict the effect of the suppressor at the tissue level. This is the case for suppressors that target Argonaute: they increase virus levels at the intracellular level, but can hinder virus spread on the tissue due to raised siRNA levels. Additionally, we show that targeting dsRNA is more efficient than targeting only siRNA and that dsRNA targeting is the only strategy that is able to protect the virus against a stronger silencing response.

5.1 Introduction

Viruses infect all life and often damage their host for their own benefit of replication. Hosts develop ways to fight off viruses, but viruses in turn develop counter-mechanisms against the host antiviral mechanisms.

RNA silencing is an evolutionary conserved mechanism that has an antiviral role in plants and insects (reviewed in [97, 150]). Viral dsRNA is cleaved into small interfering RNA (siRNA) by RNase III-like nucleases called Dicer of Dicer-like. These siRNAs are referred to as primary siRNAs. siRNAs associate with multiple proteins, one of which is an Argonaute protein (AGO), to form the siRNA-RISC complex. Argonaute cleaves one of the siRNA strands (the 'passenger' strand), triggering unwinding of the other, 'guide' strand and activating the siRNA-RISC complex [86]. The active complex uses the siRNA as guide to target and cleave the homologous viral RNA. Secondary siRNAs can be produced through amplification pathways that use host encoded RNA-dependent RNA polymerase (RDR). The silencing signal, most likely siRNA, is able to spread from cell-to-cell inhibiting spread of the virus ([63] and Chapter 4).

Viruses have developed a variety of silencing suppressors that act on different parts of the RNA silencing pathway. One widespread strategy is the sequestering of siRNAs, inhibiting the formation of active RISC and

preventing spread from cell-to-cell. siRNA binding by silencing suppressors has most likely evolved independently in different virus genera, for example P15 in pecluviruses, γB in hordeiviruses, P21 in closteroviruses, HC-Pro in potyviruses and P19 in tombusviruses [98].

Other virus encoded silencing suppressors can bind all lengths of dsRNA, sequestering siRNAs as well as preventing dsRNA cleavage [98]. Examples are CP (or P38) of *Turnip crinkle virus* a carmovirus, and P14 of *Pothos latent virus* an Aureusvirus.

Many silencing suppressors target siRNA or dsRNA directly. There are however two known suppressors that interact with plant Argonaute, AGO1. Silencing suppressor P0 of *Polerovirus* has shown to be a strong suppressor of RNA silencing in a transient expression assay with a GFP transgene [117]. Recently it has been shown that P0 binding to AGO1 triggers AGO1 degradation, resulting in a failure in the assembly of active RISC [8, 13]. The 2b suppressor of *Cucumber mosaic virus* also targets AGO1. However, 2b does not interfere with the ability of AGO1 to associate with siRNA. It is therefore suggested that 2b blocks the ability of AGO1 to cleave the passenger strand of the siRNA, leading to an inactive AGO1-siRNA complex [169]. This hypothesis is supported by the observation that the 2b suppressor suppresses secondary siRNA accumulation [37].

Most silencing suppressors were previously known as pathogenic factors, before their function was known. Because the endogenous pathways of silencing share components with antiviral silencing, it could be the case that silencing suppressors interfere with host gene regulation through microRNA (miRNA) resulting in virus induced symptoms and developmental phenotypes. Indeed, interaction of silencing suppressors with Argonaute affects the endogenous miRNA pathway of the host, resulting in severe abnormalities in development [8, 13]. Although siRNA binding suppressors bind only double-stranded complexes, both P21 and P19 have shown to interfere with miRNA expression, most likely by binding miRNA precursors [21, 116]. CP, a dsRNA binding suppressor, weakly inhibited the miRNA pathway which could explain the developmental phenotypes observed due to CP expression [21]. These results indicate that silencing suppressors contribute to viral induced symptoms by interfering with the miRNA pathway.

Previously we studied antiviral RNA silencing within the cell [58]. We have shown that a change in Dicer cleavage rate is representative for a general change in silencing strength. Depending on the Dicer cleavage rate the virus equilibrium can be almost unaffected, oscillations can occur, or the

virus can be cleared. For a low Dicer cleavage rate the equilibrium amount of virus is slightly decreased and the virus grows slower than without silencing. For high Dicer cleavage rate the virus is not able to grow and is cleared directly after introduction. For intermediate Dicer cleavage rates oscillations in virus levels can occur. The secondary response of RNA silencing can increase these oscillations to such extend that the virus is cleared after a single growth peak. We have also studied antiviral silencing within cells in combination with the spread of viruses and a silencing signal on a tissue (Chapter 4). The movement of siRNAs can suppress viral growth in some cells, while the virus is able to grow in other cells. The patterns that arise are very similar to chlorotic patterns observed in plants, confirming the hypothesis that RNA silencing can be responsible for virus symptoms on plant leaves. Although we have studied various aspects of antiviral RNA silencing we did not study the effect of silencing suppressors, while they are very important in symptom development in plants.

We here extend our previous models with silencing suppressors encoded by viruses. We study efficacy of the different types of suppressors and the effect the suppressors have on cellular and tissue level dynamics. We find that silencing suppressors can indeed increase intracellular virus levels, which results in increased spread of the virus over the tissue. Unexpectedly, targeting Argonaute can decrease virus spread over the tissue, while it does increase virus levels at the cellular level. We show that binding dsRNA or targeting Argonaute is especially effective against the secondary response of RNA silencing.

5.2 Methods

The model takes both intracellular and tissue-level dynamics into account.

The intracellular model consists of a replicating plus-strand RNA virus and the RNA silencing pathway [58]. A schematic representation of the model is shown in Figure 5.1. The equations (see Section 5.5) describe the dynamics of viral plus- and minus-strand RNA, dsRNA, RNA-dependent RNA polymerase, virions, primary and secondary siRNAs, RISC, and Argonaute. Viral plus-stranded RNA is translated into a poly-protein, that is auto-cleaved into separate proteins. One of the proteins is RNA-dependent RNA polymerase (RdRP). RdRP associates with plus-strand RNA to synthesise a complementary strand, and forms a dsRNA complex. The dsRNA separates into a plus- and minus-strand that can both associate with RdRP again. RdRP has a higher affinity for minus-strand RNA, and multiple

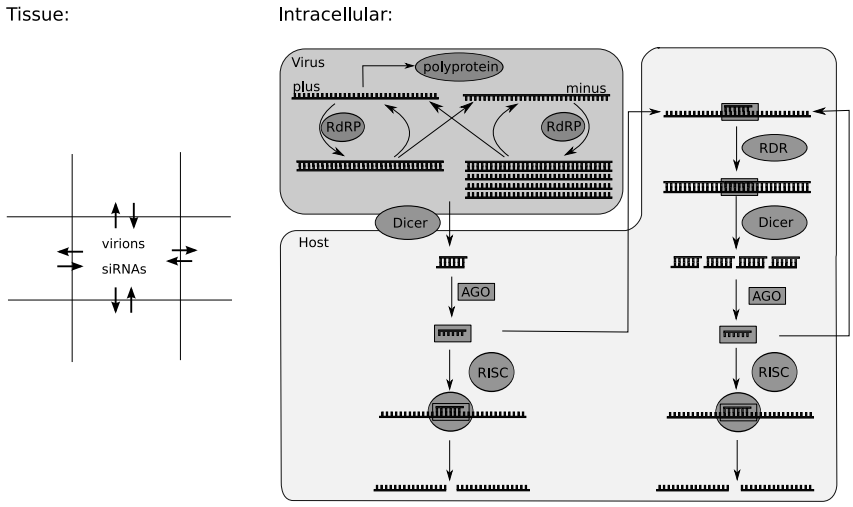

Figure 5.1: Schematic representation of the model. For each cell on the tissue the intracellular dynamics are calculated. Viral plus-strand RNA is translated into RdRP, which replicates plus- and minus-strand RNA. Viral single- or double-stranded RNA is cleaved into siRNA by Dicer. siRNA associates with Argonaute (AGO) and one strand is disposed. The Argonaute-siRNA complex associates with other proteins to form RISC, and cleaves the target RNA. The secondary response involves production of dsRNA by host encoded RDR. Amplification can be unprimed, primed or guided by the Argonaute-siRNA complex. siRNAs and virions move from cell to cell on the grid. A description and the equations of the model can be found in Section 5.5.

RdRPs can produce plus-strand RNA from a single minus-strand template. This phenomenon is known as semi-conservative synthesis of plus-stranded RNA. Plus-stranded RNA is packaged in virions, we use here a function of the number of plus-stranded RNA instead of modelling a separate coat protein.

Viral double- or single-stranded RNA is degraded into siRNAs. siRNAs can have a plus- or minus-strand polarity and will target only the plus- or minus-strand. siRNAs can bind to Argonaute and form the siRNA-Argonaute complex. This complex can bind to the other components of RISC to form the active RISC complex. Via RISC the siRNAs cause degradation of viral RNA.

We include the RNA silencing secondary response in the model, in which host encoded RDR synthesises dsRNA from viral templates. This amplification can be unprimed, or primed or guided by the siRNA-Argonaute complex. In the case of unprimed amplification RDR synthesises

dsRNA from plus- or minus-strand viral RNA. Primed amplification takes place when the siRNA-Argonaute complex binds to virus plus- or minus-strand RNA and triggers RDR to synthesise dsRNA. Guided amplification is similar to primed amplification, only the siRNA-Argonaute complex does not bind to the RNA, but is merely a guide. In guided amplification one siRNA-Argonaute complex can guide amplification of multiple transcripts. We study each type of amplification separately.

To study RNA silencing and viral infection in a tissue we use a spatial model (described in Chapter 4). The grid represents a number of coupled plant cells. For each cell the intracellular dynamics are calculated using the model described above. Virions can move to the four neighbouring cells. We move a finite number of virions to neighbouring cells to avoid the triggering of viral replication by incomplete particles. Virions are unpacked into plus-strand RNA. The spread of siRNAs is implemented in the same way.

We extend the intracellular model with equations for virus encoded silencing suppressors. All types of suppressors are translated from the plus-strand with the same rate as RdRP, and decay with a fixed rate. Silencing suppressors do not move from cell-to-cell. We study four groups of silencing suppressors: siRNA binding, dsRNA binding, Argonaute decay and Argonaute inactivation.

The siRNA binding suppressor associates with primary and secondary siRNAs that target the plus- or minus-strand. siRNA that associated with the suppressor become inactive and are removed from the siRNA pool. The altered equations can be found in Appendix 5.5.2.

The second type of suppressor binds to all types of siRNA, dsRNA produced by the virus during replication, and dsRNA produced through the secondary silencing response. The viral dsRNA-suppressor complex splits in plus- and minus-strand RNA, RdRP and suppressor. Dicer is not able to cleave siRNA from a dsRNA-suppressor complex. All siRNAs and dsRNA produced by the secondary pathway become inactive when bound to the suppressor. The altered equations can be found in Appendix 5.5.3.

The suppressor that targets Argonaute for decay binds to Argonaute and the suppressor-Argonaute complex is removed from the Argonaute pool. The equations can be found in Appendix 5.5.4.

The last suppressor inactivates Argonaute by binding to it. The Argonaute-suppressor complex binds primary and secondary siRNA as a normal Argonaute. The siRNAs that bind to the suppressor-Argonaute complex become inactive and are removed. The equations can be found

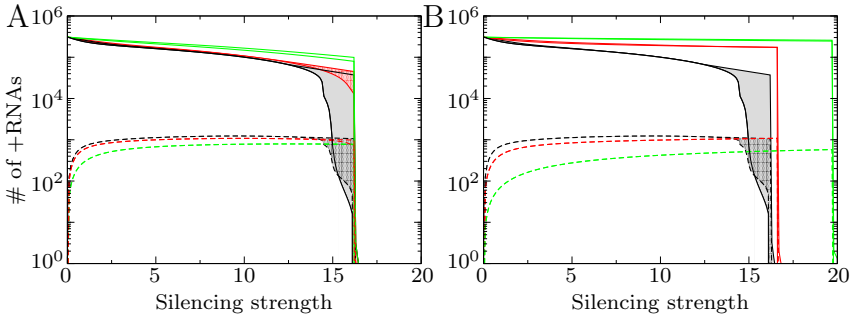

Figure 5.2: Effect of a siRNA and dsRNA binding suppressors on intracellular RNA silencing. Shown are the number of plus-strand RNAs (solid lines) and the total number of free siRNAs (dashed lines) 300 hours post infection for increasing silencing strength (Dicer cleavage rate). (A) Results for a siRNA binding suppressor and (B) for a dsRNA binding suppressor. Black lines: no silencing suppressor; red lines: with silencing suppressor, binding rate to siRNA or dsRNA $w = 0.00001$; green lines: with silencing suppressor, binding rate to siRNA or dsRNA $w = 0.0001$. Oscillations in virus and siRNA levels are observed in the filled areas.

in Appendix 5.5.5.

5.3 Results and Discussion

We study the effect of various silencing suppressors at the cellular and tissue-level. At the cellular level we monitor intracellular virus levels for increasing silencing efficiency with and without suppressors. At the tissue level we study virus spread, and virus and siRNA levels with and without silencing suppressor. We start to study the primary response, and then continue with studying the effect of the different amplification pathways. For simplicity we only study the case where Dicer cleaves dsRNA, and not single-stranded RNA.

5.3.1 Suppressors that target siRNA or dsRNA

siRNA binding by a suppressor can benefit viral growth in three ways. Firstly, siRNAs can no longer associate with Argonaute, resulting in decreased degradation of the virus through RISC. Secondly, siRNAs associated with the silencing suppressor can no longer spread from cell to cell. Thirdly, sequestering of siRNAs prevents the use of siRNAs in secondary pathways. In addition to the advantages of siRNA binding, dsRNA

binding prevents dsRNA cleavage by Dicer and inhibits the production of secondary siRNAs.

Initially, we investigate the effect of siRNA and dsRNA binding suppressors within the cell. We vary Dicer cleavage rate on dsRNA as representative for silencing strength, and monitor the maximum and final virus levels 300 hours post infection. Without silencing suppressor the virus reaches a high equilibrium for low silencing strength, the virus is cleared for a high silencing strength, and levels oscillate for intermediate silencing strength (black lines, Figure 5.2A and B). There is a sharp transition to the region where the virus is cleared, we refer to this point as the 'silencing point'. Dashed lines show siRNA levels. When we add the siRNA binding protein, the virus is able to grow to higher levels, intracellular siRNA levels are reduced and oscillations disappear (red and green lines, Figure 5.2A). However, the suppressor is not able to shift the silencing point to higher silencing strength. The benefit of the siRNA binding suppressor within the cell therefore lies not in defending the virus against a stronger silencing response, but in increasing virus levels when the virus is not cleared by RNA silencing.

When the suppressor binds both siRNA and dsRNA the bifurcation diagrams look different (Figure 5.2B). To compare the results to the siRNA binding suppressor we use the same binding rates as previously. Binding both dsRNA and siRNA is more efficient than binding only siRNA, and results in an increase in viral RNA levels while decreasing siRNA levels 2-10 fold at the same time. Additionally, the dsRNA binding suppressor shifts the silencing point to higher silencing strength, meaning that a stronger silencing response is needed to silence the virus completely. This was not possible when only siRNAs were bound by the suppressor (Figure 5.2A).

Although the siRNA binding suppressor seems rather inefficient at the cellular level, at the tissue level siRNA binding can have two beneficial effects for the virus. Firstly, intracellular virus levels are increased, resulting in more virions and increased viral spread. Secondly, siRNA levels are decreased, limiting the spread of the RNA silencing response. Both effects could increase viral spread.

In Figure 5.3 the effect of a siRNA binding suppressor on a leaf area is shown. 10 strands of virus plus-strand RNA are introduced at the beginning of the simulation in the cell at the centre of the grid. Screenshots are made 300 hours post infection (hpi) for intermediate silencing strength (Dicer cleavage rate is 15 cleavages per hour), or for a low silencing strength (Dicer cleavage rate is 5 cleavages per hour). With intermediate silencing

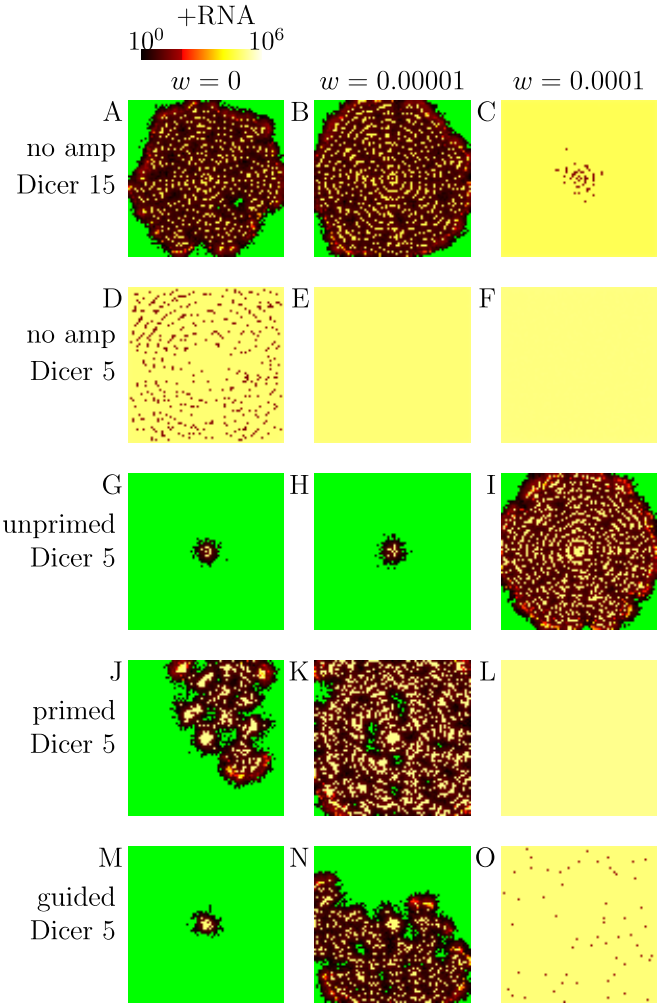

Figure 5.3: Infection patterns 300 hpi with and without siRNA binding suppressor and with different types of secondary responses. The first column shows results without silencing suppressor, the second column with suppressor with binding rate $w = 0.00001$, and in the third column $w = 0.001$. (A-C) screenshots for an intermediate Dicer cleavage rate (15 cleavages per hour) without secondary response; (D-F) screenshots for a low Dicer cleavage rate (5 cleavages per hour) without secondary response; (G-I) screenshots for a low Dicer cleavage rate with unprimed amplification; (J-L) with primed amplification; (M-O) with guided amplification. Colours according to the colour-ramp shown at the top.

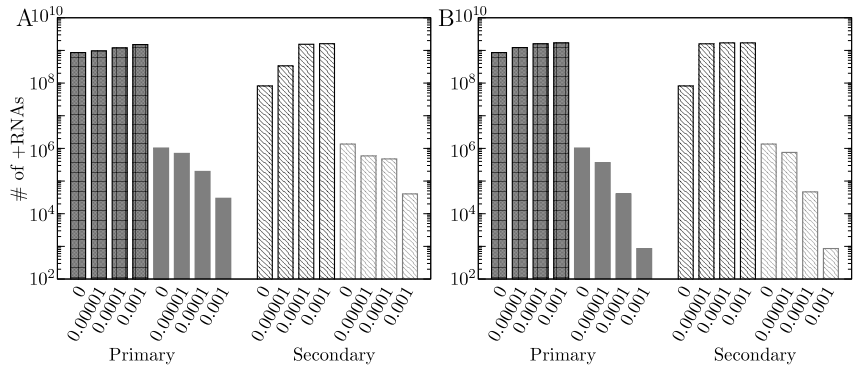

Figure 5.4: Total number of virus plus-strand RNA and free siRNAs present in the entire area 300 hpi. Bars are calculated for different binding rates of the suppressor to siRNA or dsRNA (parameter w). (A) values for different siRNA binding rates and (B) for different dsRNA binding rates of the suppressors. Shown are values for the primary silencing response (5 Dicer cleavages per hour) and for the response with primed amplification. Black bars represent total virus plus-strand RNA levels and grey bars represent siRNA levels. Solid bars show results for the primary silencing response, dashed bars for the response with primed amplification.

strength we observe a mosaic-like pattern that spreads slowly over the entire area (Figure 5.3A). When the virus encodes a suppressor, it is able to spread faster over the area (Figure 5.3B).

However, the strength of the suppressor is not sufficient to increase the number of cells in which the virus can reach high levels. When the strength of the suppressor increases 10-fold the virus spreads faster and reaches high levels in almost all or all cells (Figure 5.3C). When silencing strength is low (Figure 5.3D-F), the silencing suppressor is able to reduce the effect of silencing to such extend that the virus reaches high levels in all cells. Concluding, this strategy of silencing suppression increases virus levels and virus spread over the tissue.

The RNA silencing pathway however, has a secondary pathway that increases its efficiency. It has been shown that siRNA production in antiviral defence strongly depends on the secondary response [39]. We add a strong secondary response (10 siRNAs are produced from one dsRNA) to the primary pathway with a low Dicer cleavage rate. The unprimed secondary response limits viral growth to an initial spot (Figure 5.3G). A weak siRNA binding suppressor is not able to increase virus spread when unprimed amplification is present, but a higher binding rate to siRNA does result in increased spread (Figure 5.3G-I). The siRNA binding suppressor is

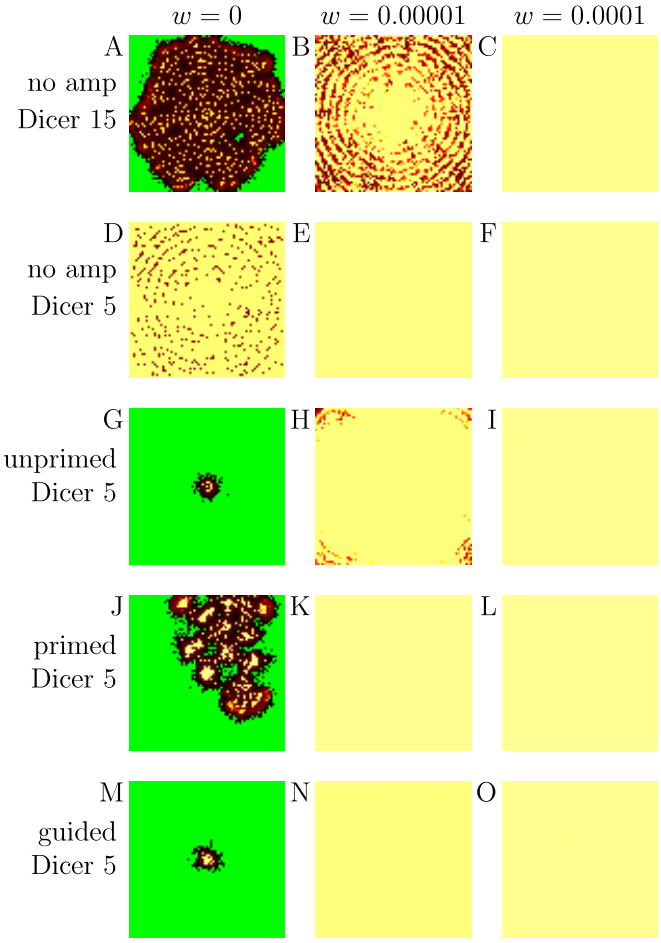

Figure 5.5: Infection patterns 300 hpi with and without dsRNA binding suppressor and with different types of secondary responses. The first column shows results without silencing suppressor, the second column with suppressor with binding rate $w = 0.00001$, and in the third column $w = 0.001$. (A-C) screenshots for an intermediate Dicer cleavage rate (15 cleavages per hour) without secondary response; (D-F) screenshots for a low Dicer cleavage rate (5 cleavages per hour) without secondary response; (G-I) screenshots for a low Dicer cleavage rate with unprimed amplification; (J-L) with primed amplification; (M-O) with guided amplification. Colours according to the colour-ramp shown in Figure 5.3.

more efficient against primed and guided amplification, and increases viral spread for very low binding affinity to siRNA (Figure 5.3J-L and 5.3M-O). This is the case because the number of siRNA-Argonaute complexes is decreased and they are used for primed and guided amplification.

To quantify the effect of the siRNA binding suppressor we measure the total number of viral plus-stranded RNA and the total number of free siRNAs present on the entire leaf area 300 hpi (Figure 5.4A). It is clear that the effect of the suppressor on the primary and secondary response is qualitatively the same. The suppressor increases viral plus-strand RNA levels and decreases the number of siRNAs at the same time. These results indicate that the siRNA binding suppressor is advantageous against both the primary and secondary response.

As at the cellular level the dsRNA binding suppressor performs better at the tissue level than siRNA binding. A lower binding rate is sufficient for the virus to infect the entire tissue (Figure 5.5A-C). This suppressor also copes very well with the RNA silencing secondary response, even with unprimed amplification (Figure 5.5G-O). This is due to the fact that both siRNAs and dsRNA are targeted by the suppressor, and dsRNA binding largely inactivates the secondary response. When the binding rate of the suppressor increases virus spread and virus levels are increased in all cases (Figure 5.4B). Both primary and secondary siRNA levels are decreased considerably (Figure 5.4B). These results are in correspondence with the observation that expression of P14, a dsRNA binding suppressor, does not prevent the accumulation of virus derived siRNAs, but that less siRNA and more viral RNA were detected compared to virus infection without the P14 suppressor [99]. This is also the case for another dsRNA binding suppressor, P38 or CP, that reduces siRNA production in infected tissue [98].

5.3.2 Suppressors that target Argonaute

Targeting Argonaute can have a number of positive effects on viral growth. Degradation or inactivation of Argonaute prevents assembly of the active RISC complex and will decrease viral degradation by the silencing response. Additionally, targeting Argonaute can decrease secondary siRNA production because the siRNA-Argonaute complex is needed for primed or guided amplification. Decreased secondary siRNA accumulation could result in a decreased number of RISC complexes, and decreased spread of siRNAs over the tissue. The inactivation of Argonaute could be more advantageous than the degradation of Argonaute, because a siRNA sink is

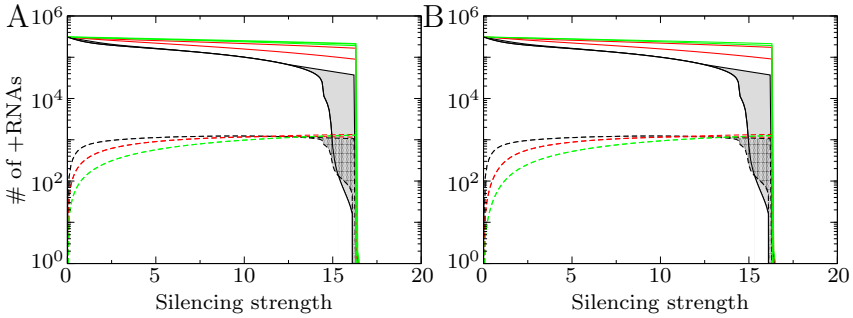

Figure 5.6: Effect of suppressors that target Argonaute on intracellular RNA silencing. Shown are the number of plus-strand RNAs (solid lines) and the total number of free siRNAs (dashed lines) 300 hours post infection for increasing silencing strength. (A) Results for an Argonaute degrading suppressor; and (B) a suppressor that inactivates Argonaute. Black lines: no silencing suppressor; red lines: with silencing suppressor, binding rate to Argonaute $z = 1$; green lines: with silencing suppressor, binding rate to Argonaute $z = 10$. Oscillations in virus and siRNA levels are observed in the filled areas.

created that may prevent primary and secondary siRNA accumulation.

The Argonaute targeting suppressors have very similar effects within the cell (Figure 5.6). Both increase virus levels, and although these suppressors do not target siRNAs, for low Dicer cleavage rates siRNA levels are lowered. This is due to the fact that Argonaute levels are reduced and siRNAs associated with Argonaute have a lower decay rate than free siRNAs. At higher Dicer cleavage rates siRNA levels are no longer decreased. Due to the raised virus levels more siRNAs are cleaved from the virus, and the larger decay experienced by the siRNA pool is no longer able to compensate. The similarity in bifurcation diagrams of suppressors that target Argonaute for degradation or inactivation indicates that the advantage of Argonaute inactivation within the cell is not substantial. Concluding, suppressors that target Argonaute increase intracellular virus levels, but are not always able to decrease siRNA levels.

The balance of these effects becomes important at the tissue level. Again we investigate the effect of the suppressor on a strong and a weak primary RNA silencing response, by studying two different Dicer cleavage rates. Without suppressor and when Dicer cleavage rate is 15 cleavages per hour the virus spreads over the tissue with a mosaic like pattern (Figure 5.7A and 5.9A). The virus reaches high levels in some cells, but is suppressed in most. When the silencing suppressor is present the virus is able to grow to high levels in each cell initially. However, because siRNA levels

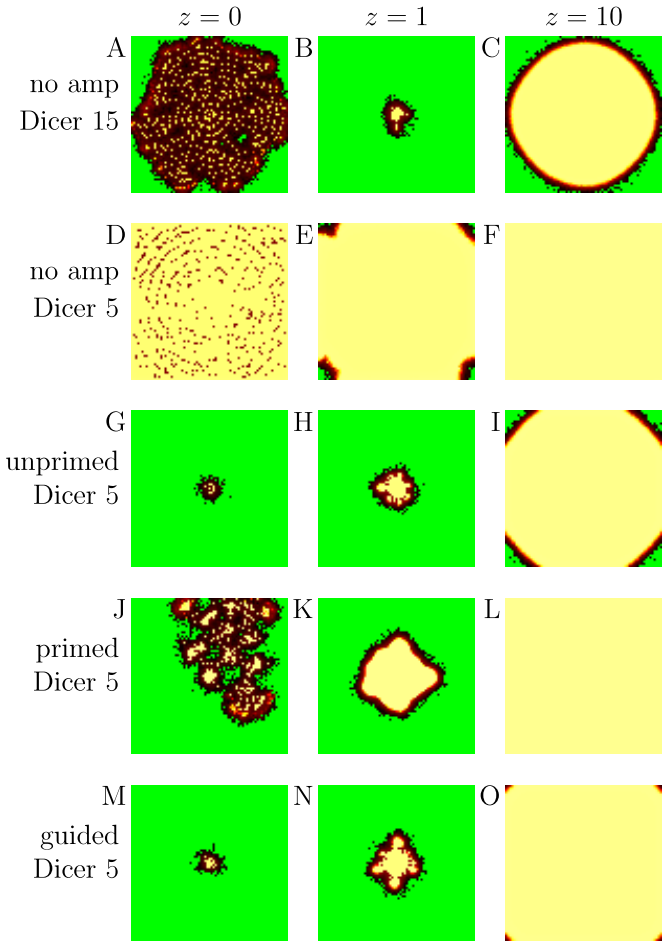

Figure 5.7: Infection patterns 300 hpi with and without Argonaute degrading suppressor and with different types of secondary responses. The first column shows results without silencing suppressor, the second column with suppressor with binding rate $z = 1$, and in the third column $z = 10$. (A-C) screenshots for an intermediate Dicer cleavage rate (15 cleavages per hour) without secondary response; (D-F) screenshots for a low Dicer cleavage rate (5 cleavages per hour) without secondary response (G-I) screenshots for a low Dicer cleavage rate with unprimed amplification; (J-L) with primed amplification; (M-O) with guided amplification. Colours according to the colour-ramp shown in Figure 5.3.

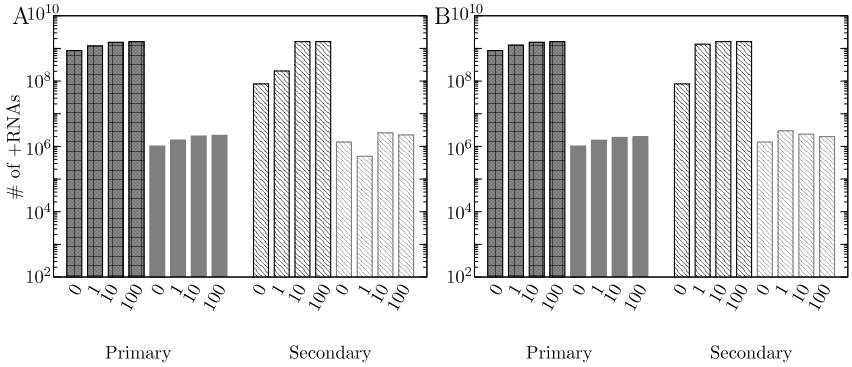

Figure 5.8: Total number of virus plus-strand RNA and free siRNAs present in the entire area 300 hpi, for suppressors that target Argonaute. Bars are calculated for different binding rates of the suppressor to Argonaute (parameter z). Results in (A) for a suppressor that targets Argonaute for degradation and (B) for a suppressor that inactivates Argonaute. Shown are values for the primary silencing response (5 Dicer cleavages per hour) and for the response with primed amplificaiton. Black bars represent total virus plus-strand RNA levels and grey bars represent siRNA levels. Solid bars show results for the primary silencing response, dashed bars for the response with primed amplification.

are not decreased all these cells produce siRNAs that spread from cell to cell and inhibit further virus spread over the tissue (Figure 5.7B and 5.9B). This negative effect was predicted by Baumberger et al. [8]. They hypothesised that the lack of prevention of siRNA production could contribute to the observation that Polerovirus cannot spread out of the phloem. In our model, the virus is able to spread further when the suppressor is stronger, and can infect the entire area (Figure 5.7C and 5.9C). When the RNA silencing response is weak (Dicer cleavage rate is 5 cleavages per hour) the virus reaches high levels in all infected cells, but there still is a slight negative effect on the rate of viral spread when the suppressor is not sufficiently strong (Figure 5.7E). The increase in free siRNA levels however, is not able to limit viral spread to a small spot as was the case for a stronger silencing response. In summary, the suppressors that target Argonaute induce a possible threat to virus spread when countering the primary RNA silencing response. It could be the case that the main benefit of the targeting of Argonaute is the suppression of the RNA silencing secondary response. To test this hypothesis we study viral spread for all three types of amplification. The weakest suppressor is not able to suppress RNA silencing to such extend that the virus can spread over the entire area (Figure 5.7 and

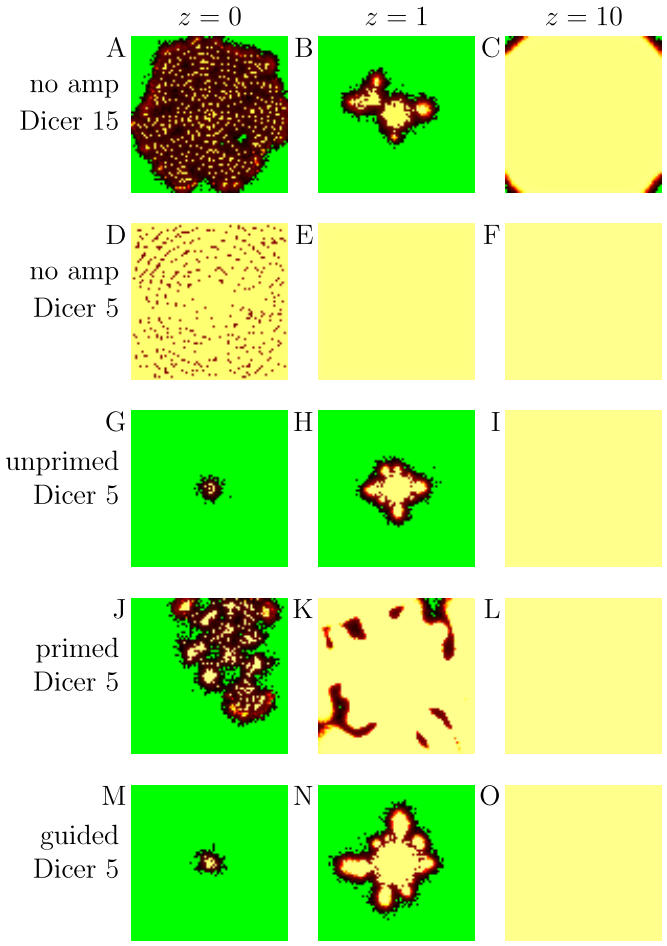

Figure 5.9: Infection patterns 300 hpi with and without Argonaute inactivating suppressor and with different types of secondary responses. The first column shows results without silencing suppressor, the second column with suppressor with binding rate $z = 1$, and in the third column $z = 10$. (A-C) screenshots for an intermediate Dicer cleavage rate (15 cleavages per hour) without secondary response; (D-F) screenshots for a low Dicer cleavage rate (5 cleavages per hour) without secondary response (G-I) screenshots for a low Dicer cleavage rate with unprimed amplification; (J-L) with primed amplification; (M-O) with guided amplification. Colours according to the colour-ramp shown in Figure 5.3.

5.9: H, K, N). When the binding rate to Argonaute is higher, this suppressor is very efficient, resulting in fast spread over the entire area (Figure 5.7 and 5.9: I, L, O). Another observation is that Argonaute inactivation has a small advantage over Argonaute degradation. Especially in the case of primed amplification virus spread is increased considerably (Figure 5.9K). This effect is also clear from the total virus and free siRNA counts shown in Figure 5.8, virus levels are almost 10-fold higher in the case of the weak Argonaute inactivating suppressor. Apart from this case, the Argonaute targeting suppressors have the same effect on virus and siRNA levels: Without amplification increased virus levels go hand in hand with increased siRNA levels. When amplification is present siRNA levels decrease or remain constant for increasing suppressor efficiency while virus levels increase 20-fold (Figure 5.8).

Our results suggest that the main benefit of Argonaute targeting suppressors is to decrease the plant secondary response. This hypothesis is supported by the observation that the 2b suppressor suppresses secondary siRNA accumulation [37]. However, we found that targeting Argonaute never results in the strong decrease in siRNAs caused by siRNA or dsRNA targeting suppressors.

5.4 Conclusion

We here studied four different types of viral encoded suppressors of RNA silencing: a siRNA binding suppressor; a dsRNA binding suppressor; a suppressor that targets Argonaute for degradation; and a suppressor that inactivates Argonaute.

Counterintuitively, we found that three of the four suppressors studied are not able to prevent clearance of the virus by a strong silencing response. Only the dsRNA binding suppressor is able to protect the virus against a stronger response. All suppressors are able to increase intracellular virus levels, although again the dsRNA binding suppressor is most efficient.

In our model, an increase in intracellular virus will automatically lead to higher primary siRNA levels. The presence of silencing suppressors can change this behaviour. dsRNA binding and siRNA binding can result in a strong decrease in intracellular siRNA levels. The suppressors that target Argonaute can also decrease intracellular siRNA levels, but only when the silencing response is weak. When the silencing response is strong there is no effect on primary siRNA levels.

At the tissue level the suppressors that target siRNA or dsRNA limit

RNA silencing, and the virus reaches higher levels in more cells and spreads faster. The dsRNA binding suppressor performs better than the siRNA binding suppressor. Targeting Argonaute is effective at the cellular level, but at the tissue level these suppressors can have a negative effect on virus spread. When the suppressors target Argonaute more efficiently they do increase virus levels and virus spread.

The negative effect of the suppressor on viral spread is in agreement with the observation that suppressor P0 (that targets Argonaute for degradation) can hinder viral growth. It has been observed that P0 is lowly expressed and that higher expression does not increase but decreases viral growth [117]. The authors suggested that this could be the case because an increase in P0 expression automatically leads to a reduced expression of other viral proteins that are coded on the same stretch of RNA, or that it could be that P0 itself carries a negative effect for virus replication. In our model, we indeed find that this type of suppressor can have a negative effect on viral spread, however higher expression of the suppressor increases viral growth and spread. Our model suggests that secondary effects as proposed by Pfeffer et al. [117] are indeed needed to explain the effects of P0 on viral replication and spread.

At high binding rates to the target, all tested suppressors increase virus levels at the tissue level. The effect of these increased virus levels on primary siRNA accumulation varies: siRNA binding and dsRNA binding suppressors can decrease siRNA levels at the tissue level, but siRNA levels are always increased by the suppressors that target Argonaute.

When we studied the addition of the secondary response, we observed that not all suppressors cope as efficiently with the primary and secondary response. siRNA binding cannot cope well with the unprimed amplification response, while dsRNA binding is efficient against all types of secondary responses. The most striking observation is virus spread is always increased by the Argonaute targeting suppressors when a secondary response is present, indicating that these suppressors may have evolved specifically against the secondary response.

The model described here included the pathways of RNA silencing, virus growth, viral suppression of silencing and some basic cell-to-cell movement. Possible extensions of the model could involve a more detailed tissue model that describes for example veins and multiple connected leaves. Additionally, the long distance silencing signal could be a major factor in determining viral spread through the plant.

Because silencing suppressors interfere with endogenous silencing path-

ways, they are implicated in symptom development. Previously we have shown that pattern formation of these symptoms on leaf tissue can be caused by viral growth and the spread of RNA silencing from cell-to-cell (Chapter 4). Because the number of silencing suppressors in a cell is directly correlated to the number of plus strands, we expect that symptoms develop in cells where the virus reaches high levels.

In summary, we have shown that suppressors that target Argonaute can be detrimental for viral spread when facing only a primary response, but are very potent against the secondary response. On the other hand siRNA binding and dsRNA binding by suppressors are always beneficial for virus spread. Whether or not symptoms develop by interference of suppressors with endogenous pathways, our results indicate that these symptoms should follow the pattern generated by the interaction between viral growth and the RNA silencing response.

5.5 Appendices

5.5.1 Basic model

The model consists of an intracellular ODE model and a spatial tissue level model.

We expand the previously described intracellular model (Section 4.5) with Argonaute. Argonaute binds to siRNA and the siRNA-Argonaute complex in turn binds to other components to from the active RISC.

RdRP
$$\frac{dR}{dt} = \frac{rP}{(P+k_t)} - d_r R - \{o(1-f)P + ofM + o_d D_m\}\mathcal{F} + hD_p + hR_a + \mathcal{G}_d(D_p + R_a) \tag{5.1}$$

+RNA
$$\frac{dP}{dt} = -o(1-f)P\mathcal{F} + hD_p + hR_a - dP - \frac{vP^5}{k_v^5 + P^5} - \frac{b_2 R_m P}{P+k_{ri}} - \mathcal{G}_{p,m}P - \mathcal{A}_u P - \mathcal{A}_p Ag_m P - \mathcal{A}_g Ag_m P \tag{5.2}$$

−RNA
$$\frac{dM}{dt} = -ofM\mathcal{F} + hD_p + hD_m(1 - \frac{1}{D_m})^{(R_a - D_m)} - dM - \frac{b_2 R_p M}{M+k_{ri}} - \mathcal{G}_{p,m}M - \mathcal{A}_u M - \mathcal{A}_p Ag_p M - \mathcal{A}_g Ag_p M \tag{5.3}$$

Virions
$$\frac{dV}{dt} = \frac{vP^5}{k_v^5 + P^5} - d_v V \tag{5.4}$$

dsRNA
$$\frac{dD_p}{dt} = o(1-f)P\mathcal{F} - hD_p - \mathcal{G}_d D_p \tag{5.5}$$

dsRNA
$$\frac{dD_m}{dt} = ofM\mathcal{F} - hD_m(1 - \frac{1}{D_m})^{(R_a - D_m)} - \mathcal{G}_d D_m \tag{5.6}$$

activeRdRP
$$\frac{dR_a}{dt} = ofM\mathcal{F} + o_d D_m \mathcal{F} - hR_a - \mathcal{G}_d R_a \tag{5.7}$$

+siRNA
$$\frac{dSi_p}{dt} = \mathcal{G}_{p,m}P + 0.5\mathcal{G}_d(D_p + D_m) - d_{si}Si_p - b_0 AgSi_p \tag{5.8}$$

−siRNA
$$\frac{dSi_m}{dt} = \mathcal{G}_{p,m}M + 0.5\mathcal{G}_d(D_p + D_m) - d_{si}Si_m - b_0 AgSi_m \tag{5.9}$$

free RISC
$$\frac{dR_f}{dt} = i - d_r R_f - b_1 R_f(Ag_p + Ag_m) \tag{5.10}$$

+RISC
$$\frac{dR_p}{dt} = b_1 R_f Ag_p - d_r R_p \tag{5.11}$$

−RISC
$$\frac{dR_m}{dt} = b_1 R_f Ag_m - d_r R_m \tag{5.12}$$

dsRNA amp
$$\frac{dD_e}{dt} = \mathcal{A}_u(P+M) + \mathcal{A}_p(Ag_m P + Ag_p M) + \mathcal{A}_g(Ag_m P + Ag_p M) - \mathcal{G}_d D_e \tag{5.13}$$

$$\text{sec. } +\text{siRNA} \quad \frac{dSis_p}{dt} = 0.5\mathcal{G}_d D_e - d_{si} Sis_p - b_0 Ag Sis_p \tag{5.14}$$

$$\text{sec. } -\text{siRNA} \quad \frac{dSis_m}{dt} = 0.5\mathcal{G}_d D_e - d_{si} Sis_m - b_0 Ag Sis_m \tag{5.15}$$

$$\text{Argonaute} \quad \frac{dAg}{dt} = i - d_r Ag - b_0 Ag(Si_p + Sis_p + Si_m + Sis_m) \tag{5.16}$$

$$\text{Ag\&Si+} \quad \frac{dAg_p}{dt} = b_0 Ag(Si_p + Sis_p) - d_r Ag_p - b1R_f Ag_p - \mathcal{A}_p Ag_p M \tag{5.17}$$

$$\text{Ag\&Si}- \quad \frac{dAg_m}{dt} = b_0 Ag(Si_m + Sis_m) - d_r Ag_m - b1R_f Ag_m - \mathcal{A}_p Ag_m P \tag{5.18}$$

Equations 5.1-5.7 describe viral replication and the degradation by the RNA silencing response. Equations 5.8-5.18 describe the dynamics of proteins and RNAs part of the RNA silencing response. The biological meaning of the variables is mentioned to the left of the equations. All parameter values, together with a short description, can be found in Table 5.1. $\mathcal{F}$, $\mathcal{G}$ and $\mathcal{A}$ are functions for the complex formation between RdRP and RNA strands, Dicer cleavage and amplification, respectively.

Viral replication is implemented as follows. Viral plus-strand RNA (P) is translated into RdRP (R), and forms virions (V). RdRP binds to plus-strand RNA and synthesises dsRNA (D_p), which separates into plus- and minus-stranded RNA (M). RdRP can also bind to minus-strand RNA to form dsRNA (D_m). More than one RdRP can bind to this double-stranded complex, we refer to these as 'active RdRPs' (R_a).

The complex formation ($\mathcal{F}$) between RdRP and RNA strands is saturated for both viral RNA and RdRP (the Beddington-DeAngelis functional response [9, 35]):

$$\mathcal{F} = \frac{oR}{R + P + M + D_m + k_r} \tag{5.19}$$

Viral single- or double-stranded RNA is degraded into primary siRNAs by Dicer. siRNAs can target the plus-strand (Si_m) or the minus-strand (Si_p). siRNAs cleaved from double-stranded RNA will target plus-strand or minus-strand RNA with a 1:1 ratio. Secondary siRNA (Sis_p and Sis_m) is cleaved from dsRNA produced by host encoded RDR (D_e).

The Dicer cleavage function is saturated for D_e, D_p, D_m, P and M. The Dicer cleavage functions, one for cleaving dsRNA and one for ssRNA, are saturated according to the ratio between single- and double-stranded RNA

cleavage (q) by Dicer:

$$\mathcal{G}_d = \frac{(1-q)c_d D_i}{(1-q)(D_p+D_m+D_e)+q(P+M)+k_d} \tag{5.20}$$

$$\mathcal{G}_s = \frac{qc_s D_i}{(1-q)(D_p+D_m+D_e)+q(P+M)+k_d} \tag{5.21}$$

Free Argonaute (Ag) associates with primary and secondary siRNA. Ag_p and Ag_m represent siRNA-Argonaute complexes with either a plus- or minus-strand siRNA. These complexes can associate with proteins to form the active RISC (R_p and R_m). RISC degrades the viral plus- or minus-strand RNA. The siRNA-Argonaute complex is also used to in the secondary amplification pathways. The amplification terms are:

$$\mathcal{A}_u = \frac{a_u}{(P+M+k_a)} \tag{5.22}$$

$$\mathcal{A}_g = \mathcal{A}_p = \frac{a_{p,g}}{(Ag_p M + Ag_m P + k_a)} \tag{5.23}$$

with $\mathcal{A}_u$ is unprimed amplification of ssRNA into dsRNA by RDR, and $\mathcal{A}_p$ and $\mathcal{A}_g$ primed and guided amplification. In the case of primed amplification a siRNA-Argonaute complex binds to ssRNA which triggers RDR to synthesise dsRNA. With guided amplification the siRNA-Argonaute complex does not bind to the ssRNA but serves only as guide for the RDR and is not degraded during the process as is the case with primed amplification.

The above equations are calculated for each cell on the tissue. Virions and siRNAs can move to the four neighbours of a cell. In each cell virions are unpacked into plus-strand RNA. To avoid triggering of viral growth or RNA silencing by incomplete particles we move virions and siRNAs with a particle based system. A fraction of virions and siRNAs is evenly distributed among the neighbours. Excess virions are distributed randomly, and when the number of moving particles is smaller than one, we draw a number to decide if a particle moves to a random neighbour.

5.5.2 siRNA binding

We add an equation for the silencing suppressor (S) to the intracellular model. We show the altered equations with the new terms in bold print:

$$\text{Suppressor} \qquad \frac{\mathbf{S}}{\mathbf{dt}} = \frac{\mathbf{rP}}{(\mathbf{P}+\mathbf{k_t})} - \mathbf{d_s S} - \mathbf{w}(\mathbf{Si_p}+\mathbf{Sis_p}+\mathbf{Si_m}+\mathbf{Sis_m})\mathbf{S} \tag{5.24}$$

$$+\text{siRNA} \qquad \frac{dSi_p}{dt} = \mathcal{G}_{p,m}P + 0.5\mathcal{G}_d(D_p+D_m) - d_{si}Si_p - b_0 AgSi_p - \mathbf{wSi_pS} \tag{5.25}$$

$$-\text{siRNA} \qquad \frac{dSi_m}{dt} = \mathcal{G}_{p,m}M + 0.5\mathcal{G}_d(D_p+D_m) - d_{si}Si_m - b_0 AgSi_m - \mathbf{wSi_mS} \tag{5.26}$$

$$\text{sec. } +\text{siRNA} \qquad \frac{dSis_p}{dt} = 0.5\mathcal{G}_d D_e - d_{si}Sis_p - b_0 AgSis_p - \mathbf{wSis_pS} \tag{5.27}$$

$$\text{sec. } -\text{siRNA} \qquad \frac{dSis_m}{dt} = 0.5\mathcal{G}_d D_e - d_{si}Sis_m - b_0 AgSis_m - \mathbf{wSis_mS} \tag{5.28}$$

Suppressor protein is translated from the plus-strand with maximum rate r and saturation constant k_t and decays with rate d_s. The suppressor associates with primary and secondary siRNAs with rate w. The association terms wSi_pS, wSi_mS, $wSis_pS$ and $wSis_mS$ are subtracted from the siRNA equations. Those siRNAs are no longer able to associate with Argonaute, and cannot spread from cell to cell.

5.5.3 dsRNA binding

The equations for the virus replication cycle and both the primary and secondary RNA silencing pathway are altered to implement the suppressor:

$$\begin{aligned}\text{Suppressor} \qquad \frac{\mathbf{S}}{\mathbf{dt}} &= \frac{\mathbf{rP}}{(\mathbf{P}+\mathbf{k_r})} - \mathbf{d_s S} - \mathbf{w}(\mathbf{D_p}+\mathbf{D_m}+\mathbf{D_e})\mathbf{S} \\ &\quad -\mathbf{w}(\mathbf{Si_m}+\mathbf{Sis_m}+\mathbf{Si_p}+\mathbf{Sis_p})\mathbf{S} + \mathbf{hS_{dp}} \\ &\quad +\mathbf{hS_{dm}}(\mathbf{1}-\frac{\mathbf{1}}{\mathbf{S_{dm}}})^{(\mathbf{S_{ra}}-\mathbf{S_{dm}})}\end{aligned} \tag{5.29}$$

$$\begin{aligned}\text{RdRP} \qquad \frac{dR}{dt} &= \frac{rP}{(P+k_t)} - d_r R - \{o(1-f)P + ofM + o_d D_m + \mathbf{o_d S_{dm}}\}\mathcal{F} \\ &\quad + hD_p + \mathbf{hS_{dp}} + hR_a + \mathbf{hS_{ra}} + \mathcal{G}_d(D_p+R_a)\end{aligned} \tag{5.30}$$

$$\begin{aligned}+\text{RNA} \qquad \frac{dP}{dt} &= -o(1-f)P\mathcal{F} + hD_p + \mathbf{hS_{dp}} + hR_a + \mathbf{hS_{ra}} - dP \\ &\quad - \frac{vP^5}{k_v^5+P^5} - \frac{b_2 R_m P}{P+k_{ri}} - \mathcal{G}_{p,m}P - \mathcal{A}_u P - \mathcal{A}_p Ag_m P - \mathcal{A}_g Ag_m P\end{aligned} \tag{5.31}$$

−RNA
$$\frac{dM}{dt} = -ofM\mathcal{F} + hD_p + \mathbf{hS_{dp}} + hD_m(1-\frac{1}{D_m})^{(R_a-D_m)} + \mathbf{hS_{dm}}(\mathbf{1}-\frac{\mathbf{1}}{\mathbf{S_{dm}}})^{(\mathbf{S_{ra}}-\mathbf{S_{dm}})} - dM - \frac{b_2R_pM}{M+k_{ri}} - \mathcal{G}_{p,m}M - \mathcal{A}_uM - \mathcal{A}_pAg_pM - \mathcal{A}_gAg_pM \quad (5.32)$$

dsRNA
$$\frac{dD_p}{dt} = o(1-f)P\mathcal{F} - hD_p - \mathcal{G}_dD_p - \mathbf{wD_pS} \quad (5.33)$$

dsRNA&sup
$$\frac{\mathbf{dS_{dp}}}{\mathbf{dt}} = \mathbf{wD_pS} - \mathbf{hS_{dp}} \quad (5.34)$$

dsRNA
$$\frac{dD_m}{dt} = ofM\mathcal{F} - hD_m(1-\frac{1}{D_m})^{(R_a-D_m)} - \mathcal{G}_dD_m - \mathbf{wD_mS} \quad (5.35)$$

dsRNA&sup
$$\frac{\mathbf{dS_{dm}}}{\mathbf{dt}} = \mathbf{wD_mS} - \mathbf{hS_{dm}}(\mathbf{1}-\frac{\mathbf{1}}{\mathbf{S_{dm}}})^{(\mathbf{S_{ra}}-\mathbf{S_{dm}})} \quad (5.36)$$

activeRdRP
$$\frac{dR_a}{dt} = ofM\mathcal{F} + o_dD_m\mathcal{F} - hR_a - \mathcal{G}_dR_a - \mathbf{wR_aS} \quad (5.37)$$

activeRdRPonSDs
$$\frac{\mathbf{dS_{ra}}}{\mathbf{dt}} = \mathbf{wR_aS} + \mathbf{o_dS_{dm}}\mathcal{F} - \mathbf{hS_{ra}} \quad (5.38)$$

+siRNA
$$\frac{dSi_p}{dt} = \mathcal{G}_{p,m}P + 0.5\mathcal{G}_d(D_p+D_m) - d_{si}Si_p - b_0AgSi_p - \mathbf{wSi_pS} \quad (5.39)$$

−siRNA
$$\frac{dSi_m}{dt} = \mathcal{G}_{p,m}M + 0.5\mathcal{G}_d(D_p+D_m) - d_{si}Si_m - b_0AgSi_m - \mathbf{wSi_mS} \quad (5.40)$$

dsRNA amp
$$\frac{dD_e}{dt} = \mathcal{A}_u(P+M) + \mathcal{A}_p(Ag_mP+Ag_pM) + \mathcal{A}_g(Ag_mP+Ag_pM) - \mathcal{G}_dD_e - \mathbf{wD_eS} \quad (5.41)$$

sec. +siRNA
$$\frac{dSis_p}{dt} = 0.5\mathcal{G}_dD_e - d_{si}Sis_p - b_0AgSis_p - \mathbf{wSis_pS} \quad (5.42)$$

sec. −siRNA
$$\frac{dSis_m}{dt} = 0.5\mathcal{G}_dD_e - d_{si}Sis_m - b_0AgSis_m - \mathbf{wSis_mS} \quad (5.43)$$

With new variables S suppressor protein, S_{dp} suppressor associated with dsRNA from the plus-strand, S_{dm} suppressor associated with dsRNA from the minus-strand, S_{ra} active RdRPs on S_{dm}. Suppressor protein is translated from plus-strand RNA with maximum rate r and saturation constant k_r, and has a decay rate d_r. Suppressor associates with Si_p, Sis_p, Si_m, Sis_m, D_m, D_p and D_e with rate w. The association terms are subtracted from the corresponding equations. We assume that the suppressor-siRNA complex and the suppressor-D_e complex remain inactive after association. The complexes of D_p and D_m with suppressor, S_{dp} and S_{dm}, dissociate in plus- and minus-strand RNA, RdRP and suppressor with rate h. To maintain semi-conservative replication of plus-strand RNA from the minus strand

when suppressor associates with D_m, the mean number of active RdRPs is removed from the normal R_a pool and added to the S_{ra} pool. Because viral replication now functions also through the Suppressor-dsRNA complexes, $\mathcal{F}$ is altered:

$$\mathcal{F} = \frac{oR}{R+P+M+D_m+S_{dm}+k_r} \tag{5.44}$$

5.5.4 Targeting Argonaute for degradation

We add this type of suppressor to the model. As previously described, the suppressor is produced by translation from the plus-strand.

$$\text{Suppressor} \qquad \frac{\mathbf{S}}{\mathbf{dt}} = \frac{\mathbf{rP}}{(\mathbf{P}+\mathbf{k_r})} - \mathbf{d_r S} - \frac{\mathbf{zSAg}}{\mathbf{S}+\mathbf{k_{sup}}} \tag{5.45}$$

$$\text{Argonaute} \qquad \frac{dAg}{dt} = i - d_r Ag - b_0 Ag(Si_p + Sis_p + Si_m + Sis_m) - \frac{\mathbf{zSAg}}{\mathbf{S}+\mathbf{k_{sup}}} \tag{5.46}$$

The decay term $-\frac{zSAg}{S+k_{sup}}$ is also added to the Argonaute equation. The suppressor binds to the Argonaute and then triggers degradation of the complex. Once the suppressor has bound Argonaute that particular Argonaute protein cannot bind to siRNA, and is removed from the Argonaute pool.

5.5.5 Inactivating Argonaute

The equation for the suppressor is the same as for P0, we now add an equation for inactive free Argonaute (Ag_s) that associates with siRNA as the normal free Argonaute with rate b_0:

$$\text{Suppressor} \qquad \frac{\mathbf{S}}{\mathbf{dt}} = \frac{\mathbf{rP}}{(\mathbf{P}+\mathbf{k_r})} - \mathbf{d_s S} - \frac{\mathbf{zSAg}}{\mathbf{S}+\mathbf{k_{sup}}} \tag{5.47}$$

$$\text{Argonaute} \qquad \frac{dAg}{dt} = i - d_r Ag - b_0 Ag(Si_p + Sis_p + Si_m + Sis_m) - \frac{\mathbf{zSAg}}{\mathbf{S}+\mathbf{k_{sup}}} \tag{5.48}$$

$$\text{Arg\&sup} \qquad \frac{\mathbf{Ag_s}}{\mathbf{dt}} = \frac{\mathbf{zSAg}}{\mathbf{S}+\mathbf{k_{sup}}} - \mathbf{d_r Ag_s} - \mathbf{b_0 Ag}(\mathbf{Si_p} + \mathbf{Si_m} + \mathbf{Sis_p} + \mathbf{Sis_m}) \tag{5.49}$$

$$+\text{siRNA} \qquad \frac{dSi_p}{dt} = \mathcal{G}_{p,m}P + 0.5\mathcal{G}_d(D_p + D_m) - d_{si}Si_p - b_0AgSi_p - \mathbf{b_0Ag_sSi_p} \tag{5.50}$$

$$-\text{siRNA} \qquad \frac{dSi_m}{dt} = \mathcal{G}_{p,m}M + 0.5\mathcal{G}_d(D_p + D_m) - d_{si}Si_m - b_0AgSi_m - \mathbf{b_0Ag_sSi_m} \tag{5.51}$$

$$\text{sec. } +\text{siRNA} \qquad \frac{dSis_p}{dt} = 0.5\mathcal{G}_dD_e - d_{si}Sis_p - b_0AgSis_p - \mathbf{b_0Ag_sSis_p} \tag{5.52}$$

$$\text{sec. } -\text{siRNA} \qquad \frac{dSis_m}{dt} = 0.5\mathcal{G}_dD_e - d_{si}Sis_m - b_0AgSis_m - \mathbf{b_0Ag_sSis_m} \tag{5.53}$$

siRNAs that associate with inactive Argonaute are removed from the free siRNA pool.

5.5.6 Parameter values

We use parameter values from our previous studies ([58] and Chapter 4). Parameter values can be found in table 5.1. The only new parameters are b_0, the rate of siRNA-Argonaute complex formation; w and z, the binding rates of the suppressors to their target; and k_{sup} the saturation constant for suppressor-Argonaute complex formation.

Table 5.1: Parameter values used. #mol is number of molecules.

Model	Par.	Meaning	Value	units
Intracellular	r	maximum translation rate x #ribosomes	15*5000	#mol hr^{-1}
	o	max rate of complex formation ssRNA	1	hr^{-1}
	o_d	max rate of complex formation dsRNA	100	hr^{-1}
	f	ratio of binding plus or minus RNA	0.9	-
	h	dsRNA-RDR splitting rate	10	hr^{-1}
	v	max virion production rate	500	#mol hr^{-1}
	D_i	number of Dicer molecules	500	#mol
	c_d	max Dicer cleavage rate for dsRNA	0-15	#mol hr^{-1}
	c_s	max Dicer cleavage rate for ssRNA	0-10	#mol hr^{-1}
	b_0	rate siRNA-Argonaute (AGO) complex formation	0.005	#mol $^{-1}$ hr^{-1}
	b_1	rate of RISC activation	0.1	#mol $^{-1}$ hr^{-1}
	b_2	RISC target cleavage rate	20	#mol $^{-1}$ hr^{-1}
	i	translation of RISC and AGO	100	#mol hr^{-1}
	a	amplification (a_u, a_p and a_g)	100	#mol hr^{-1}
	d_r	decay RdRP, RISC and AGO	0.1	hr^{-1}
	d	decay viral ssRNA	0.5	hr^{-1}
	d_{si}	decay siRNA	2	hr^{-1}
	d_v	decay virions	0.1	hr^{-1}
	k_v	saturation of virion production	10,000	#mol
	k_d	saturation of Dicer cleavage	10,000	#mol
	k_t	saturation constant for translation	1,000	#mol
	k_{ri}	saturation of RISC cleavage	1,000	#mol
	k_r	saturation of complex formation	1,000	#mol
	k_a	saturation amplification	1000	#mol
Suppressors	w	binding rate suppressor to siRNA and dsRNA	0-0.00001	#mol
	z	binding rate suppressor to Argonaute	0-100	#mol
	k_{sup}	saturation AGO suppressor	1000	#mol
Spatial	ΔSi	percentage of siRNAs exiting the cell	4	hr^{-1}
	ΔV	percentage of virions exiting the cell	1	hr^{-1}
	u	unpacking rate of virions	2	#mol hr^{-1}

CHAPTER 6

Summarising Discussion

6.1 Scope

In this thesis we studied various aspects of siRNA mediated silencing. siRNA mediated silencing is initiated by the introduction of dsRNA, transgenes and viral infection. Our first goal was to study the ability of the core pathway of RNA silencing to explain transgene and dsRNA induced silencing. To that extend we developed and studied concise models of the RNA silencing pathway in Chapter 2. Secondly, we investigated the efficacy of RNA silencing to reduce viral infections, and added a replicating RNA virus. While we studied antiviral silencing within the cell in Chapter 3, in Chapter 4 we extended our study to tissue level dynamics and symptom development in plants. Finally, we added virus encoded silencing suppressors and studied the effect and capability of the different silencing suppressors.

6.2 Review and Discussion

In **Chapter 2** we developed a model of the core pathway of RNA silencing and tested if this pathway allows for transgene and dsRNA induced silencing. Transgene induced silencing is dosage-dependent, meaning that a low number of transgenes does not trigger silencing while a high number of transgenes does. We have shown that dosage dependent transgene induced silencing is not straightforward to accomplish. The core mechanism of RNA silencing resulted in an "all-or-nothing" type of behaviour: either addition of transgenes lead to a linear increase in RNA levels, or even a single transgene was silenced. The secondary amplification response did not alter these results. To allow for transgene induced silencing the core model needs an additional feedback mechanism that was not previously described. Mechanisms that could result in dosage dependence are for example an siRNA degrading RNase, primed amplification of aberrant RNA pieces, and cooperation between aberrant RNA to trigger amplification. The cooperation between aberrant RNA pieces was not able to suppress very highly expressed transgenes and therefore less likely to be the basis of dosage dependent silencing than the other two mechanisms.

When we studied the model, there was no evidence for one of the proposed models. Just before publishing our results new experimental evidence confirmed the existence of a siRNA degrading RNase. An endogenous inhibitor of RNA silencing, *eri-1*, was found in *Caenorhabditis elegans* [75]. *eri-1* is an RNaseT enzyme that can partially degrade siRNAs and is highly conserved. Interestingly, high doses of siRNA in the mouse induce *eri-1*

expression, resulting in the phenomenon that a higher dose of siRNAs results in reduced silencing efficiency [67]. These results indicate that this exonuclease could indeed be involved in dose-dependent silencing. An *eri-1* homolog, Snipper, has also been found in *Drosophila*, but it does not seem to interfere with RNA silencing [81]. However, our models suggest that the experimental setup that lead to this conclusion cannot rule out a role of Snipper in RNA silencing. The tested transgenes coded for dsRNA, resulting in a silencing response triggered by continuous production of homologous dsRNA. It would be very interesting to test if Snipper is able to degrade siRNAs like *eri-1*.

Although a siRNA degrading RNase like *eri-i* or Snipper allows for dosage dependent silencing, it only functions when amplification is present to provide the nescessary feedback. *Drosophila* and mammals lack RDR and therefore a secondary response. In accordance, dosage dependent silencing has not been observed in mammals, but *Drosophila* is capable of dosage dependent silencing. *Drosophila* therefore must posses another mechanism to provide the feedback needed, which should be further investigated.

Recently there is increasing evidence supporting our other proposed mechanism, primed amplification of aberrant garbage RNA [151]. The mechanism is even incorporated in schematic graphs of the pathway. It is however not realised that this type of amplification is sufficient to provide a threshold for dose-dependent silencing and to avoid self-reactivity as shown in Chapter 2. Therefore, other mechanisms to avoid widespread silencing in the genome are being sought. One proposed mechanism is the avoidance of the production of uncapped RNAs by exonucleases [151]. XRN, an exonuclease, enhances transgene-induced silencing in *Arabidopsis* [55]. XRN competes for binding to aberrant transcripts with RDR and could reduce amplification and the formation of initial triggers of RNA silencing. Further modelling is necessary to study the effect of this mechanism on transgene induced silencing.

The mechanisms that allowed for dosage-dependent silencing differed in their response to an increasing number of transgenes. In the case of primed amplification of aberrant garbage pieces there is a large region of behaviour where two equilibria exist for a fixed number of transgenes. This means that a single introduction of homologous RNA could result in an equilibrium change from a silenced state to an equilibrium with high RNA levels. This bistable region is very small or absent in the case of the siRNA degrading RNase. Experiments could shed light on the existence of this

bistable region by investigating if the introduction of additional RNA can shift the system from a silenced equilibrium to a high equilibrium for a fixed number of transgenes.

Transgene and viral induced silencing differ because the virus itself is a replicating entity. In **Chapter 3** we studied the dynamics and efficacy of antiviral RNA silencing within the cell. We showed that antiviral silencing can function without amplification and that RNA silencing can limit viral growth. We found that RNA silencing caused different viral growth patterns: the virus could escape partly and grew to a decreased equilibrium; the virus was cleared from the cell; or virus levels oscillated. Although viral growth could be limited without amplification of the response, amplification did result in a new type of behaviour, causing viral clearance after an initial growth peak. We studied different Dicer activity modes, and showed than cleavage of both double- and single-stranded viral RNA is more efficient that cleavage of either type of RNA alone. Additionally, we showed that combined double- and single-strand cleavage results in the experimentally observed skewed siRNA ratio's.

We observed four qualitatively different effects of RNA silencing on viral growth, resulting in distinct viral growth curves. There is already some data on viral growth limited by RNA silencing available showing a single growth peak and decreased growth behaviour. Additional timeseries are needed to verify the role RDR, silencing efficiency, and Dicer activity predicted by our models.

Of major importance for viral infection is the spread of the virus through the host. In **Chapter 4** we extended our intracellular model of viral growth and RNA silencing with plant tissue level dynamics. The virus produces virions that can spread from cell-to-cell. The RNA silencing response in the form of siRNA can also spread, resulting in interesting dynamics at both the cellular and the tissue level. We found that RNA silencing could cause patterns on leaf tissue: the virus reached high levels in some cells, while viral growth was suppressed in other cells. These differences in viral accumulation have also been observed in experiments with mosaic viruses. We found that the siRNA influx from neighbouring cells was the driving force behind this pattern formation. It would be very interesting to see the effect of reduced or increased siRNA levels in an experimental setup. siRNA levels could be changed by for example changed RDR expression, but this of course also changes silencing strength.

In **Chapter 5** we added virus encoded suppressors of RNA silencing, since they are the virus' answer to limited viral growth by RNA silencing.

Viral suppression of RNA silencing can target different points in the RNA silencing pathway. We studied suppressors that bind to siRNA or dsRNA and suppressors that target Argonaute. We found that targeting all lengths of dsRNA was far more efficient than binding only to siRNA. Counterintuitively, we found that targeting Argonaute could limit viral growth to a single spot, while it was able to spread over the tissue without the presence of the suppressor. This was the case because targeting Argonaute could result in increased primary siRNA levels that limited virus spread. When the suppressors bound Argonaute faster, the virus could spread and reached higher levels. siRNA levels however, were always increased. The suppressors that bound siRNA or dsRNA did limit siRNA accumulation, while increasing virus levels at the same time. Interestingly, our models show that the Argonaute targeting suppressors are very potent against the amplification pathways. These results suggest that this strategy is evolved specifically against the secondary silencing response.

At first sight the results of **Chapter 2 and 3** seem to contradict, because we did not include the mechanisms we suggested in Chapter 2 in the models of antiviral silencing. In Chapter 2 we search for the necessary mechanism to result in dosage-dependent silencing, which requires more efficient silencing when RNA levels increase. In Chapter 3 however, we get this mechanism for free: virus levels can increase initially and be decreased to zero later in infection when primed or guided amplification is present. Additionally, RNA levels can oscillate, something that was not possible in Chapter 2. What is the difference between antiviral silencing and transgene induced silencing? The most important difference between viral growth and transgenes is the self-replicative behaviour of the virus. Virus RNA will not be generated spontaneously, meaning that a state without viral RNA is stable. This is not the case for the RNA generated from transgenes. Additionally, virus growth rate is not constant but has a maximum for intermediate RNA levels. A decrease in viral levels by RNA silencing can result in oscillations because the virus will rebound due to the high growth rate of the virus for intermediate virus levels. A stronger decrease in RNA levels by silencing increases these oscillations to such extend that the stable equilibrium for zero RNAs is reached. In this way self-replication can result in oscillations and a single growth peak behaviour. To ensure that self-replication and not another difference between the models is the driving force behind the different behaviour observed in Chapter 2 and 3, we have replaced the influx and decay of RNAs in the model of Chapter 2 with self-replicative RNA. We found that the self-replication can indeed result

in oscillations or single growth peak behaviour.

We did not test exhaustively the effect of the siRNA degrading RNase and primed amplification of garbage pieces in the models of antiviral silencing. However, we expect that primed amplification of garbage RNA does not change the qualitative behaviour observed in the models. It is not more efficient or faster than primed or guided amplification, and the temporal and spatial behaviour of the RNA silencing response will not change after virus introduction. The RNase however, induces a delay in the offset of silencing, which could affect the type and scale of the patterns observed on the tissue.

6.3 Analysing the models

The models in **Chapter 2** were concise, and we could extensively analyse the effect of all parameters. Additionally, we could prove that new interactions were needed because simple modifications of the known interactions could never result in dosage dependent silencing.

The models in **Chapter 3, 4 and 5** were more complex, with many parameters and variables. Despite problems associated with big models, we were able to study the models thoroughly with low dimensional bifurcation diagrams. This was possible because of the nature of the RNA silencing pathway. Many parameters behave similarly: parameter changes lead to either an increase or decrease in the strength and speed of the silencing response. The same holds for parameters part of virus replication: a change in parameters affects only the growth rate and the final virus levels reached. In this way clusters of parameters that have the same effect could be studied, and we could analyse the models with low dimensional bifurcation diagrams.

However in our models, like many models of biological systems, equilibrium analysis is not sufficient. Transients can be very important, and can be the decisive factor between viral clearance or escape. These transients became more and more important when we studied the spatial model with movement of siRNAs.

6.4 Future directions

Although the work described in this thesis studies the pathway of RNA silencing and the interactions with viruses from different angles, there are many aspects still to be studied.

One possible extension of the model is the addition of more detailed tissue dynamics, like for example the presence of veins through which both siRNAs and virions can spread. To study viral spread and systemic RNA silencing, we could expand to modelling multiple leafs and compare our results with experimental setups (f.e. [131, 152]). We could also combine the model of transgene induced silencing with tissue dynamics. The co-suppression experiments in Petunia showed that over-expression of chalcone synthase (that gives a purple colour to the flowers) results in white or white patterned flowers. This situation differs from viral growth because the chalcone synthase is over-expressed in every cell. It would be possible that siRNA movement affects the mRNA accumulation, resulting in the white patches.

Another interesting direction would be to study the evolutionary dynamics of antiviral RNA silencing. Viruses want to prevent cleavage of their RNA by Dicer. One way to do this is by the use of dsRNA binding silencing suppressors, but Dicer also cleaves siRNA from single-stranded RNA. Viruses would therefore evolve RNAs that are not easily cleaved by Dicer, but they have to maintain their functionality. On the other hand viruses can use RNA silencing for their own benefit. It has been shown that mammalian and insect viruses encode miRNAs (cleaved by the host) that regulate virus gene expression and replication [29, 68, 134].

A very different direction with the developed model is to adapt it to study siRNA delivery in mammalian tissue. Many studies investigate the ability of siRNA to suppress target gene expression in tumours. When the adapted intracellular model is combined with a spatial model on tumour growth [95], we could gain insight in siRNA spread and effectivity in such a tissue.

In this thesis we studied only siRNA mediated silencing. The equations however, could be altered to model gene regulation by miRNAs. Some modelling already has been done in this area. Levine et al. [87] have developed a model of gene regulation by miRNA in which miRNA can diffuse on a one dimensional tissue, and they showed that miRNA can reinforce spatial expression patterns. Similarly, a concise model of gene expression and miRNA could be coupled to tissue dynamics describing a developing tissue [96] to study the localisation and function of miRNAs during development.

6.5 Conclusion

In this thesis we have applied a stepwise approach that began with a model of the core pathway of RNA silencing and ended with the complex system of antiviral RNA silencing and silencing suppression on a tissue. We have shown that model studies are indispensable to understand complex cellular pathways. On the one hand we have shown that the generally accepted pathway of RNA silencing was insufficient to explain the experimental findings on transgene induced silencing it was supposed to explain. On the other hand we have shown that the interaction of RNA silencing and viral growth is indeed able to generate infection patterns for which the link to RNA silencing was still tentative. Further work to investigate the dynamics and role of RNA silencing in both infection and development should be done.

Bibliography

[1] **Ahlquist P** (2002) RNA-dependent RNA polymerases, viruses, and RNA silencing. Science 296: 1270–1273.

[2] **Al-Kaff NS, Covey SN, Kreike MM, Page AM, Pinder R, Dale PJ** (1998) Transcriptional and posttranscriptional plant gene silencing in response to a pathogen. Science 279: 2113–2115.

[3] **Aravind L, Watanabe H, Lipman DJ, Koonin EV** (2000) Lineage-specific loss and divergence of functionally linked genes in eukaryotes. Proc Natl Acad Sci USA 97: 11319–11324.

[4] **Atkinson PH, Matthews RE** (1970) On the origin of dark green tissue in tobacco leaves infected with tobacco mosaic virus. Virology 40: 344–356.

[5] **Bartlett DW, Davis ME** (2006) Insights into the kinetics of siRNA-mediated gene silencing from live-cell and live-animal bioluminescent imaging. Nucleic Acids Res 34: 322–333.

[6] **Baulcombe D** (2004) RNA silencing in plants. Nature 431: 356–363.

[7] **Baulcombe DC** (2007) Molecular biology. Amplified silencing. Science 315: 199–200.

[8] **Baumberger N, Tsai CH, Lie M, Havecker E, Baulcombe DC** (2007) The Polerovirus silencing suppressor P0 targets ARGONAUTE proteins for degradation. Curr Biol 17: 1609–1614.

[9] **Beddington J** (1975) Mutual interference between parasites or predators and its effect on searching efficiency. J Animal Ecol 44: 331–340.

[10] **Bergstrom CT, McKittrick E, Antia R** (2003) Mathematical models of RNA silencing: unidirectional amplification limits accidental self-directed reactions. Proc Natl Acad Sci USA 100: 11511–11516.

[11] **Bernstein E, Caudy AA, Hammond SM, Hannon GJ** (2001) Role for a bidentate ribonuclease in the initiation step of RNA interference. Nature 409: 363–366.

[12] **Blevins T, Rajeswaran R, Shivaprasad PV, Beknazariants D, Si-**

Ammour A, Park HS, Vazquez F, Robertson D, Meins Jr F, Hohn T, Pooggin MM (2006) Four plant Dicers mediate viral small RNA biogenesis and DNA virus induced silencing. Nucleic Acids Res 34: 6233–6246.

[13] **Bortolamiol D, Pazhouhandeh M, Marrocco K, Genschik P, Ziegler-Graff V** (2007) The Polerovirus F box protein P0 targets ARGONAUTE1 to suppress RNA silencing. Curr Biol 17: 1615–1621.

[14] **Brodersen P, Voinnet O** (2006) The diversity of RNA silencing pathways in plants. Trends Genet 22: 268–280.

[15] **Brosnan CA, Mitter N, Christie M, Smith NA, Waterhouse PM, Carroll BJ** (2007) Nuclear gene silencing directs reception of long-distance mRNA silencing in *Arabidopsis*. Proc Natl Acad Sci USA 104: 14741–14746.

[16] **Brown KM, Chu CY, Rana TM** (2005) Target accessibility dictates the potency of human RISC. Nat Struct Mol Biol 12: 469–470.

[17] **Caplen NJ, Parrish S, Imani F, Fire A, Morgan RA** (2001) Specific inhibition of gene expression by small double-stranded RNAs in invertebrate and vertebrate systems. Proc Natl Acad Sci USA 98: 9742–9747.

[18] **Casas-Mollano JA, Rohr J, Kim EJ, Balassa E, Van Dijk K, Cerutti H** (2008) Diversification of the Core RNA Interference Machinery in *Chlamydomonas reinhardtii* and the Role of DCL1 in Transposon Silencing. Genetics 179: 69–81.

[19] **Celotto AM, Graveley BR** (2002) Exon-specific RNAi: a tool for dissecting the functional relevance of alternative splicing. RNA 8: 718–724.

[20] **Cerutti H, Casas-Mollano JA** (2006) On the origin and functions of RNA-mediated silencing: from protists to man. Curr Genet 50: 81–99.

[21] **Chapman EJ, Prokhnevsky AI, Gopinath K, Dolja VV, Carrington JC** (2004) Viral RNA silencing suppressors inhibit the microRNA pathway at an intermediate step. Genes Dev 18: 1179–1186.

[22] **Chen Y, Cheng G, Mahato RI** (2008) RNAi for treating hepatitis B viral infection. Pharm Res 25: 72–86.

[23] **Chiu YL, Rana TM** (2003) sirna function in RNAi: a chemical modification analysis. RNA 9: 1034–1048.

[24] **Chuang CF, Meyerowitz EM** (2000) Specific and heritable genetic interference by double-stranded RNA in *Arabidopsis thaliana*. Proc Natl Acad Sci USA 97: 4985–4990.

[25] **Clemens MJ, Elia A** (1997) The double-stranded RNA-dependent protein kinase PKR: structure and function. J Interferon Cytokine Res 17: 503–524.

[26] **Cogoni C, Irelan JT, Schumacher M, Schmidhauser TJ, Selker EU, Macino G** (1996) Transgene silencing of the al-1 gene in vegetative cells of *Neurospora* is mediated by a cytoplasmic effector and does not depend on DNA-DNA interactions or DNA methylation. EMBO J 15: 3153–3163.

[27] **Cogoni C, Romano N, Macino G** (1994) Suppression of gene expression by homologous transgenes. Antonie Van Leeuwenhoek 65: 205–209.

[28] **Covey SN, Al-Kaff NS, Lángara A, Turner DS** (1997) Plants combat infection by gene silencing. Nature 385: 781–782.

[29] **Cullen BR** (2006) Viruses and microRNAs. Nat Genet 38: S25–S30.
[30] **Dahari H, Ribeiro RM, Rice CM, Perelson AS** (2007) Mathematical modeling of subgenomic hepatitis C virus replication in Huh-7 cells. J Virol 81: 750–760.
[31] **Dalmay T, Hamilton A, Rudd S, Angell S, Baulcombe DC** (2000) An RNA-dependent RNA polymerase gene in *Arabidopsis* is required for posttranscriptional gene silencing mediated by a transgene but not by a virus. Cell 101: 543–553.
[32] **Dawson WO** (1999) Tobacco mosaic virus virulence and avirulence. Philos Trans R Soc Lond B Biol Sci 354: 645–651.
[33] **De Carvalho F, Gheysen G, Kushnir S, Van Montagu M, Inze D, Castresana C** (1992) Suppression of beta-1,3-glucanase transgene expression in homozygous plants. EMBO J 11: 2595–2602.
[34] **De Vries W, Haasnoot J, Van der Velden J, Van Montfort T, Zorgdrager F, Paxton W, Cornelissen M, Van Kuppeveld F, De Haan P, Berkhout B** (2008) Increased virus replication in mammalian cells by blocking intracellular innate defense responses. Gene Ther 15: 545–552.
[35] **DeAngelis D, Goldstein R** (1975) A model for trophic interaction. Ecology 56: 881–892.
[36] **Dehio C, Schell J** (1994) Identification of plant genetic loci involved in a posttranscriptional mechanism for meiotically reversible transgene silencing. Proc Natl Acad Sci USA 91: 5538–5542.
[37] **Diaz-Pendon JA, Li F, Li WX, Ding SW** (2007) Suppression of antiviral silencing by cucumber mosaic virus 2b protein in *Arabidopsis* is associated with drastically reduced accumulation of three classes of viral small interfering RNAs. Plant Cell 19: 2053–2063.
[38] **Ding SW, Voinnet O** (2007) Antiviral immunity directed by small RNAs. Cell 130: 413–426.
[39] **Donaire L, Barajas D, Martinez-Garcia B, Martinez-Priego L, Pagan I, Llave C** (2008) Structural and genetic requirements for the biogenesis of tobacco rattle virus-derived small interfering RNAs. J Virol 82: 5167–5177.
[40] **Dorlhac de Borne F, Vincentz M, Chupeau Y, Vaucheret H** (1994) Co-suppression of nitrate reductase host genes and transgenes in transgenic tobacco plants. Mol Gen Genet 243: 613–621.
[41] **Dougherty WG, Lindbo JA, Smith HA, Parks TD, Swaney S, Proebsting WM** (1994) RNA-mediated virus resistance in transgenic plants: exploitation of a cellular pathway possibly involved in RNA degradation. Mol Plant Microbe Interact 7: 544–552.
[42] **Dougherty WG, Parks TD** (1995) Transgenes and gene suppression: telling us something new? Curr Opin Cell Biol 7: 399–405.
[43] **Dunoyer P, Voinnet O** (2008) Mixing and matching: the essence of plant systemic silencing? Trends Genet 24: 151–154.
[44] **Dzianott A, Bujarski JJ** (2004) Infection and RNA recombination of Brome mosaic virus in *Arabidopsis thaliana*. Virology 318: 482–492.

[45] **Elbashir SM, Harborth J, Lendeckel W, Yalcin A, Weber K, Tuschl T** (2001) Duplexes of 21-nucleotide RNAs mediate RNA interference in cultured mammalian cells. Nature 411: 494–498.

[46] **Elghonemy S, Davis WG, Brinton MA** (2005) The majority of the nucleotides in the top loop of the genomic 3' terminal stem loop structure are cis-acting in a West Nile virus infectious clone. Virology 331: 238–246.

[47] **Elmayan T, Vaucheret H** (1996) Expression of single copies of a strongly expressed 35s transgene can be silenced post-transcriptionally. Plant J 9: 787–797.

[48] **Fire A, Xu S, Montgomery MK, Kostas SA, Driver SE, Mello CC** (1998) Potent and specific genetic interference by double-stranded RNA in *Caenorhabditis elegans*. Nature 391: 806–811.

[49] **Forrest EC, Cogoni C, Macino G** (2004) The RNA-dependent RNA polymerase, QDE-1, is a rate-limiting factor in post-transcriptional gene silencing in *Neurospora crassa*. Nucleic Acids Res 32: 2123–2128.

[50] **Freitag M, Lee DW, Kothe GO, Pratt RJ, Aramayo R, Selker EU** (2004) DNA methylation is independent of RNA interference in *Neurospora*. Science 304: 1939.

[51] **Galagan JE, Selker EU** (2004) RIP: the evolutionary cost of genome defense. Trends Genet 20: 417–423.

[52] **Galvani A, Sperling L** (2001) Transgene-mediated post-transcriptional gene silencing is inhibited by 3' non-coding sequences in *Paramecium*. Nucleic Acids Res 29: 4387–4394.

[53] **Galvani A, Sperling L** (2002) RNA interference by feeding in *Paramecium*. Trends Genet 18: 11–12.

[54] **Garcia-Perez RD, Houdt HV, Depicker A** (2004) Spreading of post-transcriptional gene silencing along the target gene promotes systemic silencing. Plant J 38: 594–602.

[55] **Gazzani S, Lawrenson T, Woodward C, Headon D, Sablowski R** (2004) A link between mRNA turnover and RNA interference in *Arabidopsis*. Science 306: 1046–1048.

[56] **Girard A, Hannon GJ** (2008) Conserved themes in small-RNA-mediated transposon control. Trends Cell Biol 18: 136–148.

[57] **Grewal SI, Jia S** (2007) Heterochromatin revisited. Nat Rev Genet 8: 35–46.

[58] **Groenenboom MA, Hogeweg P** (2008) The dynamics and efficacy of antiviral RNA silencing: a model study. BMC Syst Biol 2: 28.

[59] **Groenenboom MA, Maree AF, Hogeweg P** (2005) The RNA silencing pathway: the bits and pieces that matter. PLoS Comput Biol 1: 155–165.

[60] **Haley B, Zamore PD** (2004) Kinetic analysis of the RNAi enzyme complex. Nat Struct Mol Biol 11: 599–606.

[61] **Hamilton A, Voinnet O, Chappell L, Baulcombe D** (2002) Two classes of short interfering RNA in RNA silencing. EMBO J 21: 4671–4679.

[62] **Hamilton AJ, Baulcombe DC** (1999) A species of small antisense RNA

in posttranscriptional gene silencing in plants. Science 286: 950–952.

[63] **Himber C, Dunoyer P, Moissiard G, Ritzenthaler C, Voinnet O** (2003) Transitivity-dependent and -independent cell-to-cell movement of RNA silencing. EMBO J 22: 4523–4533.

[64] **Hinas A, Reimegard J, Wagner EG, Nellen W, Ambros VR, Soderbom F** (2007) The small RNA repertoire of *Dictyostelium discoideum* and its regulation by components of the RNAi pathway. Nucleic Acids Res 35: 6714–6726.

[65] **Hirai K, Kubota K, Mochizuki T, Tsuda S, Meshi T** (2008) Antiviral RNA silencing is restricted to the marginal region of the dark green tissue in the mosaic leaves of tomato mosaic virus-infected tobacco plants. J Virol 82: 3250–3260.

[66] **Ho T, Pallett D, Rusholme R, Dalmay T, Wang H** (2006) A simplified method for cloning of short interfering RNAs from Brassica juncea infected with Turnip mosaic potyvirus and Turnip crinkle carmovirus. J Virol Methods 136: 217–223.

[67] **Hong J, Qian Z, Shen S, Min T, Tan C, Xu J, Zhao Y, Huang W** (2005) High doses of siRNAs induce eri-1 and adar-1 gene expression and reduce the efficiency of RNA interference in the mouse. Biochem J 390: 675–679.

[68] **Hussain M, Taft RJ, Asgari S** (2008) An insect virus-encoded microRNA regulates viral replication. J Virol 0: O.

[69] **Hutvagner G, Simard MJ** (2008) Argonaute proteins: key players in RNA silencing. Nat Rev Mol Cell Biol 9: 22–32.

[70] **Hutvágner G, Zamore PD** (2002) RNAi: nature abhors a double-strand. Curr Opin Genet Dev 12: 225–232.

[71] **Jorgensen RA, Atkinson RG, Forster RL, Lucas WJ** (1998) An RNA-based information superhighway in plants. Science 279: 1486–1487.

[72] **Jorgensen RA, Cluster PD, English J, Que Q, Napoli CA** (1996) Chalcone synthase cosuppression phenotypes in petunia flowers: comparison of sense vs. antisense constructs and single-copy vs. complex T-DNA sequences. Plant Mol Biol 31: 957–973.

[73] **Jovel J, Walker M, Sanfacon H** (2007) Recovery of *Nicotiana benthamiana* plants from a necrotic response induced by a nepovirus is associated with RNA silencing but not with reduced virus titer. J Virol 81: 12285–12297.

[74] **Kawasaki H, Taira K** (2005) Transcriptional gene silencing by short interfering RNAs. Curr Opin Mol Ther 7: 125–131.

[75] **Kennedy S, Wang D, Ruvkun G** (2004) A conserved siRNA-degrading RNase negatively regulates RNA interference in *C. elegans*. Nature 427: 645–649.

[76] **Kennerdell JR, Carthew RW** (1998) Use of dsRNA-mediated genetic interference to demonstrate that frizzled and frizzled 2 act in the wingless pathway. Cell 95: 1017–1026.

[77] **Klahre U, Crete P, Leuenberger SA, Iglesias VA, Meins Jr F** (2002)

High molecular weight RNAs and small interfering RNAs induce systemic posttranscriptional gene silencing in plants. Proc Natl Acad Sci USA 99: 11981–11986.

[78] **Klattenhoff C, Theurkauf W** (2008) Biogenesis and germline functions of piRNAs. Development 135: 3–9.

[79] **Kloosterman WP, Plasterk RH** (2006) The diverse functions of microRNAs in animal development and disease. Dev Cell 11: 441–450.

[80] **Kumar A** (2008) RNA interference: a multifaceted innate antiviral defense. Retrovirology 5: 17.

[81] **Kupsco JM, Wu MJ, Marzluff WF, Thapar R, Duronio RJ** (2006) Genetic and biochemical characterization of *Drosophila* Snipper: A promiscuous member of the metazoan 3'hExo/ERI-1 family of 3' to 5' exonucleases. RNA 12: 2103–2117.

[82] **Lechtenberg B, Schubert D, Forsbach A, Gils M, Schmidt R** (2003) Neither inverted repeat T-DNA configurations nor arrangements of tandemly repeated transgenes are sufficient to trigger transgene silencing. Plant J 34: 507–517.

[83] **Lee CT, Risom T, Strauss WM** (2007) Evolutionary conservation of microRNA regulatory circuits: an examination of microRNA gene complexity and conserved microRNA-target interactions through metazoan phylogeny. DNA Cell Biol 26: 209–218.

[84] **Lee RC, Ambros V** (2001) An extensive class of small RNAs in *Caenorhabditis elegans*. Science 294: 862–864.

[85] **Lee RC, Feinbaum RL, Ambros V** (1993) The *C. elegans* heterochronic gene lin-4 encodes small RNAs with antisense complementarity to lin-14. Cell 75: 843–854.

[86] **Leuschner PJ, Ameres SL, Kueng S, Martinez J** (2006) Cleavage of the siRNA passenger strand during RISC assembly in human cells. EMBO Rep 7: 314–320.

[87] **Levine E, McHale P, Levine H** (2007) Small regulatory RNAs may sharpen spatial expression patterns. PLoS Comput Biol 3: e233.

[88] **Li YX, Farrell MJ, Liu R, Mohanty N, Kirby ML** (2000) Double-stranded RNA injection produces null phenotypes in zebrafish. Dev Biol 217: 394–405.

[89] **Lindbo JA, Silva-Rosales L, Proebsting WM, Dougherty WG** (1993) Induction of a highly specific antiviral state in transgenic plants: Implications for regulation of gene expression and virus resistance. Plant Cell 5: 1749–1759.

[90] **Lipardi C, Wei Q, Paterson BM** (2001) RNAi as random degradative PCR: siRNA primers convert mRNA into dsRNAs that are degraded to generate new siRNAs. Cell 107: 297–307.

[91] **Liu Y, Taverna SD, Muratore TL, Shabanowitz J, Hunt DF, Allis CD** (2007) RNAi-dependent H3K27 methylation is required for heterochromatin formation and DNA elimination in *Tetrahymena*. Genes Dev 21: 1530–1545.

[92] **Lodish HF, Jacobsen M** (1972) Regulation of hemoglobin synthesis. Equal rates of translation and termination of - and -globin chains. J Biol Chem 247: 3622–3629.

[93] **Ma JB, Yuan YR, Meister G, Pei Y, Tuschl T, Patel DJ** (2005) Structural basis for 5'-end-specific recognition of guide RNA by the *A. fulgidus* Piwi protein. Nature 434: 666–670.

[94] **Makeyev EV, Bamford DH** (2002) Cellular RNA-dependent RNA polymerase involved in posttranscriptional gene silencing has two distinct activity modes. Mol Cell 10: 1417–1427.

[95] **Marée AFM, Grieneisen VA, Hogeweg P** (2007) The Cellular Potts Model and biophysical properties of cells, tissues and morphogenesis. In: **Anderson ARA, Chaplain MAJ, Rejniak KA**, editors, Single-Cell-Based Models in Biology and Medicine, Basel: Birkhäuser Verlag, pp. 107–136.

[96] **Marée AFM, Grieneisen VA, Hogeweg P** (2008) Modelling chick gastrulation and somitogenesis on the interface of subcellular and cellular processes. Manuscript in preparation.

[97] **Marques JT, Carthew RW** (2007) A call to arms: coevolution of animal viruses and host innate immune responses. Trends Genet 23: 359–364.

[98] **Merai Z, Kerenyi Z, Kertesz S, Magna M, Lakatos L, Silhavy D** (2006) Double-stranded RNA binding may be a general plant RNA viral strategy to suppress RNA silencing. J Virol 80: 5747–5756.

[99] **Merai Z, Kerenyi Z, Molnar A, Barta E, Valoczi A, Bisztray G, Havelda Z, Burgyan J, Silhavy D** (2005) Aureusvirus P14 is an efficient RNA silencing suppressor that binds double-stranded RNAs without size specificity. J Virol 79: 7217–7226.

[100] **Mette MF, Aufsatz W, Van der Winden J, Matzke MA, Matzke AJ** (2000) Transcriptional silencing and promoter methylation triggered by double-stranded RNA. EMBO J 19: 5194–5201.

[101] **Molnar A, Csorba T, Lakatos L, Varallyay E, Lacomme C, Burgyan J** (2005) Plant virus-derived small interfering RNAs originate predominantly from highly structured single-stranded viral RNAs. J Virol 79: 7812–7818.

[102] **Molnar A, Schwach F, Studholme DJ, Thuenemann EC, Baulcombe DC** (2007) mirnas control gene expression in the single-cell alga *Chlamydomonas reinhardtii*. Nature 447: 1126–1129.

[103] **Montgomery MK, Xu S, Fire A** (1998) RNA as a target of double-stranded RNA-mediated genetic interference in *Caenorhabditis elegans*. Proc Natl Acad Sci USA 95: 15502–15507.

[104] **Moore CJ, Sutherland PW, Forster RL, Gardner RC, MacDiarmid RM** (2001) Dark green islands in plant virus infection are the result of posttranscriptional gene silencing. Mol Plant Microbe Interact 14: 939–946.

[105] **Morris KV, Chan SW, Jacobsen SE, Looney DJ** (2004) Small interfering RNA-induced transcriptional gene silencing in human cells. Science 305: 1289–1292.

[106] **Mourrain P, Beclin C, Elmayan T, Feuerbach F, Godon C, Morel JB, Jouette D, Lacombe AM, Nikic S, Picault N, Remoue K, Sanial M, Vo TA, Vaucheret H** (2000) *Arabidopsis* SGS2 and SGS3 genes are required for posttranscriptional gene silencing and natural virus resistance. Cell 101: 533–542.

[107] **Murphy D, Dancis B, Brown JR** (2008) The evolution of core proteins involved in microRNA biogenesis. BMC Evol Biol 8: 92.

[108] **Napoli C, Lemieux C, Jorgensen R** (1990) Introduction of a Chimeric Chalcone Synthase Gene into Petunia results in reversible co-suppression of homologous genes in trans. Plant Cell 2: 279–289.

[109] **Nolan T, Braccini L, Azzalin G, De Toni A, Macino G, Cogoni C** (2005) The post-transcriptional gene silencing machinery functions independently of DNA methylation to repress a LINE1-like retrotransposon in *Neurospora crassa*. Nucleic Acids Res 33: 1564–1573.

[110] **Pak J, Fire A** (2007) Distinct populations of primary and secondary effectors during RNAi in C. elegans. Science 315: 241–244.

[111] **Pal-Bhadra M, Bhadra U, Birchler JA** (2002) RNAi related mechanisms affect both transcriptional and posttranscriptional transgene silencing in Drosophila. Mol Cell 9: 315–327.

[112] **Palauqui JC, Elmayan T, Pollien JM, Vaucheret H** (1997) Systemic acquired silencing: transgene-specific post-transcriptional silencing is transmitted by grafting from silenced stocks to non-silenced scions. EMBO J 16: 4738–4745.

[113] **Palauqui JC, Vaucheret H** (1995) Field trial analysis of nitrate reductase co-suppression: a comparative study of 38 combinations of transgene loci. Plant Mol Biol 29: 149–159.

[114] **Palmiter RD** (1973) Ovalbumin messenger ribonucleic acid translation. Comparable rates of polypeptide initiation and elongation on ovalbumin and globin messenger ribonucleic acid in a rabbit reticulocyte lysate. J Biol Chem 248: 2095–2106.

[115] **Pantaleo V, Szittya G, Burgyan J** (2007) Molecular bases of viral RNA targeting by viral small interfering RNA-programmed RISC. J Virol 81: 3797–3806.

[116] **Papp I, Mette MF, Aufsatz W, Daxinger L, Schauer SE, Ray A, Van der Winden J, Matzke M, Matzke AJ** (2003) Evidence for nuclear processing of plant micro RNA and short interfering RNA precursors. Plant Physiol 132: 1382–1390.

[117] **Pfeffer S, Dunoyer P, Heim F, Richards KE, Jonard G, Ziegler-Graff V** (2002) P0 of beet Western yellows virus is a suppressor of posttranscriptional gene silencing. J Virol 76: 6815–6824.

[118] **Pillai RS, Bhattacharyya SN, Filipowicz W** (2007) Repression of protein synthesis by miRNAs: how many mechanisms? Trends Cell Biol 17: 118–126.

[119] **Pirollo KF, Chang EH** (2008) Targeted delivery of small interfering RNA: approaching effective cancer therapies. Cancer Res 68: 1247–1250.

[120] **Player MR, Torrence PF** (1998) The 2-5A system: modulation of viral and cellular processes through acceleration of RNA degradation. Pharmacol Ther 78: 55–113.

[121] **Qu F, Ye X, Hou G, Sato S, Clemente TE, Morris TJ** (2005) RDR6 has a broad-spectrum but temperature-dependent antiviral defense role in *Nicotiana benthamiana*. J Virol 79: 15209–15217.

[122] **Que Q, Wang HY, English JJ, Jorgensen RA** (1997) The Frequency and Degree of Cosuppression by Sense Chalcone Synthase Transgenes Are Dependent on Transgene Promoter Strength and Are Reduced by Premature Nonsense Codons in the Transgene Coding Sequence. Plant Cell 9: 1357–1368.

[123] **Ratcliff F, Harrison BD, Baulcombe DC** (1997) A similarity between viral defense and gene silencing in plants. Science 276: 1558–1560.

[124] **Regoes RR, Crotty S, Antia R, Tanaka MM** (2005) Optimal replication of poliovirus within cells. Am Nat 165: 364–373.

[125] **Rohr J, Sarkar N, Balenger S, Jeong BR, Cerutti H** (2004) Tandem inverted repeat system for selection of effective transgenic RNAi strains in *Chlamydomonas*. Plant J 40: 611–621.

[126] **Roignant JY, Carre C, Mugat B, Szymczak D, Lepesant JA, Antoniewski C** (2003) Absence of transitive and systemic pathways allows cell-specific and isoform-specific RNAi in *Drosophila*. RNA 9: 299–308.

[127] **Romano N, Macino G** (1992) Quelling: transient inactivation of gene expression in *Neurospora crassa* by transformation with homologous sequences. Mol Microbiol 6: 3343–3353.

[128] **Ruiz MT, Voinnet O, Baulcombe DC** (1998) Initiation and maintenance of virus-induced gene silencing. Plant Cell 10: 937–946.

[129] **Sasaki T, Shimizu N** (2007) Evolutionary conservation of a unique amino acid sequence in human DICER protein essential for binding to Argonaute family proteins. Gene 396: 312–320.

[130] **Schiebel W, Haas B, Marinkovic S, Klanner A, Sanger HL** (1993) RNA-directed RNA polymerase from tomato leaves. II. Catalytic in vitro properties. J Biol Chem 268: 11858–11867.

[131] **Schwach F, Vaistij FE, Jones L, Baulcombe DC** (2005) An RNA-dependent RNA polymerase prevents meristem invasion by potato virus X and is required for the activity but not the production of a systemic silencing signal. Plant Physiol 138: 1842–1852.

[132] **Schwarz DS, Hutvagner G, Haley B, Zamore PD** (2002) Evidence that siRNAs function as guides, not primers, in the *Drosophila* and human RNAi pathways. Mol Cell 10: 537–548.

[133] **Segers GC, Zhang X, Deng F, Sun Q, Nuss DL** (2007) Evidence that RNA silencing functions as an antiviral defense mechanism in fungi. Proc Natl Acad Sci USA 104: 12902–12906.

[134] **Seo GJ, Fink L, O'Hara B, Atwood WJ, Sullivan CS** (2008) Evolutionary conserved function of a viral microRNA. J Virol 0: O.

[135] **Shabalina SA, Koonin EV** (2008) Origins and evolution of eukaryotic

RNA interference. Trends Ecol Evol 0: O.

[136] **Shiu PK, Metzenberg RL** (2002) Meiotic silencing by unpaired DNA: properties, regulation and suppression. Genetics 161: 1483–1495.

[137] **Sigova A, Rhind N, Zamore PD** (2004) A single Argonaute protein mediates both transcriptional and posttranscriptional silencing in *Schizosaccharomyces pombe*. Genes Dev 18: 2359–2367.

[138] **Sijen T, Fleenor J, Simmer F, Thijssen KL, Parrish S, Timmons L, Plasterk RH, Fire A** (2001) On the role of RNA amplification in dsRNA-triggered gene silencing. Cell 107: 465–476.

[139] **Sijen T, Plasterk RH** (2003) Transposon silencing in the *Caenorhabditis elegans* germ line by natural RNAi. Nature 426: 310–314.

[140] **Sijen T, Steiner FA, Thijssen KL, Plasterk RH** (2007) Secondary siRNAs result from unprimed RNA synthesis and form a distinct class. Science 315: 244–247.

[141] **Stein P, Svoboda P, Anger M, Schultz RM** (2003) RNAi: mammalian oocytes do it without RNA-dependent RNA polymerase. RNA 9: 187–192.

[142] **Tabara H, Sarkissian M, Kelly WG, Fleenor J, Grishok A, Timmons L, Fire A, Mello CC** (1999) The rde-1 gene, RNA interference, and transposon silencing in *C. elegans*. Cell 99: 123–132.

[143] **Takayama KM, Inouye M** (1990) Antisense RNA. Crit Rev Biochem Mol Biol 25: 155–184.

[144] **Taylor CB, Green PJ** (1995) Identification and characterization of genes with unstable transcripts (GUTs) in tobacco. Plant Mol Biol 28: 27–38.

[145] **Triboulet R, Mari B, Lin YL, Chable-Bessia C, Bennasser Y, Lebrigand K, Cardinaud B, Maurin T, Barbry P, Baillat V, Reynes J, Corbeau P, Jeang KT, Benkirane M** (2007) Suppression of microRNA-silencing pathway by HIV-1 during virus replication. Science 315: 1579–1582.

[146] **Uchil PD, Satchidanandam V** (2003) Characterization of RNA synthesis, replication mechanism, and in vitro RNA-dependent RNA polymerase activity of Japanese encephalitis virus. Virology 307: 358–371.

[147] **Ullu E, Tschudi C, Chakraborty T** (2004) RNA interference in protozoan parasites. Cell Microbiol 6: 509–519.

[148] **van Blokland R, van der Geest N, Mol JNM, Kooter JM** (1994) Transgene-mediated suppression of chalcone synthase expression in Petunia hybrida results from an increase in RNA turnover. Plant J 6: 861–877.

[149] **Van der Krol AR, Mur LA, Beld M, Mol JN, Stuitje AR** (1990) Flavonoid genes in petunia: addition of a limited number of gene copies may lead to a suppression of gene expression. Plant Cell 2: 291–299.

[150] **Voinnet O** (2005) Induction and suppression of RNA silencing: insights from viral infections. Nat Rev Genet 6: 206–220.

[151] **Voinnet O** (2008) Use, tolerance and avoidance of amplified RNA silencing by plants. Trends Plant Sci 13: 317–328.

[152] **Voinnet O, Lederer C, Baulcombe DC** (2000) A viral movement protein prevents spread of the gene silencing signal in *Nicotiana benthamiana*.

Cell 103: 157–167.

[153] **Voinnet O, Vain P, Angell S, Baulcombe DC** (1998) Systemic spread of sequence-specific transgene RNA degradation in plants is initiated by localized introduction of ectopic promoterless DNA. Cell 95: 177–187.

[154] **Wang Y, Liu CL, Storey JD, Tibshirani RJ, Herschlag D, Brown PO** (2002) Precision and functional specificity in mRNA decay. Proc Natl Acad Sci USA 99: 5860–5865.

[155] **Wassenegger M, Krczal G** (2006) Nomenclature and functions of RNA-directed RNA polymerases. Trends Plant Sci 11: 142–151.

[156] **Wei Q, Lipardi C, Paterson BM** (2003) Analysis of the 3(')-hydroxyl group in *Drosophila* siRNA function. Methods 30: 337–347.

[157] **Wightman B, Ha I, Ruvkun G** (1993) Posttranscriptional regulation of the heterochronic gene lin-14 by lin-4 mediates temporal pattern formation in C. elegans. Cell 75: 855–862.

[158] **Wilkins C, Dishongh R, Moore SC, Whitt MA, Chow M, Machaca K** (2005) RNA interference is an antiviral defence mechanism in *Caenorhabditis elegans*. Nature 436: 1044–1047.

[159] **Willmann MR, Poethig RS** (2007) Conservation and evolution of miRNA regulatory programs in plant development. Curr Opin Plant Biol 10: 503–511.

[160] **Wu-Scharf D, Jeong B, Zhang C, Cerutti H** (2000) Transgene and transposon silencing in *Chlamydomonas reinhardtii* by a DEAH-box RNA helicase. Science 290: 1159–1162.

[161] **Xie Z, Fan B, Chen C, Chen Z** (2001) An important role of an inducible RNA-dependent RNA polymerase in plant antiviral defense. Proc Natl Acad Sci USA 98: 6516–6521.

[162] **Yang E, Van Nimwegen E, Zavolan M, Rajewsky N, Schroeder M, Magnasco M, Darnell Jr JE** (2003) Decay rates of human mRNAs: correlation with functional characteristics and sequence attributes. Genome Res 13: 1863–1872.

[163] **Yang SJ, Carter SA, Cole AB, Cheng NH, Nelson RS** (2004) A natural variant of a host RNA-dependent RNA polymerase is associated with increased susceptibility to viruses by *Nicotiana benthamiana*. Proc Natl Acad Sci USA 101: 6297–6302.

[164] **Yao MC, Chao JL** (2005) RNA-guided DNA deletion in *Tetrahymena*: an RNAi-based mechanism for programmed genome rearrangements. Annu Rev Genet 39: 537–559.

[165] **Yoo BC, Kragler F, Varkonyi-Gasic E, Haywood V, Archer-Evans S, Lee YM, Lough TJ, Lucas WJ** (2004) A systemic small RNA signaling system in plants. Plant Cell 16: 1979–2000.

[166] **Yu D, Fan B, MacFarlane SA, Chen Z** (2003) Analysis of the involvement of an inducible *Arabidopsis* RNA-dependent RNA polymerase in antiviral defense. Mol Plant Microbe Interact 16: 206–216.

[167] **Yuan YR, Pei Y, Ma JB, Kuryavyi V, Zhadina M, Meister G, Chen HY, Dauter Z, Tuschl T, Patel DJ** (2005) Crystal structure of *A.*

aeolicus Argonaute, a site-specific DNA-guided endoribonuclease, provides insights into RISC-mediated mRNA cleavage. Mol Cell 19: 405–419.

[168] **Zamore PD, Tuschl T, Sharp PA, Bartel DP** (2000) RNAi: double-stranded RNA directs the ATP-dependent cleavage of mRNA at 21 to 23 nucleotide intervals. Cell 101: 25–33.

[169] **Zhang X, Yuan YR, Pei Y, Lin SS, Tuschl T, Patel DJ, Chua NH** (2006) Cucumber mosaic virus-encoded 2b suppressor inhibits *Arabidopsis* Argonaute1 cleavage activity to counter plant defense. Genes Dev 20: 3255–3268.

[170] **Zhao T, Li G, Mi S, Li S, Hannon GJ, Wang XJ, Qi Y** (2007) A complex system of small RNAs in the unicellular green alga *Chlamydomonas reinhardtii*. Genes Dev 21: 1190–1203.

[171] **Zofall M, Grewal SI** (2006) RNAi-mediated heterochromatin assembly in fission yeast. Cold Spring Harb Symp Quant Biol 71: 487–496.

Nederlandse samenvatting

In dit proefschrift bespreken we wiskundige modellen van **RNA silencing**. RNA silencing zou vertaald naar het nederlands "RNA tot zwijgen brengen" of "RNA stil maken" betekenen. In het onderzoek wordt standaard de Engelse term RNA Silencing gebruikt, en dat zullen wij in deze samenvatting ook doen. RNA silencing is een afweermechanisme dat planten en dieren gebruiken om zich te verdedigen tegen bijvoorbeeld virussen. We zullen eerst wat biologische achtergrond uitleggen voor we het onderzoek beschreven in dit proefschrift zullen samenvatten.

Introductie

RNA silencing vindt plaats op RNA niveau. RNA lijkt qua chemische structuur op DNA. DNA is een lang molecuul wat wordt bewaard in de kern van elke cel en bevat de informatie om eiwitten te maken. Eiwitten zijn de moleculen waaruit alle organismen zijn opgebouwd.

De informatie op het DNA is gecodeerd door middel van nucleotiden. Er zijn vier soorten nucleotiden, aangeduid door de letters A, T, G en C. DNA bestaat uit twee strengen met letters die op elkaar passen. A past op T en G past op C. De volgorde van de nucleotiden bepaalt wat er voor informatie op het DNA staat. Een stuk DNA wat de informatie over één eiwit bevat wordt een gen genoemd. Voor de vertaling van DNA naar een eiwit moet de informatie de celkern uit. Dat is waar RNA om de hoek komt kijken. De informatie van een gen op het DNA wordt gekopieerd naar RNA, wat uit de celkern kan. Eenmaal uit de celkern gaat het RNA naar een ribosoom, dat is een soort fabriekje in de cel. Het ribosoom leest

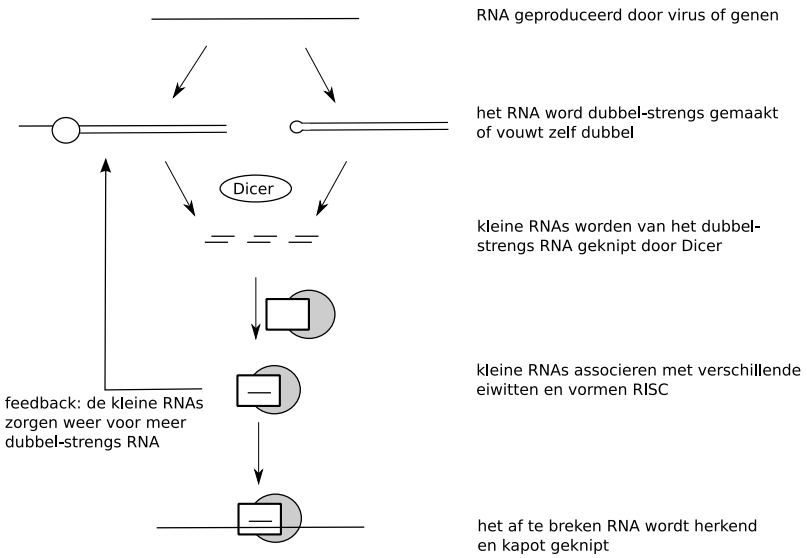

Figuur 7.1: Een schematische weergave van mechanisme van RNA silencing. Genen produceren RNA wat dubbelstrengs wordt gemaakt of wat vanzelf dubbel vouwt. Virussen produceren zelf dsRNA. dsRNA wordt door Dicer in kleine stukjes geknipt. Deze kleine RNAs associeren met verschillende eiwitten en vormen RISC. RISC herkent het af te breken RNA en knipt het kapot. Er zijn ook feedback mechanismen die zorgen voor de productie van meer dsRNA, wat weer voor meer kleine RNAs zorgt.

het RNA af en zet dan het juiste eiwit in elkaar.

Samengevat is RNA noodzakelijk voor het functioneren van elk organisme. Waarom is er dan een mechanisme, RNA silencing, om RNA af te breken? Eén reden is dat er soms door een foutje teveel RNA ontstaat, wat er toe kan leiden dat er veel te veel van een bepaald eiwit wordt gemaakt. Een andere reden is dat niet alleen planten en dieren RNA gebruiken: ook virussen gebruiken RNA. Een virus komt in een planten- of dierencel en gebruikt de apparatuur van de cel om daar eiwitten te maken van zijn eigen RNA. RNA silencing kan er voor zorgen dat het RNA van het virus wordt afgebroken. Wat wel van belang is dat alleen het juiste RNA wordt afgebroken, anders gaan er dingen mis met het organisme zelf.

Veel mensen hebben onderzocht hoe RNA silencing werkt. Het schema in Figuur 7.1 laat de interacties zien. RNA wordt geproduceerd door een gen of virus. Normaal bestaat RNA uit één keten van letters, maar tijdens RNA silencing wordt er ook gebruik gemaakt van dubbelstrengs RNA (dsRNA), wat uit twee ketens bestaat die op elkaar passen. Virussen

maken zelf dsRNA, en er is ook een eiwit in de cel dat dsRNA maakt van een enkele RNA streng. Het is ook mogelijk dat een stukje RNA dubbel klapt waardoor er lokaal een stukje dsRNA ontstaat. Het dsRNA wordt door een eiwit, Dicer, in kleine stukjes geknipt. Deze kleine stukjes RNA binden aan een aantal eiwitten en vormen zo het complex RISC ("RNA Induced Silencing Complex"). In RISC wordt één van de strengen van de kleine RNA weggegooid, de andere wordt bewaard. Dit kleine stukje RNA komt uit één van de twee strengen van het originele dsRNA en past precies op het RNA uit de tegenoverliggende streng. Op deze manier kan het RISC-complex RNAs opsporen en afbreken die bij de kleine RNA horen. Zo wordt alleen het juiste RNA afgebroken. Er zijn ook feedback mechanismen die meer dsRNA maken wat weer in kleine RNAs geknipt kan worden. Deze mechanismen maken gebruik van een eiwit wat enkelstrengs RNA herkent en daar dubbelstrengs RNA van maakt. Het is mogelijk dat dit eiwit gewoon RNA omzet in dsRNA, of dat de kleine RNAs eerst aan een RNA binden, waarna het eiwit er dsRNA van maakt.

In dit proefschrift gebruiken we wiskundige modellen om RNA silencing te bestuderen. Het mechanisme van RNA silencing is op te splitsen in kleine stappen (Figuur 7.1). Deze stappen worden in het model gezet. Het model houdt bij hoeveel RNA er is, hoeveel kleine stukjes er zijn, hoeveel er is van Dicer en RISC, enzovoort. Het doel van dit soort modellen is om iets te leren over het systeem waar je een model van hebt gemaakt. Onderzoekers kunnen namelijk wel bedenken hoe een mechanisme zou kunnen werken, maar de manieren waarop eiwitten en RNA op elkaar in kunnen werken zijn nooit vooraf voorspelbaar. We zijn begonnen met twee modellen die het gedrag van RNA silencing binnenin de cel beschrijven. Daarna hebben we de modellen uitgebreid om het gedrag van RNA silencing in een weefsel te beschrijven: meerdere cellen naast elkaar.

Onbekende interacties voorspeld

In **Hoofdstuk 2** van dit proefschrift hebben we gekeken of de bestaande kennis over RNA silencing wel alle facetten van RNA silencing kon verklaren. We hebben ons op twee verschillende processen geconcentreerd, namelijk 1) RNA silencing door de introductie van dsRNA en 2) RNA silencing dat werkt tegen genen die teveel RNA maken.

Onderzoek heeft laten zien dat je een gen tijdelijk kan onderdrukken met RNA silencing door dsRNA toe te voegen. Dat dsRNA wordt dan meteen door Dicer in kleine RNAs geknipt, die zorgen voor afbraak van het RNA geproduceerd door het gen.

Ander onderzoek heeft laten zien dat RNA silencing werkt tegen genen die teveel RNA produceren. Het eerste experiment (uit 1990) dat dit liet zien, was een experiment met petunia's. De onderzoekers wilden de bloemen van de petunia's extra paars maken. De paarse kleur van de bloemen wordt veroorzaakt door een bepaald eiwit. De onderzoekers verwachtten dat de bloemen paarser zouden worden als de plant meer kopieën van dit gen had. Dit was niet het geval, want de bloemen werden juist wit of kregen witte vlekken (zie de illustratie op de voorkant van dit proefschrift). De onderzoekers kwamen er achter dat het RNA dat bij de paarsmakende genen hoort, werd afgebroken in de cel voordat er eiwit van werd gemaakt. Later onderzoek liet zien dat RNA silencing alleen geactiveerd wordt als er genoeg extra kopieën van het gen in kwestie aanwezig zijn. We hebben een model gemaakt met daarin alle ontdekte interacties van RNA silencing. We ontdekten dat toegevoegd dsRNA inderdaad kan zorgen dat het RNA van een gen wordt afgebroken. Deze reactie is tijdelijk, want na een tijdje is het dsRNA uitgewerkt en komt de hoeveelheid RNA weer op het oude niveau.

Al snel bleek dat het tweede proces, de activatie van RNA silencing door extra kopieën van een gen, niet verklaard kon worden door de bekende interacties. Om dat proces te verklaren waren extra, nog niet ontdekte interacties nodig. Op basis van ons model hebben we een aantal mechanismen voorgesteld die zouden kunnen werken. Het leuke is dat dat de twee mechanismen die in ons model het beste werkten, nu ook zijn gevonden in experimenten. In dit hoofdstuk hebben we dus laten zien dat het gebruik van modellen erg nuttig, en zelfs noodzakelijk, kan zijn om te begrijpen hoe een mechanisme als RNA silencing werkt. Door het model kwamen we erachter dat de bestaande kennis onvoldoende was om het gedrag van RNA silencing compleet te begrijpen en konden we achterhalen welke onontdekte mechanismen er waarschijnlijk in de natuur aan het werk waren.

RNA silencing tegen een virusinfectie

In **Hoofdstuk 3** hebben we gekeken naar de situatie dat RNA silencing een virus bestrijdt. Het verschil met ons eerdere onderzoek is dat de hoeveelheid van een virus zelf groeit: er komen steeds meer kopieën van het virale RNA, terwijl we eerder van een constante hoeveelheid "aanjager" uitgingen: het dsRNA uit het vorige onderdeel. Bij het begin van een virusinfectie is er maar weinig viraal RNA, dat neemt toe in de tijd en verzadigt uiteindelijk op een maximaal niveau. We hebben ontdekt dat RNA silencing deze groeicurve op drie manieren kan veranderen.

1) Als RNA silencing heel efficiënt is, wordt al het virus afgebroken voor het kan groeien. 2) Als RNA silencing niet zo efficiënt is, ontstaat een evenwicht met minder viraal RNA dan zonder RNA silencing. Deze groeicurve is ook gemeten in planten met een virusinfectie. 3) Als de efficientie van RNA silencing tussen de twee uitersten ligt, kunnen er oscillaties optreden. Dit betekent dat de hoeveelheid virus en kleine RNAs blijft schommelen tussen een hoge en een lage waarde. We hebben laten zien dat de aanwezigheid van een feedback mechanisme er toe kan leiden dat er nog een andere groeicurve optreedt, waarbij het virus begint te groeien maar later in de infectie toch nog helemaal wordt afgebroken. Ook deze groeicurve is door onderzoekers in experimenten waargenomen.

Virusbestrijdende RNA silencing in een weefsel

In **Hoofdstuk 4** hebben we ons model van anti-virale RNA silencing uitgebreid. Eerder beschreef het alleen de hoeveelheid RNA en eiwitten binnen één cel, en dit hebben we uitgebreid naar meerdere cellen die met elkaar in verbinding staan. Het virus maakt deeltjes, die zich van de ene naar de andere cel verspreiden en zo andere cellen infecteren. De kleine RNAs die het virus bestrijden, verspreiden zich ook naar andere cellen. We waren geinteresseerd in het gedrag van RNA-silencing in een weefsel van meerdere cellen, omdat onderzoekers al hebben laten zien dat de hoeveelheid virus en kleine RNAs niet overal hetzelfde is. Op bladeren die geinfecteerd zijn met virus onstaan vaak gele vlekken door de infectie (zie de illustratie op de voorkant van dit proefschrift). Men heeft laten zien dat er veel virus is in cellen in de lichte plekken en dat er weinig virus is op de groene plekken. De kleine RNAs komen voor in de gele plekken en op de randen van groene met gele plekken. Het was niet bekend waardoor deze plekken konden ontstaan. Met ons ruimtelijke model hebben we laten zien dat dit soort patronen ontstaat door de interacties tussen RNA silencing, virusgroei en de verplaatsing van virus en kleine RNAs door het weefsel.

Virus vecht terug tegen RNA silencing

Nu laten virussen zich niet zomaar tegenwerken door RNA silencing. Ze hebben eiwitten ontwikkeld die RNA silencing tegengaan. Deze eiwitten kunnen verschillende stappen in RNA silencing belemmeren. Er zijn eiwitten die de kleine RNAs opnemen, zodat ze niet kunnen zorgen voor de afbraak van het virus en zich ook niet meer van cel naar cel kunnen verspreiden. Andere eiwitten binden zich niet alleen vast aan de kleine RNAs

maar ook aan het dsRNA, zodat het dsRNA van het virus niet in stukjes geknipt kan worden door Dicer. De laatste groep van hinderende soort eiwitten zorgt dat er geen RISC gevormd kan worden door een onderdeel van RISC af te breken of te inactiveren. In **Hoofdstuk 5** hebben we deze onderdrukkers van RNA silencing aan het model toegevoegd. Alle soorten onderdrukkers zorgden ervoor dat de hoeveelheid viraal RNA in een cel toenam. Verrassend was, dat dit niet hoefde te betekenen dat er in het ruimtelijke model meer cellen werden geinfecteerd. Dit was het geval voor de silencing onderdrukkers die een onderdeel van RISC als aangrijppunt hadden. Ons model liet zien dat het afbreken of inactiveren van RISC als gevolg kon hebben dat de hoeveelheid kleine RNAs toenam. Deze verspreiden dan van cel naar cel en kunnen de infectie van het virus voor blijven, waardoor het virus belemmerd wordt in zijn groei. We hebben laten zien dat deze onderdrukkers wel goed werken tegen het al in de literatuur bekende feedback mechanisme. In ons model werkten de eiwitten die dsRNA en siRNA binden het beste om de virusbestrijdende werking van RNA silencing te blokkeren.

Conclusie

In dit proefschrift hebben wiskundige modellen van biologische verschijnselen nieuw licht geworpen op de ingewikkelde interacties van RNA silencing. Daardoor zijn extra interacties voorspeld, die later ook in experimenten zijn bevestigd. Verder kan het model dat meerdere nabije cellen beschrijft (een 'weefsel') goed voorspellen waarom sommige gedeeltes van een weefsel met virus-infectie veel virusdeeltjes bevat, terwijl naburige gedeeltes juist rijk zijn in de kleine RNAs die RNA silencing aanjagen. Tenslotte hebben we gemodelleerd hoe virussen terug kunnen vechten door de verschillende stappen van RNA silencing te hinderen.

We hopen dat collega-onderzoekers de resultaten uit dit proefschrift gebruiken om beter dan voorheen te voorspellen hoe RNA silencing functioneert. Dat kan leiden tot experimenten die gericht op zoek gaan naar nog onbekende interacties, of tot onderzoek naar andere rollen van RNA silencing. Het gaat om een onderzoeksgebied met een rijke complexiteit, waarin theoretische modellen en experimenteel werk elkaar sterk aanvullen en versterken.

Curriculum vitae

Marian Groenenboom was born on June 29, 1979 in Tilburg. In 1991 she attended the Cobbenhagencollege in Tilburg where she gained her VWO diploma in 1997. In the same year she started with her studies in Biology at the University of Utrecht. She specialised in Theoretical Biology at the group of Paulien Hogeweg at the University of Utrecht, and in evolutionary biology at the group of Dolph Schluter at the University of British Columbia in Vancouver, Canada. After obtaining her Masters degree in 2003 she started her PhD with Paulien Hogeweg in Utrecht, and the results of these studies are described in this thesis.

List of Publications

Groenenboom, MAC & Hogeweg, P Space and the persistence of male-killing endosymbionts in insect populations *Proc. R. Soc. Lond., Ser. B: Biol. Sci.* Vol. 269, no. 1509, 2509–2518 (2002).

Groenenboom, MAC, Marée, AFM, and Hogeweg, P The RNA Silencing Pathway: The Bits and Pieces That Matter. *PLoS Comput Biol* 1(2) (2005) .

Taylor, EB, Boughman, JW, Groenenboom, M, Sniatynski, M, Schluter, D & Gow, JL Speciation in reverse: morphological and genetic evidence of the collapse of a three-spined stickleback (*Gasterosteus aculeatus*) species pair. *Molecular Ecology* 15(2) 343–355 (2006).

Groenenboom, MAC & Hogeweg, P The dynamics and efficacy of antiviral RNA silencing: a model study. *BMC Systems Biology* 2:28 (2008).

Groenenboom, MAC & Hogeweg, P RNA silencing can explain chlorotic infection patterns on plant leaves. *BMC Systems Biology, in press.*

Groenenboom, MAC & Hogeweg, P Viral suppression of RNA silencing. *In preparation.*

Dankwoord

Op deze plek wil ik graag iedereen bedanken die mij heeft geholpen bij het tot stand komen van dit proefschrift.

Als eerste wil ik graag mijn promotor Paulien Hogeweg bedanken. Paulien, je weet dat ik het niet altijd even makkelijk heb gehad, maar jij hebt me er altijd weer doorheen geholpen. Niet alleen op wetenschappelijk gebied, ook op het persoonlijke vlak stond je altijd voor me klaar en hier ben ik je erg dankbaar voor.

Graag wil ik ook de leden van de beoordelingscommissie, Rob de Boer, Rustom Antia, Simon Levin en Albert Goldbeter bedanken.

Ik wil de vakgroep bedanken voor de gezelligheid en hulp met allerlei problemen. Milan, je bent erg geduldig en stond altijd voor me klaar als ik weer een (vaak nogal suf) wiskundig probleem had. Daniel, ook al zaten we toch wel 80% van de tijd allebei met onze koptelefoons op, ik heb veel gehad aan je steun in de stressvolle periode die het afronden van dit proefschrift vooraf ging. Rikkert, Kirsten en Jos, bedankt voor de leuke en soms erg serieuze gesprekken tijdens tripjes naar de winkel en de snoep- of chocomelautomaat. Stan, Jan-Kees, Verônica, Nobuto, Anton en Otto, bedankt voor jullie hulp bij alle programmeer-, makefile-, Inkscape- en LaTeX-issues. Giel, bedankt voor het lezen en verbeteren van mijn nederlandse samenvatting.

Buiten de vakgroep heb ik veel steun gehad van mijn familie en vrienden, met name natuurlijk Marije, Margreet, Astrid en mijn ouders. Frank, bedankt voor het altijd voor me klaar staan in deze hectische tijd. Ik hoop samen met jou en ons kindje een fijne tijd tegemoet te gaan.